

Isotopic and Fuel Lattice Parameter Trends in Extended Enrichment and Higher Burnup LWR Fuel

Volume II: BWR Fuel



Riley Cumberland
Ryan Sweet
Ugur Merturek
Robert Hall
William A. Wieselquist

March 2021

DOCUMENT AVAILABILITY

Reports produced after January 1, 1996, are generally available free via US Department of Energy (DOE) SciTech Connect.

Website www.osti.gov

Reports produced before January 1, 1996, may be purchased by members of the public from the following source:

National Technical Information Service
5285 Port Royal Road
Springfield, VA 22161
Telephone 703-605-6000 (1-800-553-6847)
TDD 703-487-4639
Fax 703-605-6900
E-mail info@ntis.gov
Website <http://classic.ntis.gov/>

Reports are available to DOE employees, DOE contractors, Energy Technology Data Exchange representatives, and International Nuclear Information System representatives from the following source:

Office of Scientific and Technical Information
PO Box 62
Oak Ridge, TN 37831
Telephone 865-576-8401
Fax 865-576-5728
E-mail reports@osti.gov
Website <http://www.osti.gov/contact.html>

This report was prepared as an account of work sponsored by an agency of the United States Government. Neither the United States Government nor any agency thereof, nor any of their employees, makes any warranty, express or implied, or assumes any legal liability or responsibility for the accuracy, completeness, or usefulness of any information, apparatus, product, or process disclosed, or represents that its use would not infringe privately owned rights. Reference herein to any specific commercial product, process, or service by trade name, trademark, manufacturer, or otherwise, does not necessarily constitute or imply its endorsement, recommendation, or favoring by the United States Government or any agency thereof. The views and opinions of authors expressed herein do not necessarily state or reflect those of the United States Government or any agency thereof.

Nuclear Energy Fuel Cycle Division

**ISOTOPIC AND FUEL LATTICE PARAMETER TRENDS IN EXTENDED
ENRICHMENT AND HIGHER BURNUP LWR FUEL**

VOLUME II: BWR FUEL

Riley Cumberland, Ryan Sweet, Ugur Mertuyurek, Robert Hall, William A. Wieselquist

Date Published: March 2021

Prepared by
OAK RIDGE NATIONAL LABORATORY
Oak Ridge, TN 37831-6283
managed by
UT-BATTELLE, LLC
for the
US DEPARTMENT OF ENERGY
under contract DE-AC05-00OR22725

CONTENTS

1.	INTRODUCTION.....	3
1.1	EXPECTED EFFECTS OF HBU AND EE ON FUEL MANAGEMENT	4
2.	LATTICE PHYSICS MODEL DESCRIPTION.....	6
3.	LATTICE PHYSICS RESULTS.....	10
3.1	FLUX SPECTRUM	10
3.2	REACTIVITY AND COEFFICIENTS.....	11
3.3	MACROSCOPIC CROSS SECTIONS.....	15
3.3.1	Lattice Cross Sections	15
3.3.2	Kinetics Parameters.....	17
4.	SENSITIVITY AND UNCERTAINTY	19
4.1	NUCLIDE WORTH RANKING	19
4.2	SAMPLER/POLARIS DEPLETION UNCERTAINTY	21
5.	ISOTOPIC INVENTORY.....	24
5.1	DECAY HEAT TRENDS	24
5.2	ISOTOPES RELEVANT TO ACTIVITY	36
5.3	ISOTOPES RELEVANT TO ACCIDENT RELEASE SOURCE TERM	41
5.4	ISOTOPES RELEVANT TO RADIATION SHIELDING SOURCE TERM	43
5.5	ISOTOPES FOR CRITICALITY	49
5.6	COMPARISON OF 252g AND 56g MULTIGROUP LIBRARIES	53
6.	CONCLUSIONS	56
7.	REFERENCES.....	59
	APPENDIX A. EFFECT OF CROSS SECTION LIBRARY	A-1
	APPENDIX B. ARCHIVE FILE CONTENT	B-1

LIST OF FIGURES

Figure 1. Layout of 5max-4.5av wt% DOM (left) and 5max-4.5av wt% VAN lattices (right)	8
Figure 2. Layout of 8.5max-6.5av wt% DOM (left) and 8.5max-5.9av wt% VAN lattices (right).	8
Figure 3. Layout of 10max-7.4av wt% DOM (left) and 10max-7.4av wt% VAN lattices (right).	9
Figure 4. Fast/ Thermal flux ration at 40% void fraction.	11
Figure 5. Total flux.	11
Figure 6. HFP depletion k_{inf} at 40%void fraction	12
Figure 7. HFP DTC at 40% void fraction	13
Figure 8. HFP MVC.....	14
Figure 9. HFP CBW at 40% void fraction.	14
Figure 10. HFP macroscopic thermal absorption cross section	15
Figure 11. HFP macroscopic fast absorption cross section	16
Figure 12. HFP macroscopic thermal fission cross section	16
Figure 13. HFP macroscopic fast fission cross section.....	17
Figure 14. Effective delayed neutron fraction	18
Figure 15. Uncertainty in k_{inf} at 40 % void fraction due to nuclear data uncertainties.....	23
Figure 16. Decay heat as a function of cooling time for all cases	25
Figure 17. Decay heat as a function of cooling time (effect of enrichment and burnup)	26
Figure 18. Decay heats as a fraction of full power vs cooling time.....	26
Figure 19. Decay heat relative to 60 GWd/MTU 5max-4.5av 40% DOM case	27
Figure 20. Decay heat difference with to 60 GWd/MTU 5max-4.5av 40% DOM case.....	28
Figure 21. In-core abundances of ^{144}Pr beta chain isotopes for 10max-7.4av wt% initial enrichment.....	31
Figure 22. Activity as a function of cooling time for all 16 lattices.	36
Figure 23. Relative difference in activity with the reference case a function of cooling time.	37
Figure 24. Difference in activity with the reference case a function of cooling time.....	37
Figure 25. In-core abundances for isotopes in the activation chain for ^{244}Cm and ^{246}Cm	48
Figure 26. Relative difference in SF neutron emission on total SF neutron emission basis for time point 80 GWd/MTU 10max-7.4av wt% vs the reference case for 40% void fraction.	48
Figure 27. Difference in reactivity between the 252 and 56 g cross section libraries for the 10% limit dominant and vanished lattices.	A-1
Figure 28. Comparison of the Doppler temperature coefficient (DTC) for the 252 and 56 g cross section libraries for the 10% limit dominant and vanished lattices.	A-2
Figure 29. Comparison of the moderator void coefficient (MVC) for the 252 and 56 g cross section libraries for the 10% limit dominant and vanished lattices.	A-2

LIST OF TABLES

Table 1. GE14 BWR fuel lattice modeling parameters	6
Table 2. Lattice Descriptions	7
Table 3. Nuclide worth (Δk) at 40% void fraction.....	20
Table 4. Predictions and relative standard deviations in isotope inventories	22
Table 5. Contributions of each isotope to total percent change in decay heat from enrichment increase	29
Table 6. Contributions of each isotope to total percent change in decay heat from burnup increase	30
Table 7. Contributions of each isotope to total percent change in decay heat from combined enrichment and burnup increase.....	30
Table 8. Difference in isotopic decay heats resulting from enrichment increase at various cooling times	32
Table 9. Difference in isotopic decay heats resulting from burnup increase at various cooling times	32
Table 10. Difference in isotopic decay heats resulting from burnup and enrichment increase at various cooling times	33
Table 11. Signed RMS change in isotope decay heat relative to total for enrichment increase from 5max-4.5av% to 10max-7.4av% enrichment.....	34
Table 12. Signed RMS change in isotope decay heat relative to total for burnup increase from 60 to 80 GWd/MTU at 10max-7.4av% enrichment.....	34
Table 13. Signed RMS change in isotope decay heat relative to total for enrichment and burnup increase from 5max-4.5av wt% 60 GWd/MTU to 10max-7.4av wt% enrichment at 80 GWd/MTU	35
Table 14. Signed RMS change in isotopic decay heat due to changes in lattice design and void fraction for 10max-7.4av wt% DOM lattice at 80 GWd/MTU	35
Table 15. Contributions of each isotope to total percent change in activity from enrichment increase	39
Table 16. Contributions of each isotope to total percent change in activity from burnup increase	39
Table 17. Contributions of each isotope to total percent change in activity from combined enrichment and burnup increase	40
Table 18. Signed RMS change in isotopic activity due to changes in lattice design and void fraction for 10max-7.4av wt% DOM lattice at 80 GWd/MTU	41
Table 19. Relative differences of selected release isotopes activities due to enrichment increase	42
Table 20. Relative differences of selected release isotopes activities due to burnup increase	42
Table 21. Relative differences of selected release isotopes activities due to both enrichment and burnup increase	43
Table 22. Signed RMS relative differences in abundance of selected release isotopes due to changes in lattice design and void fraction for 10max-7.4av wt% DOM lattice at 80 GWd/MTU	43
Table 23. Relative differences of selected shielding isotopes activities due to enrichment increase	45

Table 24. Relative differences of selected shielding isotopes activities due to burnup increase	45
Table 25. Relative differences of selected shielding isotopes activities due to both enrichment and burnup increase	46
Table 26. Signed RMS relative differences in abundance of selected shielding isotopes vs the dominant lattice with 10% void for 10% maximum enriched lattices burned to 80 GWd/MTU	47
Table 27. Relative differences of criticality isotope masses due to enrichment increase.....	50
Table 28. Relative differences of criticality isotope masses due to burnup increase	51
Table 29. Relative differences of criticality isotope masses due to both enrichment and burnup increase	52
Table 30. Relative differences of criticality isotope masses due to changes in lattice design and void fraction for 10max-7.4av wt% DOM lattice at 80 GWd/MTU	53
Table 31. Relative difference between 252- and 56-group cross section structures on isotope results (other comparisons shown for reference).	55

ACRONYMS

ATF	accident-tolerant fuel
BOC	beginning of cycle
BW	[soluble] boron worth
BWR	Boiling Water Reactor
CRW	control rod worth
DOM	dominant
DTC	Doppler temperature coefficient
EE	extended enrichment
ENDF	Evaluated Nuclear Data File
EOC	end of cycle
GWd/MTU	gigawatt-days per metric ton of uranium
HALEU	high assay low-enriched uranium
HFP	hot full power
IAEA	International Atomic Energy Agency
IFBA	integral fuel burnable absorber
JEFF	Joint Evaluated Fission and Fusion File
LWR	light water reactor
MTC	moderator temperature coefficient
MVC	moderator void coefficient
PWR	pressurized water reactor
RMS	root mean square
SFP	spent fuel pool
S/U	sensitivity and uncertainty
VAN	vanished

SUMMARY

Commercial light water reactor (LWR) operators and fuel vendors in the United States are pursuing changes to nuclear fuel that include extended enrichment (EE) and accident-tolerant fuel (ATF) designs to further improve reactor safety and plant economics. Extended fuel enrichments above 5% ^{235}U pin enrichment and up to 10% ^{235}U are a subset of high assay low-enriched uranium (HALEU) that may be deployed in commercial US LWRs in the near term. ATF features, such as cladding coatings or alternative cladding materials, are designed to improve fuel system performance under accident conditions. One goal of EE is to improve fuel cycle economy by enabling fuel to be depleted to higher burnup than the typical current limits (62 gigawatt-days per metric ton of uranium [GWD/MTU]). Adoption of EE, ATF, and high burnup (HBU) fuels in the US commercial fleet requires a clear understanding of the effects on core physics parameters and used fuel isotopic content, as well as confidence in the accuracy of computer code predictions over an expanded range of materials, enrichment, and burnup. A thorough understanding of the applicability and adequacy of benchmark data (e.g., criticality, decay heat, isotopic content) for computer code validation is necessary to ensure that appropriate safety margins are maintained.

As part of the US Nuclear Regulatory Commission (NRC) agreement number 31310019N0008, “SCALE Code Development, Assessment and Maintenance,” the effects of EE, ATF, and HBU are being assessed for selected representative LWR fuel designs. The project is divided into phases, and this report summarizes the findings of the Phase 1 work, which focuses on lattice physics parameter and used fuel isotopic changes for a conventional GE14 10×10 boiling water reactor (BWR) design with GNF-2 part length rod patterns to model a modern BWR assembly design.

This activity is part of Phase 1 of HALEU/HBU/ATF SCALE code preparedness activities beginning in

Q2 FY20 and ending in Q2 FY21. This report addresses the following NRC user needs within the Nuclear Reactor Regulation (NRR) and Nuclear Material Safety and Safeguards offices.

- Identify data needs for high burnup and enrichment >5% in SCALE.
- Compare isotopics from baseline (~62 GWD/MTU rod average) to 75 GWD/MTU rod-average and quantify impact on reactivity, decay heat, and radioactive source terms in prototypical applications in each area.
- Compare isotopics from baseline (5%) to 8%, and quantify impact on reactivity, decay heat, and radioactive source terms in prototypical applications in each area.
- These NRC user needs are expected to change and adapt to the ever-changing commercial nuclear landscape. Phase 2 HALEU/HBU/ATF SCALE activities are expected to focus on core level (PARCS) assessments as well as code development efforts recommended by Phase 1 activities. If new user needs are available, activities identified for Phase 2 will be re-mapped and re-prioritized according to the updated user needs.

Calculations were performed using Polaris and ORIGEN sequences in SCALE to evaluate the effects of EE and HBU fuels on depletion characteristics of a representative commercial BWR fuel assembly. Uncertainties in Polaris calculations due to nuclear data uncertainties were

calculated Sampler sequence. All calculations were performed using a pre-release version of SCALE 6.3 with the 56 -group ENDF/B-VII.1 cross section library. The investigation focused on differences between depletions of better-understood LWR fuel (5 wt% ^{235}U maximum pin enrichment with lattices depleted to 60 GWd/MTU) and depletion for maximum pin enrichments up to 10 wt% and lattice burnup up to 80 GWd/MTU.

Key quantities of interest include (1) lattice physics parameters (reactivity, reactivity coefficients, cross sections, and kinetics parameters), (2) isotopic inventory at various decay times, (3) uncertainty in k_{inf} arising directly from cross section uncertainties and indirectly from uncertainties in the discharged isotopic content. Limited comparisons between predictions using SCALE 56-group ENDF/B-VII.1 cross sections and SCALE 252-group ENDF/B-VII.1 cross sections are also presented. No unexpected or anomalous trends were found that would call into question the accuracy of the Polaris code using SCALE 56-group ENDF/B-VII.1 cross sections for depletion, lattice physics, and isotopic content calculations of the analyzed BWR fuel with enrichments up to 8 wt% and burnup up to 80 GWd/MTU. For multiple physical quantities of interest, increases in enrichment and increases in burnup had opposing and offsetting effects.

1. INTRODUCTION

Commercial light water reactor (LWR) operators and fuel vendors in the United States are pursuing evolutionary changes to nuclear fuel that include extended enrichment (EE) fuel (^{235}U maximum pin enrichment within 5–10wt%) and accident-tolerant fuel (ATF) designs intended to improve fuel and cladding performance under accident conditions [1, 2]. One goal of this effort is to improve fuel cycle economy by enabling fuel to be depleted to higher burnup than presently possible. Adoption of these changes in the US commercial fleet requires a clear understanding of the effects on core physics parameters and used fuel isotopic content, as well as confidence in the accuracy of computer code predictions over an expanded range of materials, enrichment, and burnup. A thorough understanding of the applicability and adequacy of benchmark data (e.g., criticality, decay heat, isotopic content) for computer code validation is necessary to ensure that appropriate safety margins are maintained.

To prepare for and support these potential changes, the effects of EE, ATF, and high burnup (HBU) fuels are being assessed for selected representative LWR fuel designs. This Volume II report focuses on changes to lattice physics parameters and used fuel isotopic compositions for a conventional GNF-2 10×10 boiling water reactor (BWR) design [3]. The SCALE Polaris lattice physics code and the ORIGEN depletion and decay code are the primary investigation tools [4].

To aid in understanding the best-estimate effects of EE and HBU, various quantities of interest for UO_2 fuel ^{235}U enrichments are evaluated at 5, 8.5, and 10 wt% up to 80 GWd/MTU lattice-average burnup, with a focus on differences relative to 5 wt% enrichment up to 60 GWd/MTU.

Specific power was not varied in this study because it is implicitly included in burnup. Furthermore, specific power is not expected to change with EE and HBU due to its being set by thermal hydraulic limits. Therefore, power is not a parameter being varied in this study.

The quantities of interest include:

- Lattice physics behavior (modeled with Polaris)
 - Neutron flux and flux spectrum
 - Reactivity (k_{inf} , reactivity coefficients)
- Trends and contributing isotopic inventory of importance in four categories
 - Decay heat (short- and long-term decay times)
 - Shielding (activity at short- and long-term decay times)
 - Severe accident (important nuclides at short and long decay times)
 - Criticality (during decay)

These calculations are 2D, representing assembly average quantities and equilibrium cycles. 5 wt% is the current enrichment limit for commercial LWRs, 10 wt% bounds the maximum envisioned near-term enrichment increase, and 8.5 wt% is included as a midpoint to improve confidence in observed trends. Evaluation of 3D parameters such as axial burnup shapes will be performed in later work.

In addition to identifying the best-estimate effects of EE and HBU on quantities of interest, it is important to understand the uncertainty of EE and HBU models relative to conventional fuel models. Preliminary results of limited sensitivity and uncertainty (S/U) analyses are presented, comparing 80 GWd/MTU lattices with 10 wt% maximum pin enrichment to 60 GWd/MTU lattices with 10 wt% maximum pin enrichment and 60 GWd/MTU lattices with 5 wt% maximum pin enrichment. The primary tools for S/U analysis is Sampler/Polaris [4]. These analyses quantify uncertainty in k_{inf} and in depleted fuel isotopic content due to nuclear data uncertainty using the cross section covariance data included in pre-release version of SCALE 6.3. The following preliminary S/U data for 5 wt% 60 GWd/MTU¹ and 80 GWd/MTU fuel are presented.

- Sampler/Polaris perturbed cross section depletions (isotopic content and k_{inf} uncertainty at in-reactor hot full power [HFP] conditions)
- Isotope worth ranking by importance to k_{inf} (in-reactor HFP conditions)

Polaris models are described in Section 2. Lattice physics comparisons are presented in Section 3. Section 4 describes and summarizes the preliminary S/U analysis. Isotopic inventory comparisons are presented in Section 5.

All calculations were performed using a pre-release version of SCALE 6.3 with the 56 -group ENDF/B-VII.1 cross section library.

This volume discusses the lattice physics models (not the codes) in more detail in Section 2. The physics of the BWR system are discussed in Section 3. That foundation is then used to explore lattice physics (Section 4), S/U (Section 5) and isotopic inventories (Section 6) relevant to various analyses.

1.1 EXPECTED EFFECTS OF HBU AND EE ON FUEL MANAGEMENT

This evaluation of EE and HBU fuel is focused on existing commercial BWR fuel designs. As in the PWR case, the driving force for use of higher enrichment fuel is to achieve reduced fuel cycle costs. Again, higher enrichment without higher burnup would result in increased cost without the benefit of more energy produced. Higher burnup without increased enrichment cannot be achieved due to the requirement for sufficient fuel reactivity at the end of cycle (EOC). As is consistent with prior experience, increased enrichment results in increased achievable burnup, and the effects should be evaluated in combination.

There are at least two ways that EE may affect fuel cycle management. First, cycle length could be maintained, and the size of the reload fuel batch could be reduced. This approach would result in higher core average burnup throughout a cycle, and higher discharge fuel assembly burnup. It is also possible that increased enrichment could be used to increase cycle length (perhaps from 18 to 24 months). This strategy would increase EOC core average burnup and discharge burnup. The net effect on beginning of cycle (BOC) core average burnup would depend in part on batch

¹ Note that unless otherwise stated, enrichments in this volume refer to maximum pin enrichments, and burnups refer to lattice average burnups.

size. From a fuel cycle management perspective, EE and HBU are expected to be positively correlated for at least part of a reload cycle.

Regardless of whether increased enrichment is used to achieve smaller batch size or longer cycles, higher core average burnup is expected, as well as higher assembly discharge burnup. When combined with results from lattice physics calculations, this approximation is used to better understand some of the expected core average effects of EE and HBU.

2. LATTICE PHYSICS MODEL DESCRIPTION

The 2D lattice physics code Polaris was used to assess how the reactivity and local power across a fuel assembly changes from extended burnup and increased enrichment. For these calculations, design parameters were selected to approximate the GNF-2 10×10 BWR fuel lattice by using GE14 lattice parameters with GNF-2 vanished rod positions. Modeling parameters for the GE-14 lattice are provided in Table 1. In addition to the dominant (DOM) region of the assembly, the vanished (VAN) region was used in the analysis due to expected variation in neutronic behavior.

Table 1. GE14 BWR fuel lattice modeling parameters

Parameter	Value
Lattice size	10×10
Assembly pitch	15.24 cm [12]
Fuel rod pitch	1.295 cm [12]
Clad material	Zirc-2
UO ₂ pellet radius	0.4380 cm [12]
Clad inner radius	0.4470 cm [12]
Clad outer radius	0.5130 cm [12]
Water tube inner radius	1.20 cm [12]
Water tube outer radius	1.28 cm [12]
Channel width (inside)	13.406 cm [12]
Channel box thickness ¹	0.2032 cm [13]
Channel radius ²	0.9652 cm
Fuel temperature	1100 K
Clad temperature	600 K
Coolant temperature	580 K
UO ₂ effective density	10.64 g/cm ³ [12]
Coolant density	0.7048 g/cm ³

¹Assumed to be uniform and similar to a GE9 lattice channel thickness

²Calculated from the channel width assuming channel touches the pin cell corner for the corner pin.

The fuel assembly layouts for the reference 5max-4.5av wt% DOM (5% maximum and 4.5 % lattice average enrichment) and VAN lattices are shown in Figure 1. The gadolinia rods are shown in green, with the Gd₂O₃ weight precents under the ²³⁵U enrichments. Starting with GE14 enrichment maps in the literature [14], and vanished rod patterns for a GNF-2 VAN lattice region [12], ²³⁵U enrichments, gadolinia weight percents and gadolinia locations were modified to meet the following criteria for a more realistic lattice design:

- Maximum fuel pin enrichment 5%
- Depletion calculations starting with k_{inf} at BOC to 1.1 and gad peaking near 10 GWd/MTU
- Pin peaking factors below 1.3

Unfortunately, there is no publicly available BWR lattice design with pin enrichments above 5%. Increasing the maximum pin enrichments proportionally using the same 5% reference design enrichment map causes large power peaking factors within pins around the periphery. As expected, the initial lattice reactivity is also much higher.

Therefore, a simple iterative optimization study was performed to have a realistic looking lattice design for this work. Assuming that the EE, HALEU lattices will be subjected to similar lattice design constraints, the target k_{inf} value was as selected 1.1 at BOC while the target maximum pin peak was kept below 1.3. To suppress the initial fuel assembly reactivity and power peaking across the assembly, number of gadolinia rods were increased. The lattice designs that are used in this report, descriptions and the selected naming convention are provided in Table 2.

Table 2. Lattice Descriptions

Lattice Name	Maximum Enrichment (% ^{235}U)	Average Lattice Enrichment (% ^{235}U)	Lattice Region
5max-4.5av wt% DOM*	5.0%	4.33%	DOM
5max-4.5av wt% VAN		4.31%	VAN
8.5max-6.5av wt% DOM	8.5%	6.50%	DOM
8.5max-5.9av wt% VAN		5.92%	VAN
10max-7.4av wt% DOM	10.0%	7.45%	DOM
10max-7.4av wt% VAN		7.47%	VAN

*Reference lattice

The enrichment maps calculated for the max 8.5 and max 10% enrichment cases are shown in Figure 2 and Figure 3, respectively. Both designs include 8 different UO₂ fuel enrichments and 4 different UO₂-Gd₂O₃ enrichment combinations. Although, the number of different enrichments can be reduced with use of gad rod in the periphery and more rigorous optimizations, the current design is satisfactory for this study.

For the reference lattice, the nominal moderator void fraction was set to 40%. Depletion calculations were performed up to 80 GWd/MTU. for both dominant and vanished lattices. No design changes to conventional fuel pellets were assumed. Considering typical void fraction history that a DOM and VAN lattices will experience during their life time in the core, 10% and 40% void fraction state points were modeled for DOM while 40% and 70% void fraction state points were modeled for VAN lattices.

Two SCALE cross section libraries are available for use with Polaris: 56- and 252-group ENDF/B-VII.1. Lattice physics parameters and fuel depletion isotopic content were calculated using the 56-group library. Some 252- and 56-group library depletion k and reactivity coefficient comparisons are also provided to help determine whether EE and HBU introduce challenges for the 56-group library.

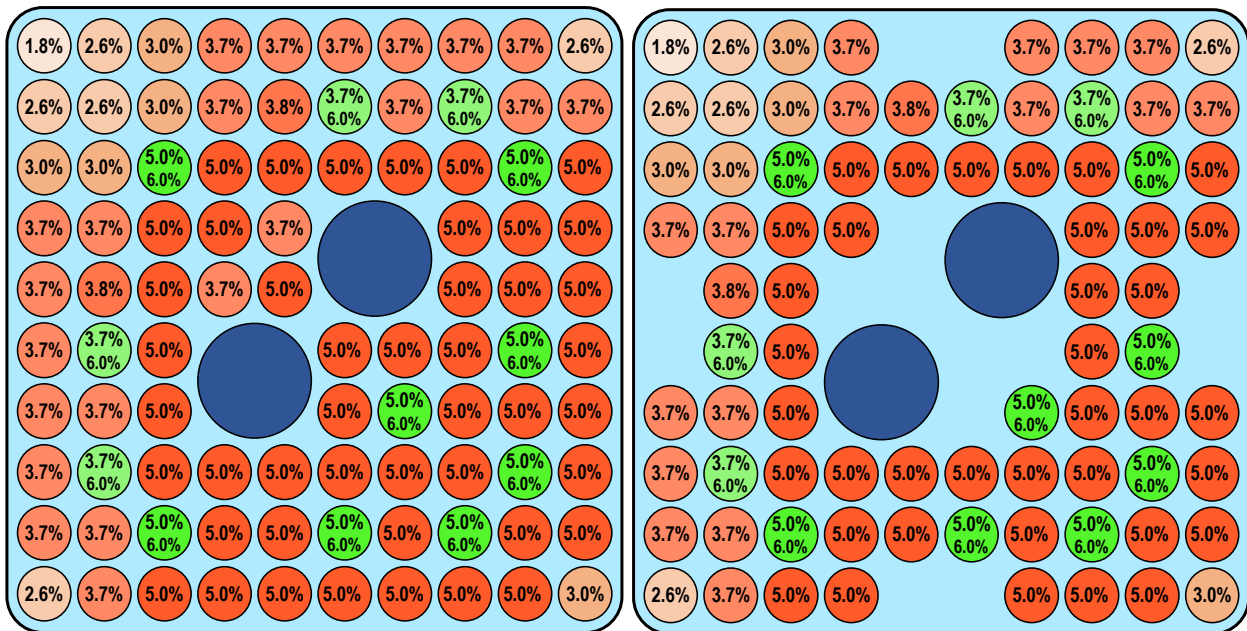


Figure 1. Layout of 5max-4.5av wt% DOM (left) and 5max-4.5av wt% VAN lattices (right)

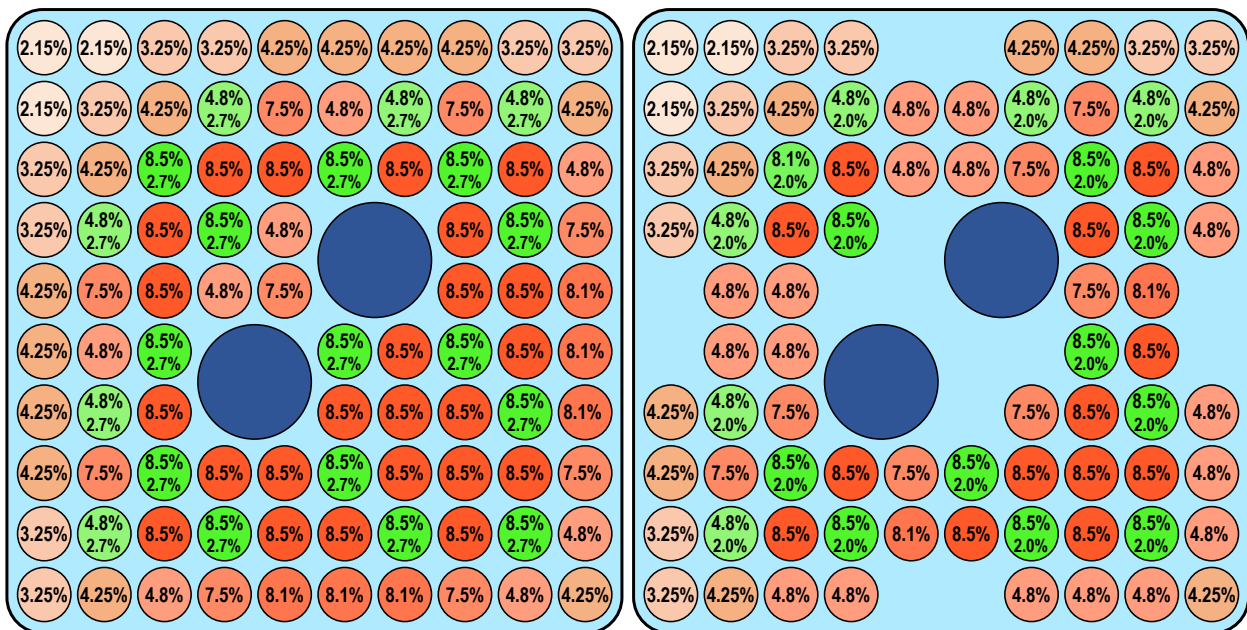


Figure 2. Layout of 8.5max-6.5av wt% DOM (left) and 8.5max-5.9av wt% VAN lattices (right).

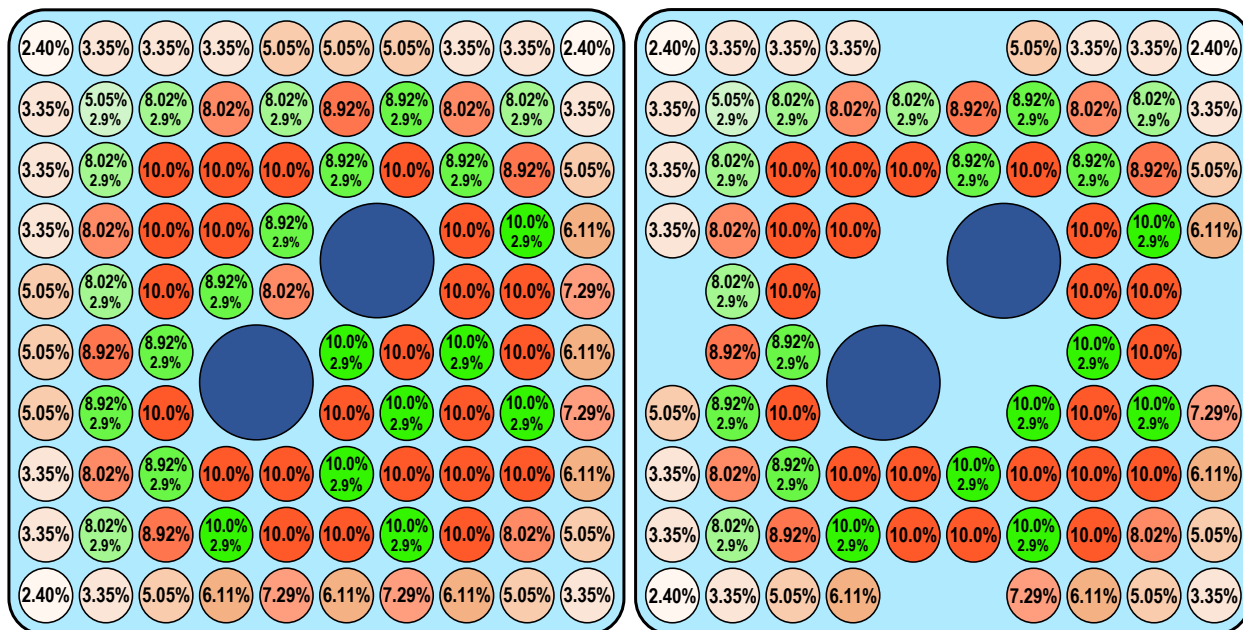


Figure 3. Layout of 10max-7.4av wt% DOM (left) and 10max-7.4av wt% VAN lattices (right).

3. LATTICE PHYSICS RESULTS

This section compares general neutronics trends observed in depletion of reference and extended enriched fuel and discusses observed differences. Extended enrichment and high burnup HFP depletions were modeled using Polaris with the model parameters described in the previous section for all 6 lattices. Reactivity for the modeled lattices is compared, as well as the ratio of fast and thermal fluxes, and the Doppler temperature coefficient (DTC) and moderator void coefficients (MVC) of reactivity.

3.1 FLUX SPECTRUM

Change in flux provides insight to many neutronic behavior observed with depletion. The fraction of fast flux to thermal flux is shown in Figure 4 as a function of burnup. Increases in the fast to thermal flux ratio demonstrate the magnitude of spectrum hardening due to increased enrichment. Similar spectrum hardening is observed between DOM and VAN lattice regions for each enrichment. All three enrichment cases follow parallel trends until practical life time of 5max-4.5av wt% lattice. Although spectrum of all three lattices become more thermal with burnup, the relative difference in spectra due to increased enrichment remains constant. In other words, EE lattices always operate at a harder spectrum than the 5max-4.5av wt% lattices throughout their lifetime.

The lattice average total flux for different lattice enrichments is also depicted in Figure 5. The observed trends in flux with burnup is mainly dominated by the gadolinia content of the lattices and gadolinia depletion until 15 GWd/MTU. The differences in flux trends in this region is due to gadolinia loading differences between 5max-4.5av wt% and 10max-7.4av wt% enriched lattices. However, in general, the differences in magnitudes and trends with depletion are caused by the flux normalization to match constant power for the lattice depletion calculations. The flux increases as fissile isotope content decreases with burnup, compensating for the reduction in number of fissions. Similarly, the flux decreases as the fissile content increases with increasing enrichment.

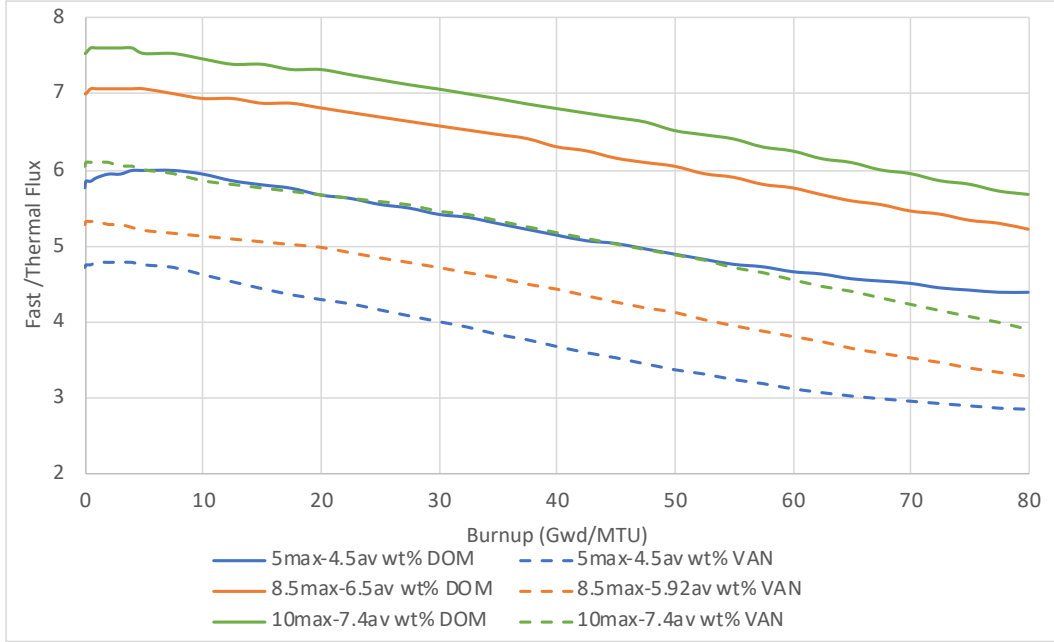


Figure 4. Fast/ Thermal flux ratio at 40% void fraction.

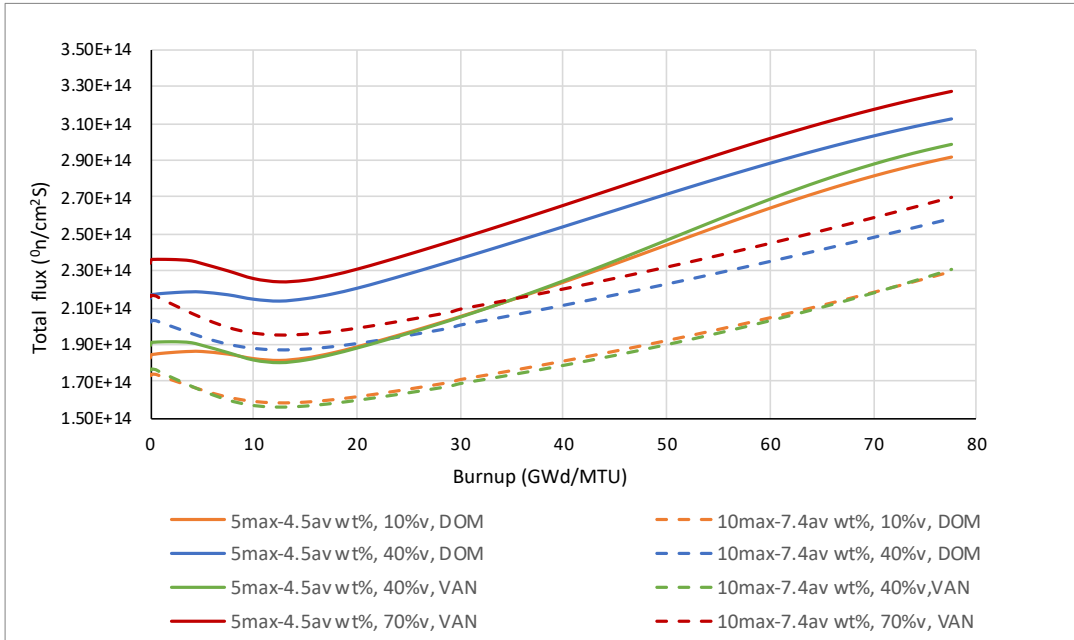


Figure 5. Total flux.

3.2 REACTIVITY AND COEFFICIENTS

Reactivity comparisons for EE/HBU depletions presented herein include HFP depletion k_{inf} , as well as reactivity coefficients and control blade worth (CBW). Coefficients and worths were calculated for each depletion step using the Polaris depletion k_{inf} at the nominal condition (1100

K fuel temperature, 580 K moderator temperature at 40% void fraction). Branch cases were performed with fuel temperatures of 900 K and 1300 K, and void fractions of 10% and 70%, and control blades inserted.

The reactivity increase with increasing enrichment and fuel content (DOM vs VAN) can be seen in Figure 6. In general, when DOM and VAN lattice depletions are compared, lattices with different enrichments show similar trends. Higher gad worth at VAN lattices causes higher reactivity peaks due to burnup of gadolinia (gad peak) than DOM lattices, while gad peaks are at consistent burnups. The reactivity of 5max-4.5av wt% lattice at 45 GWd/MTU is similar to 8.5% max lattice at 65 GWd/MTU and 10max-7.4av wt% lattice at 73 GWd/MTU (marked with a black line in the figure). If all lattices are expected have similar reactivities before they are discharged, about 20 to 30 GWd/MTU extension in lattice core lifetime can be assumed with extended enrichments.

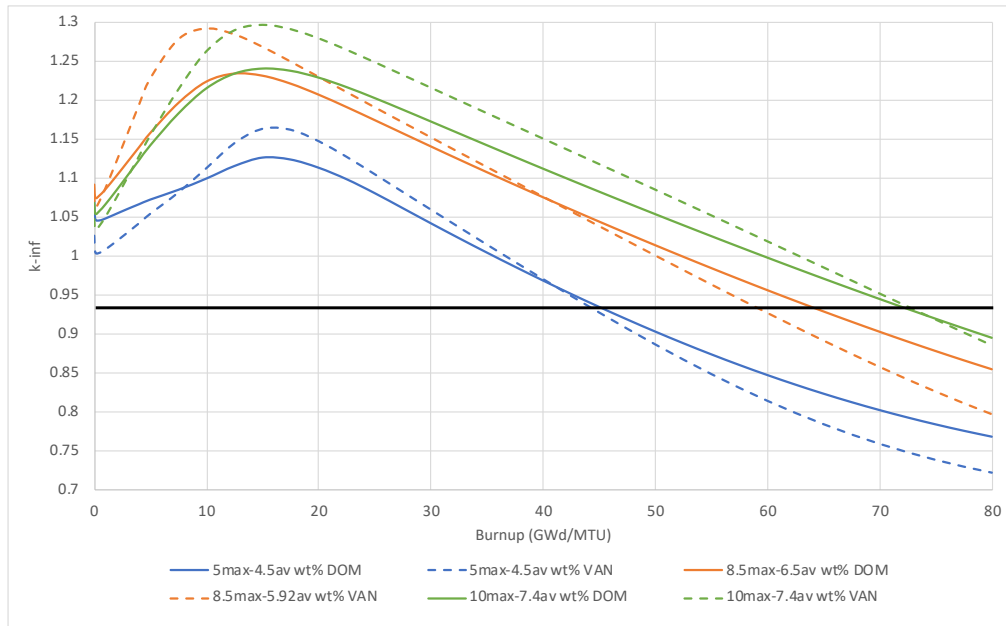


Figure 6. HFP depletion k_{inf} at 40%void fraction

As illustrated in Figure 7, the effect of DTC becomes less pronounced with increased enrichment and more pronounced with increasing burnup. Doppler broadening in ^{238}U primarily results in neutron capture (negative DTC). In fissile materials such as ^{235}U , Doppler broadening increases fission (positive DTC). Higher enrichment fuel increases the positive fissile contribution to DTC. Higher burnup reduces the positive fissile contribution to DTC. Based on the expected increase in core average burnup with increased enrichment (Figure 6) the estimated core average DTC (EOC estimate) is small due to offsetting effects of increased enrichment and increased burnup. A notable observation is the inflection in 5max-4.5av wt% VAN lattice DTC after 55 GWd/MTU. The similar behavior is observed in DTC of 8.5 % enriched VAN lattice as it plateaus around 70 GWd/MTU.

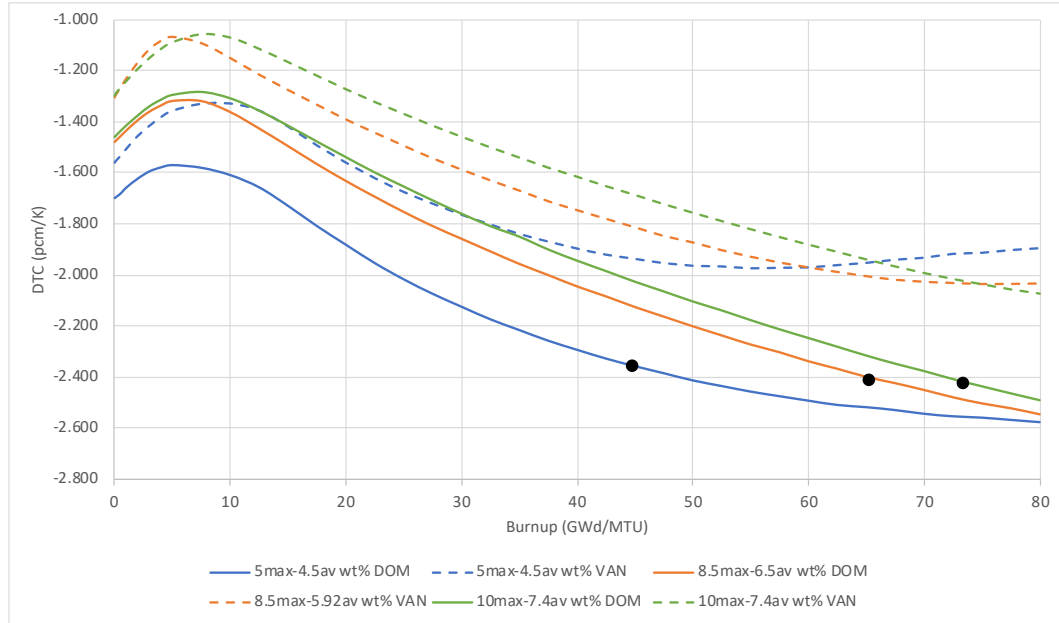


Figure 7. HFP DTC at 40% void fraction

The change in MVC with burnup and lattice enrichment is shown in Figure 8. In general, MVC becomes more positive with increased enrichment and more negative with increasing burnup. The effect of reduced moderator density on reactivity is less pronounced for VAN lattices compared DOM lattices. At BOC, a small, positive MVC with increasing enrichment beyond 7.4% average enrichment (10% max) seems possible, however it should be noted that the actual cores are not expected to have all fresh fuel of this high enrichment and gadolinia loadings are less than expected for these lattices due to incomplete enrichment map optimization. At EOC, the offsetting effects of burnup and enrichment means a fairly minor change, e.g., compare the MVC at 10% max enrichment lattice at 73 GWd/MTU (-118 pcm/%Void) to 5% max lattice at 45 GWd/MTU (-115 pcm/%Void).

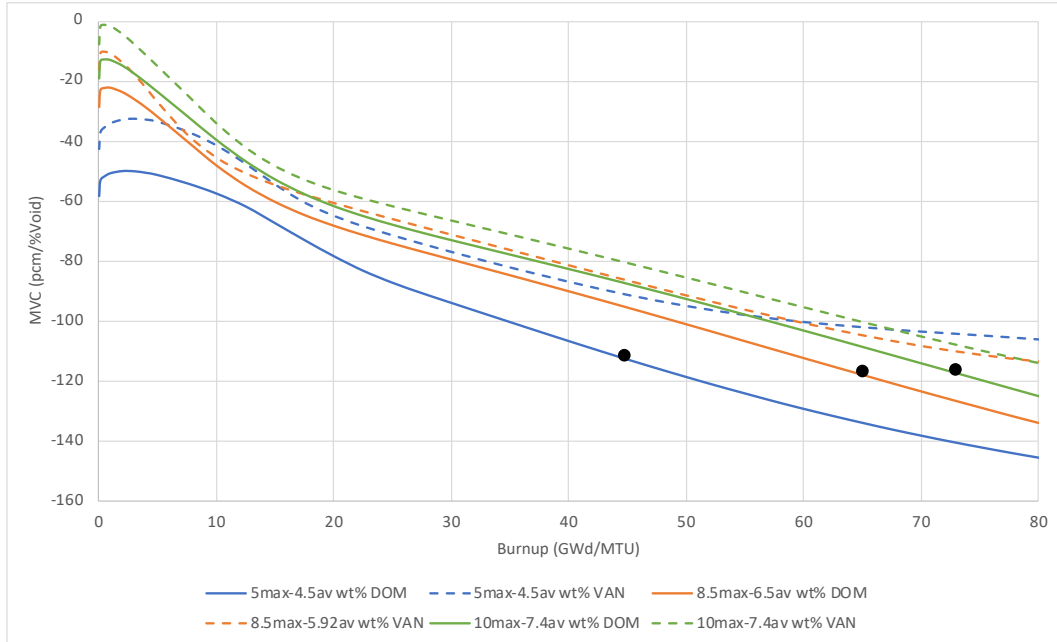


Figure 8. HFP MVC

A comparison of control blade rod worths for 5%max, 8.5%max and 10%max enriched lattices at 40% void fraction is provided in Figure 9. All lattices show the same increasing rod worth trend with burnup as the spectrum for all lattices become more thermal. However, as enrichment increases, the blade worth decreases due to hardening in spectrum with increasing enrichment. The CBW at BOC is decreased by 7000 pcm ($\sim 9\%$ / wt% ^{235}U) for the 10% maximum enrichment lattice compared to the reference lattice. This difference drops to 2000 pcm ($\sim 2\%$ / wt% ^{235}U) at EOC for the two lattices.

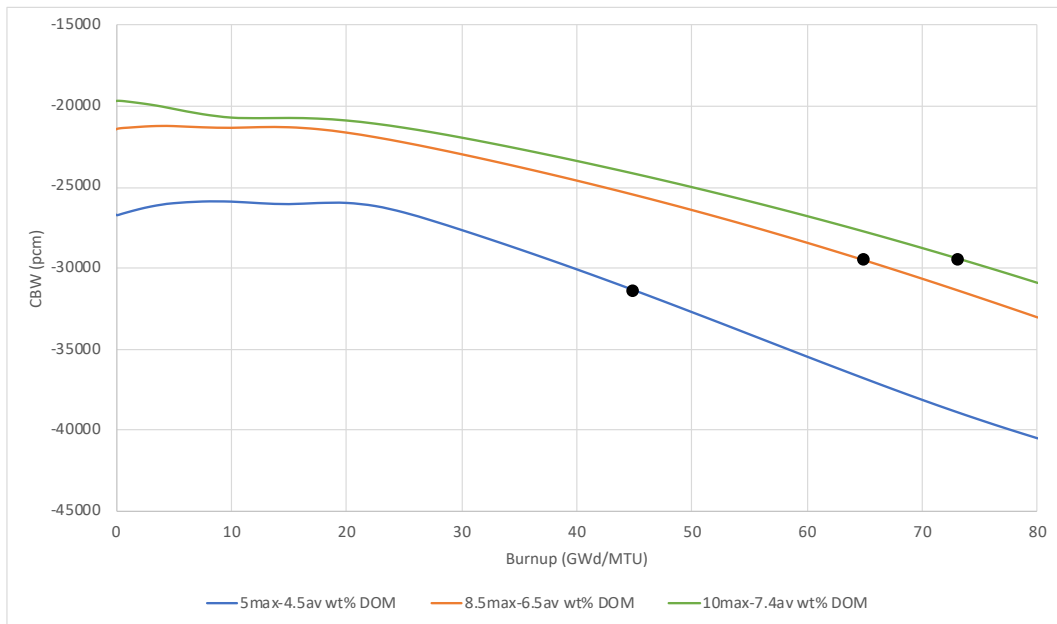


Figure 9. HFP CBW at 40% void fraction.

3.3 MACROSCOPIC CROSS SECTIONS

3.3.1 Lattice Cross Sections

Polaris lattice-averaged macroscopic absorption cross sections for thermal and fast neutrons are shown in Figure 10 and Figure 11, respectively. These figures show similar relationships among the different enrichments throughout the fuel utilization period. Both fast and thermal neutron absorption generally increases with increasing fuel enrichment for both lattices. The vanished fuel lattices consistently display less absorption cross section than the dominant region lattices. This behavior is attributed smaller fuel to moderator ratio. Regardless, both lattices show the same trend with burnup and enrichment.

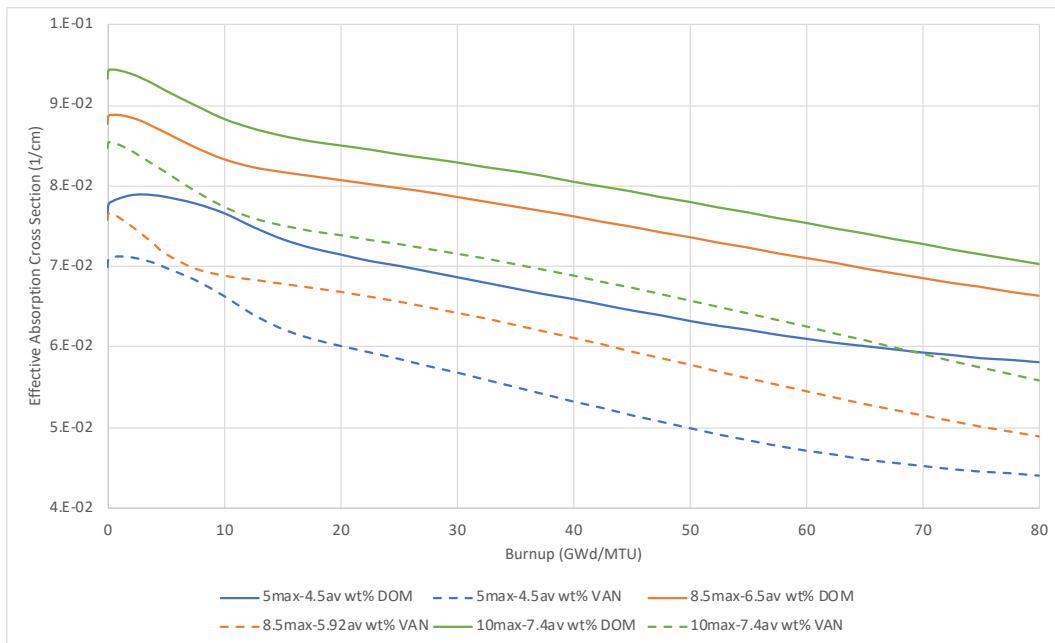


Figure 10. HFP macroscopic thermal absorption cross section

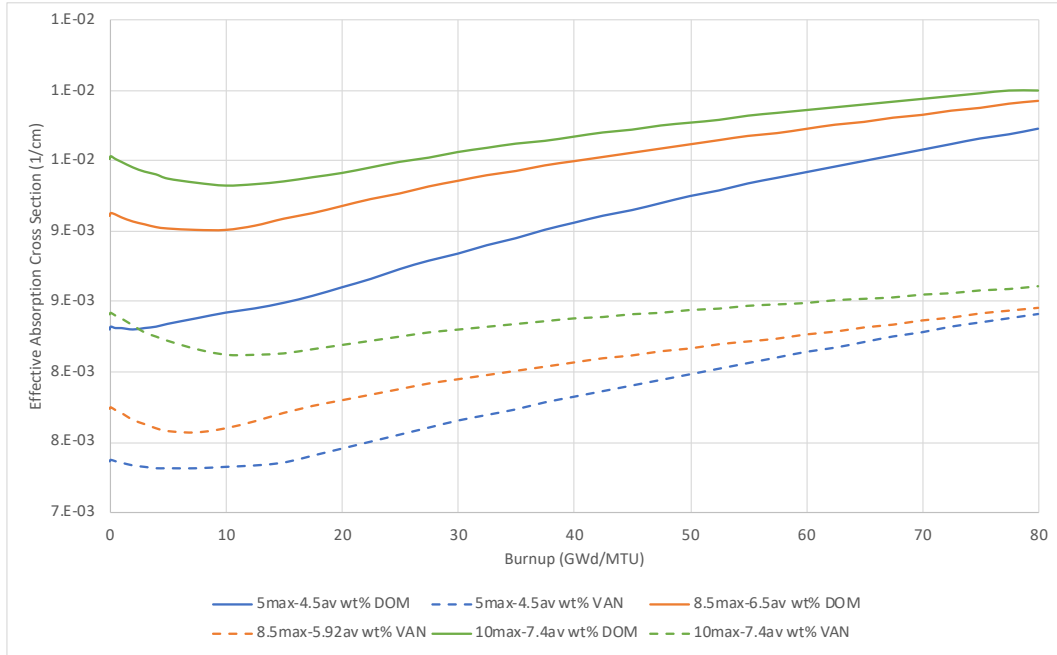


Figure 11. HFP macroscopic fast absorption cross section

Lattice-averaged macroscopic fission cross sections in Figure 12 and Figure 13 for thermal and fast neutrons, show a similar relationship among curves: increased thermal and fast fission cross sections with increased enrichment and decreased cross sections for vanished lattices. The thermal fission cross section initially increases as gadolinia is depleted because gadolinia shields out the uranium nuclei in the thermal region.

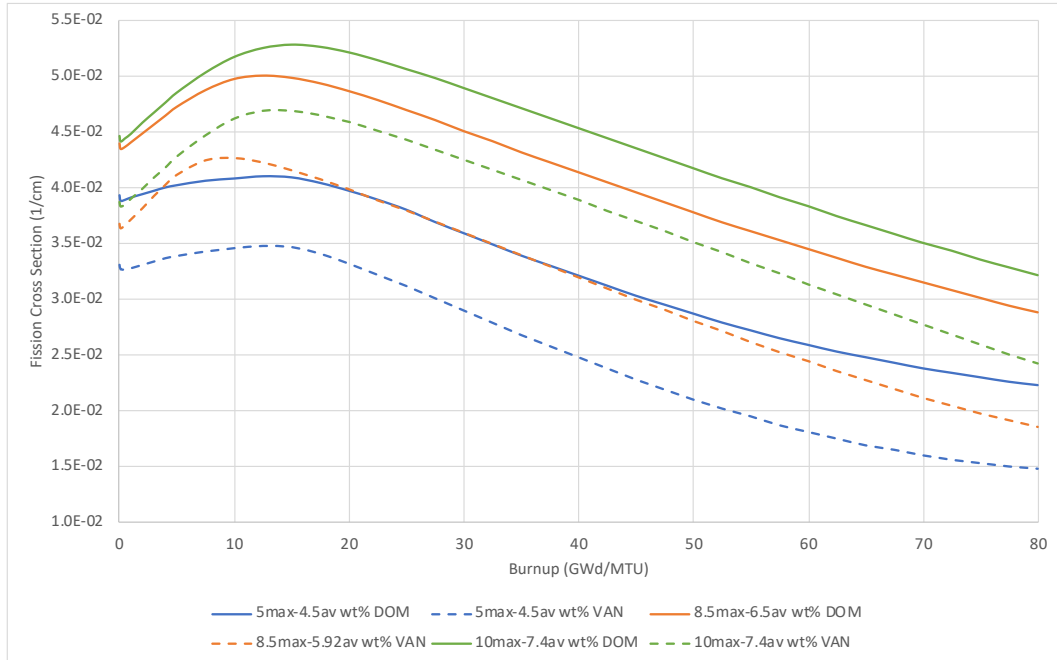


Figure 12. HFP macroscopic thermal fission cross section

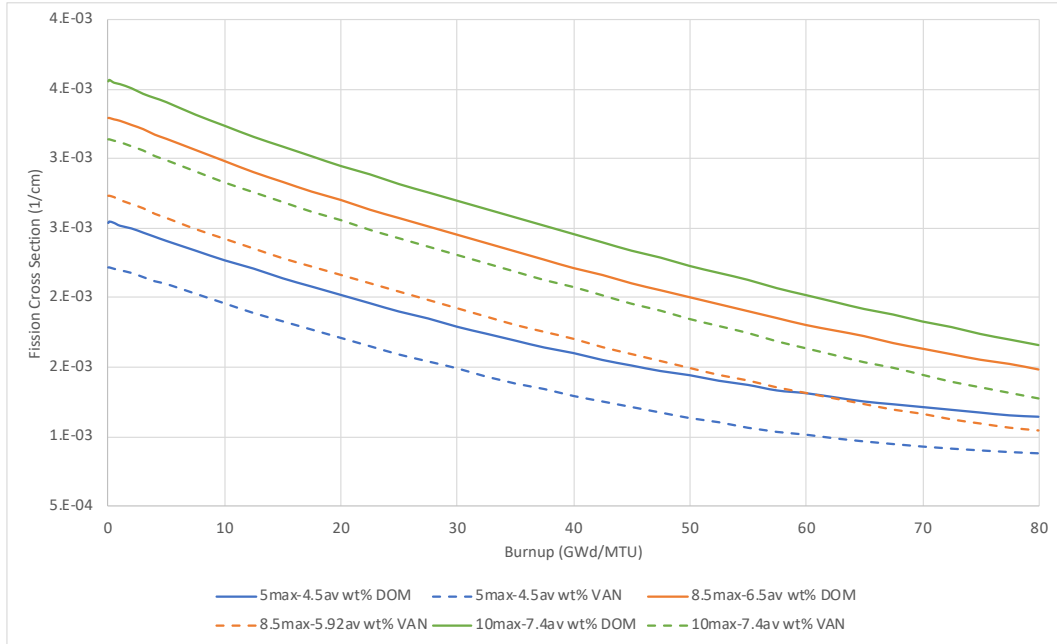


Figure 13. HFP macroscopic fast fission cross section

3.3.2 Kinetics Parameters

The total effective delayed neutron fraction (β -eff.) shown in Figure 14 increases with increasing enrichment, and it consistently decreases with increasing burnup. Among similar fuel burnups, DOM and VAN lattices for each lattice enrichment show similar delayed neutron fractions. The delayed neutron fraction is much lower for Pu fission ($\beta \sim 0.0021$ for ^{239}Pu) than for U fission ($\beta \sim 0.0064$ for ^{235}U). Higher enrichment depletion results in a lower fraction of fissions in Pu than the reference depletion at the same burnup, which results in a higher β -eff. Increased burnup in a higher enrichment core tends to offset the enrichment-only effect.

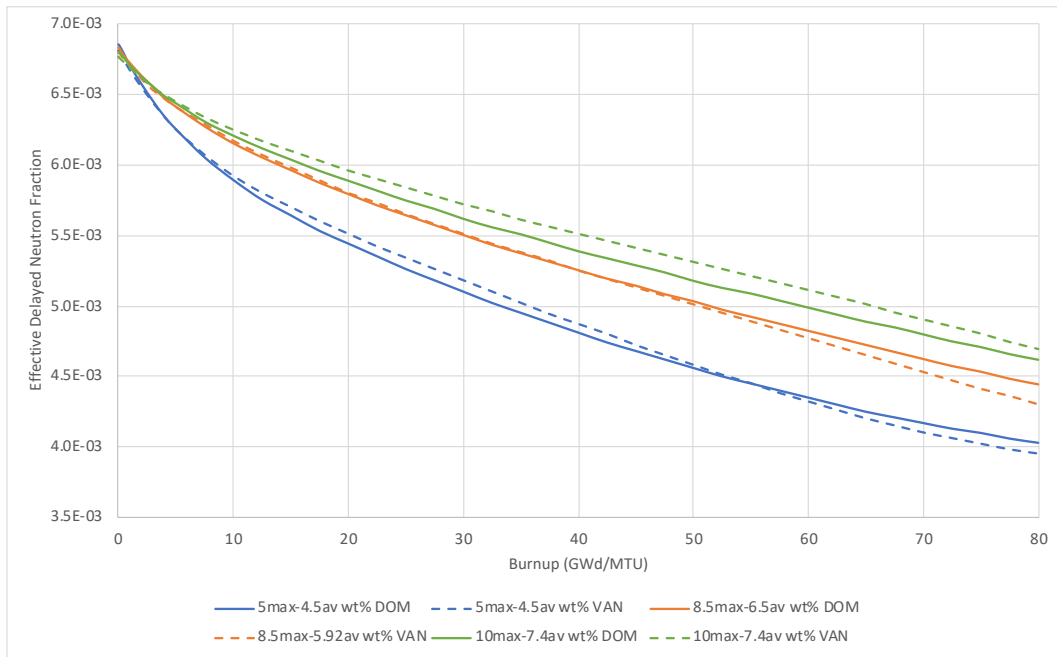


Figure 14. Effective delayed neutron fraction

4. SENSITIVITY AND UNCERTAINTY

4.1 NUCLIDE WORTH RANKING

One way to assess the similarity between the reference case and the high burnup and extended enrichment cases is to compare nuclide worth. Individual isotope worths can be computed using the simplified expression for lattice k_{inf} in Eq. 1.

$$k_{inf} = \frac{\sum_i n_i \nu \sigma_{f,i}}{\sum_i n_i \sigma_{a,i}} \quad (1)$$

where, n_i and σ_i are number densities and microscopic cross sections of the i^{th} isotope.

Using the lattice-average one-group microscopic cross sections and number densities from the Polaris depletion calculations and from ENDF/B VII.1 (only ν for ^{235}U , ^{236}U , ^{238}U , ^{239}Pu , and ^{241}Pu at 0.025 eV), the contribution of each isotope to k_{inf} can be calculated from total number of fission neutrons (numerator) and total number of absorbed neutrons (denominator) in Eq. 1. Since one-group cross sections are generated consistently with transport calculations, this simple equation for k_{inf} is accurate. Using Eq. 1, the worth of each nuclide can be ranked by ranking the change caused in k_{inf} for 1% change in concentration of each isotope.

Table 3 lists the top 25 nuclides by their respective worth. The change in reactivity worths for increased enrichment and increased burnups were calculated by comparing 10max -7.4av wt% lattice at 60 GWd/MTU and 80 GWd/MTU with the reference 5max-4.5av wt% lattice at 60 GWd/MTU for nominal, 40% void fraction. The calculated nuclide rankings for high burnup and extended enrichment are consistent with the nuclide rankings in the PWR report [15]. The top 25 nuclides account more than 94% of the total reactivity at each depletion step.

The nuclide worth ranking table provides information about the source of reactivity changes for changes in enrichment and burnup. For most isotopes the effects of enrichment and burnup are counteracting in terms of reactivity worth, with no change in sign for the worth. The findings are consistent with those throughout this report that further increases in enrichment and burnup are typically counteracting, and the behaviors are smooth extensions of expected behavior at typical enrichments and burnups.

Table 3. Nuclide worth (Δk) at 40% void fraction

Isotope	Worths (Δk) for 1% increase in isotope's composition			Percent change in worth from enrichment increase	Percent change in worth from burnup increase	Percent change in worth from enrichment and burnup increase
	5max-4.5av% 60 GWd/MTU	10max-7.4av% 60 GWd/MTU	10max-7.4av% 80 GWd/MTU			
²³⁹ Pu	2.70E-03	1.80E-03	2.20E-03	-33%	22%	-19%
²³⁸ U	-1.90E-03	-2.10E-03	-1.90E-03	11%	-10%	0%
²³⁵ U	9.20E-04	2.40E-03	1.60E-03	161%	-33%	74%
²⁴¹ Pu	1.10E-03	6.00E-04	8.70E-04	-45%	45%	-21%
²⁴⁰ Pu	-5.60E-04	-5.10E-04	-5.90E-04	-9%	16%	5%
¹ H	-5.30E-04	-5.00E-04	-4.20E-04	-6%	-16%	-21%
¹⁴³ Nd	-1.20E-04	-1.40E-04	-1.30E-04	17%	-7%	8%
¹⁰³ Rh	-1.10E-04	-1.10E-04	-1.20E-04	0%	9%	9%
¹³⁵ Xe	-1.40E-04	-1.90E-04	-1.20E-04	36%	-37%	-14%
²³⁶ U	-6.70E-05	-1.00E-04	-1.10E-04	49%	10%	64%
¹³³ Cs	-6.60E-05	-7.00E-05	-8.10E-05	6%	16%	23%
¹³¹ Xe	-6.30E-05	-7.00E-05	-7.40E-05	11%	6%	17%
²³⁷ Np	-5.50E-05	-5.50E-05	-6.60E-05	0%	20%	20%
⁹¹ Zr	-7.00E-05	-7.30E-05	-6.60E-05	4%	-10%	-6%
²⁴² Pu	-5.20E-05	-3.30E-05	-6.40E-05	-37%	94%	23%
⁹⁹ Tc	-5.00E-05	-5.30E-05	-6.20E-05	6%	17%	24%
¹⁵² Sm	-4.40E-05	-4.60E-05	-4.90E-05	5%	7%	11%
¹⁵³ Eu	-4.30E-05	-3.80E-05	-4.60E-05	-12%	21%	7%
¹⁴⁹ Sm	-4.90E-05	-7.40E-05	-4.40E-05	51%	-41%	-10%
¹⁵⁵ Eu	-4.10E-05	-3.20E-05	-4.30E-05	-22%	34%	5%
¹⁴⁵ Nd	-3.40E-05	-3.60E-05	-4.10E-05	6%	14%	21%
¹⁵⁴ Eu	-4.10E-05	-3.40E-05	-4.00E-05	-17%	18%	-2%
¹⁵¹ Sm	-4.10E-05	-4.90E-05	-3.60E-05	20%	-27%	-12%
¹⁴⁷ Pm	-3.20E-05	-4.00E-05	-3.50E-05	25%	-13%	9%
²⁴³ Am	-2.90E-05	-1.50E-05	-3.30E-05	-48%	120%	14%

4.2 SAMPLER/POLARIS DEPLETION UNCERTAINTY

Sampler is a sequence in SCALE code suit for statistical uncertainty analysis with SCALE sequences. Sampler was used with Polaris to propagate nuclear data uncertainties (cross sections, fission yields, decay constants) through depletion calculations and calculate the uncertainties in isotope inventories.

The reference 5max-4.5av wt% lattice was depleted 60 GWd/MTU and the variation in inventories of major isotopes were calculated. Similarly, relative variations in isotope inventories (Eq. 2) from depletion of 10 max-7.4 av wt% lattice at 60 GWd/MTU and 80 GWd/MTU were also calculated. All lattices were assumed to be at 40% void fraction.

Similar comparisons as in nuclide worth calculations were done in Table 4 between the three cases to show any effect of enrichment increase and extended burnup on isotope uncertainties. The difference in relative uncertainties between the cases (Eq. 3) are also shown in Table 4. In general, similar relative uncertainties are observed between the reference case, increased enrichment and increased enrichment and burnup cases. Except ^{155}Eu , all relative uncertainties in isotopic inventory either does not increase significantly or decrease with increased burnup and enrichment. The relative uncertainty for ^{155}Eu was doubled for the both 10max-7.4av wt% lattice cases compared to the reference case. However, further investigation shows that although absolute uncertainty is reduced, because of large drop (1/5) in ^{155}Eu content with increased enrichment and burnup, the relative uncertainty is larger for the two cases.

$$\sigma_{rel} = \sigma/w, \quad (2)$$

where σ is standard deviation and w is the isotope weight

$$\Delta\sigma_{rel} = \sigma_{rel} - \sigma_{rel}^{reference} \quad (3)$$

Uncertainties in k_{inf} due to nuclear data uncertainties are also plotted in Figure 15 for 5max-4.5av wt% and 10 max-7.4 av wt% DOM lattices at 40% void fraction. The standard deviation in k_{inf} was approximately 550 pcm for depletion of both lattices. The uncertainty for the reference lattice starts increase after the expected life time of the lattice (~55 GWd/MTU). No appreciable increase in uncertainty was observed for higher enrichments or burnups.

Table 4. Predictions and relative standard deviations in isotope inventories

Isotope	5max-4.5av wt%, 60 GWd/MTU		10max-7.4 wt% max, 60 GWd/MTU		10max-7.4 wt% max, 80 GWd/MTU		Enrichment increase	Enrichment and Burnup increase
	Mass (g)	σ_{rel}	Mass (g)	σ_{rel}	Mass (g)	σ_{rel}	$\Delta\sigma_{rel}$	$\Delta\sigma_{rel}$
²³⁹ Pu	1.98E-01	2.1%	1.33E-01	1.7%	1.37E-01	2.1%	-0.4%	0.0%
²³⁸ U	4.22E+01	0.0%	1.35E+01	0.0%	1.33E+01	0.0%	0.0%	0.0%
²³⁵ U	8.05E-02	3.6%	7.27E-01	0.6%	5.05E-01	1.2%	-3.0%	-2.4%
²⁴¹ Pu	6.70E-02	2.3%	2.20E-02	1.3%	3.04E-02	1.4%	-1.0%	-0.8%
²⁴⁰ Pu	1.38E-01	2.3%	3.15E-02	1.8%	4.48E-02	1.9%	-0.6%	-0.4%
¹⁴³ Nd	7.04E-02	2.8%	4.06E-02	1.5%	5.00E-02	2.0%	-1.3%	-0.7%
¹⁰³ Rh	7.21E-02	2.1%	2.29E-02	1.4%	2.87E-02	1.8%	-0.7%	-0.4%
¹³⁵ Xe	8.94E-06	4.0%	9.02E-06	1.6%	8.37E-06	2.0%	-2.4%	-2.0%
²³⁶ U	2.48E-01	1.3%	1.81E-01	1.6%	2.18E-01	1.6%	0.3%	0.3%
¹³³ Cs	1.58E-01	1.1%	5.12E-02	0.7%	6.62E-02	0.9%	-0.4%	-0.2%
¹³¹ Xe	5.27E-02	6.5%	1.92E-02	4.3%	2.34E-02	5.7%	-2.2%	-0.7%
²³⁷ Np	3.19E-02	4.2%	1.42E-02	3.8%	2.02E-02	3.6%	-0.5%	-0.6%
⁹¹ Zr	1.18E-01	0.4%	4.26E-02	0.4%	5.62E-02	0.5%	0.0%	0.1%
²⁴² Pu	7.31E-02	3.9%	4.13E-03	4.0%	8.81E-03	4.4%	0.1%	0.5%
⁹⁹ Tc	1.54E-01	0.9%	4.89E-02	0.5%	6.37E-02	0.6%	-0.4%	-0.3%
¹⁵² Sm	1.23E-02	2.8%	3.33E-03	2.5%	4.01E-03	3.1%	-0.3%	0.3%
¹⁵³ Eu	1.51E-02	3.6%	3.71E-03	2.8%	5.21E-03	3.5%	-0.8%	-0.1%
¹⁴⁹ Sm	1.04E-04	3.2%	1.64E-04	2.6%	1.38E-04	3.3%	-0.6%	0.1%
¹⁵⁵ Eu	1.29E-03	18.3%	2.67E-04	31.2%	4.49E-04	30.3%	12.9%	12.1%
¹⁴⁵ Nd	8.43E-02	2.0%	2.92E-02	1.3%	3.75E-02	1.8%	-0.7%	-0.2%
¹⁵⁴ Eu	3.12E-03	9.2%	1.03E-03	6.9%	1.61E-03	7.8%	-2.2%	-1.4%
¹⁵¹ Sm	8.35E-04	3.6%	7.68E-04	3.4%	7.71E-04	4.1%	-0.2%	0.4%
¹⁴⁷ Pm	1.30E-02	2.8%	6.02E-03	1.9%	6.18E-03	2.2%	-0.9%	-0.6%
²⁴³ Am	1.74E-02	7.8%	7.50E-04	10.0%	1.98E-03	9.2%	2.2%	1.4%
⁹⁵ Mo	1.42E-01	0.6%	4.70E-02	0.6%	6.24E-02	0.7%	0.0%	0.1%
¹⁰¹ Ru	1.56E-01	0.9%	4.42E-02	0.7%	5.91E-02	0.9%	-0.2%	-0.1%
²³⁸ Pu	2.38E-02	5.6%	5.48E-03	4.7%	1.13E-02	4.2%	-1.0%	-1.4%
¹⁰⁹ Ag	1.62E-02	9.0%	3.09E+01	0.0%	3.09E+01	0.0%	-9.0%	-9.0%
²⁴¹ Am	2.59E-03	5.8%	2.20E-03	9.6%	3.53E-03	9.1%	3.8%	3.2%
¹⁵⁶ Gd	2.36E-02	2.6%	1.57E-03	2.6%	2.45E-03	3.5%	0.0%	0.9%
¹⁴⁷ Sm	1.24E-02	2.7%	1.75E-03	5.4%	3.85E-03	4.8%	2.6%	2.1%
¹⁵⁰ Sm	3.69E-02	1.7%	5.56E-03	1.8%	7.13E-03	2.3%	0.1%	0.6%
¹⁵⁷ Gd	9.61E-06	8.5%	1.02E-02	1.4%	1.39E-02	1.8%	-7.1%	-6.7%

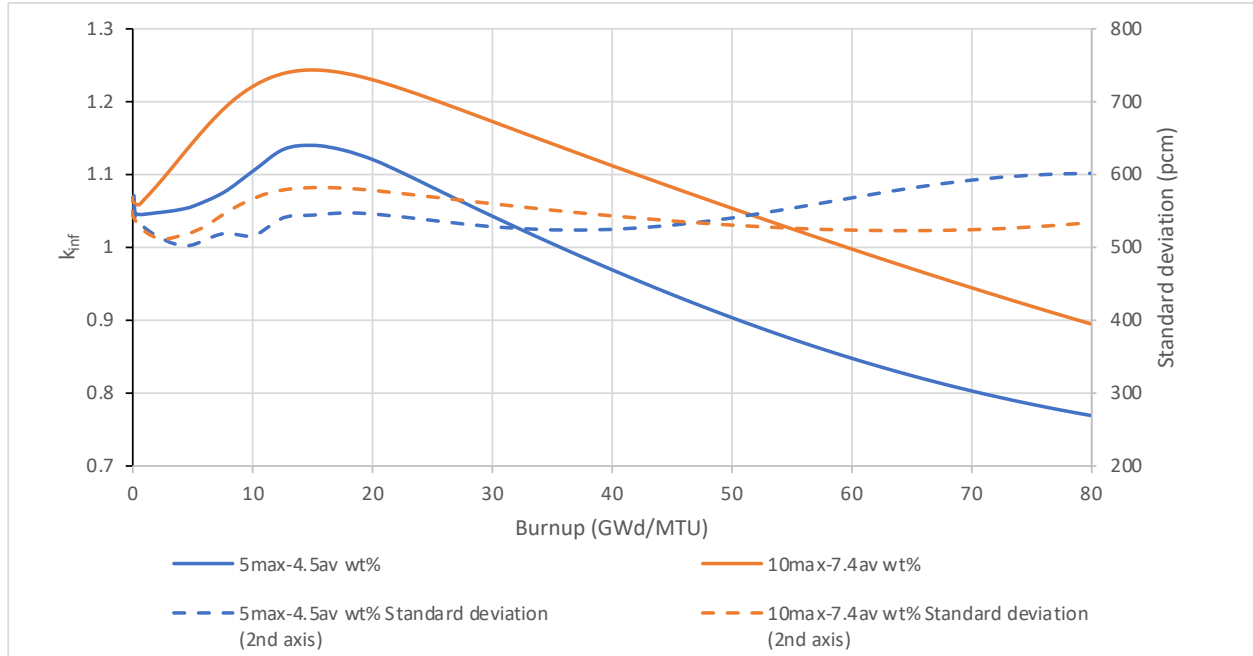


Figure 15. Uncertainty in k_{inf} at 40 % void fraction due to nuclear data uncertainties.

5. ISOTOPIC INVENTORY

The interactions between several factors and isotopic compositions are evaluated here for a total of 16 cases evaluated. All combinations of the following factors (independent variables) and factor levels (discrete values of each variable) were evaluated.

- Enrichment: 5% maximum enrichment, 10% maximum pin enrichment
- Burnup: 60 GWd/MTU, 80 GWd/MTU
- Lattice design: DOM, VAN lattice
- Void: 10% (DOM lattice only), 40%, 70% (VAN lattice only)

Five decay times were evaluated for each case in this section. The reasons for selections of the various time points are listed below:

- 0 seconds: provides a reference value for other time points
- 30 min: captures possible impacts of isotopics on core cooling events (e.g., LOCA)
- 5 days: captures possible impacts of isotopics during refueling outage/discharge
- 25 days: captures possible impacts of isotopics at the end of refueling outage/discharge
- 500 days: captures possible impacts of isotopics on early long-term storage.

Isotopes are ranked by the root mean squared (RMS) value of the isotope's percent total contribution to some quantity such as activity or decay heat given by

$$RMS_i = \sqrt{\sum_n \left(\frac{a_{in} - b_{in}}{b_n} \right)^2}, \quad (4)$$

where a_{in} and b_{in} are the values for isotope i being compared at time point n , with b_n being the total of all isotopes at time point n . The timepoint of 0 seconds of decay is not included in calculating any of the rankings. The RMS ranking presented in this section provides a measure of cumulative relative impact of an isotope to the quantity of interest over the analyzed decay period.

5.1 DECAY HEAT TRENDS

Figure 16 and Figure 17 show decay heat vs time for the burnup-enrichment combinations evaluated that bounded decay heat at 1000 days. The highest decay heat case was the VAN lattice with 5max-4.5av wt% enrichment operating at 70% void fraction and discharged at 80 GWD/MTU burnup. The lowest decay heat was the DOM lattice with 10max-7.4av wt% enrichment operating at 40% void fraction and discharged at 60 GWd/MTU burnup. All cases follow the similar decay heat curve with time after discharge. Based on discharge burnup, the decay heat curves split into two groups after 100 days of cooling. Decay heat as a fraction of full core power is also shown in Figure 18. Increased enrichment and burnup slightly increase fraction of decay heat, however, the difference is negligible and all cases start around 6% and follows the same curve (note that the decay heat assumes a sudden, complete shutdown). The relative difference in decay heat between the reference case and several representative cases (Eq. 5) with variations in void, burnup, enrichment and lattice types are shown in Figure 19.

Although, up to 60% relative differences due to small decay heat values are observed for some cases, the absolute differences shown in Figure 20 are negligible.

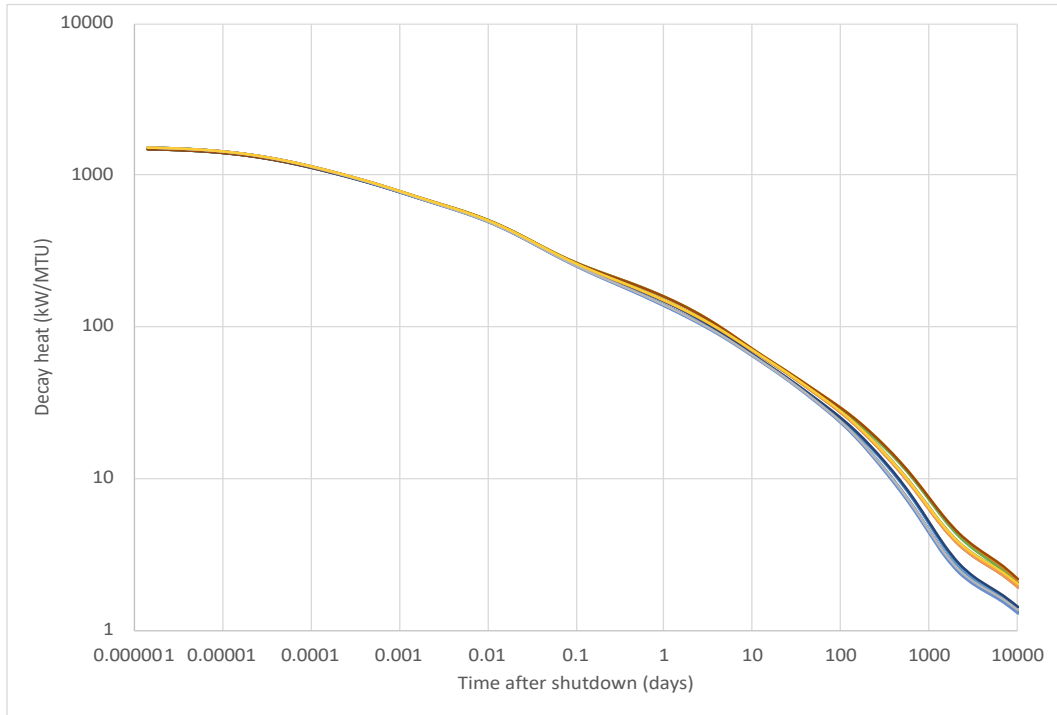


Figure 16. Decay heat as a function of cooling time for all cases

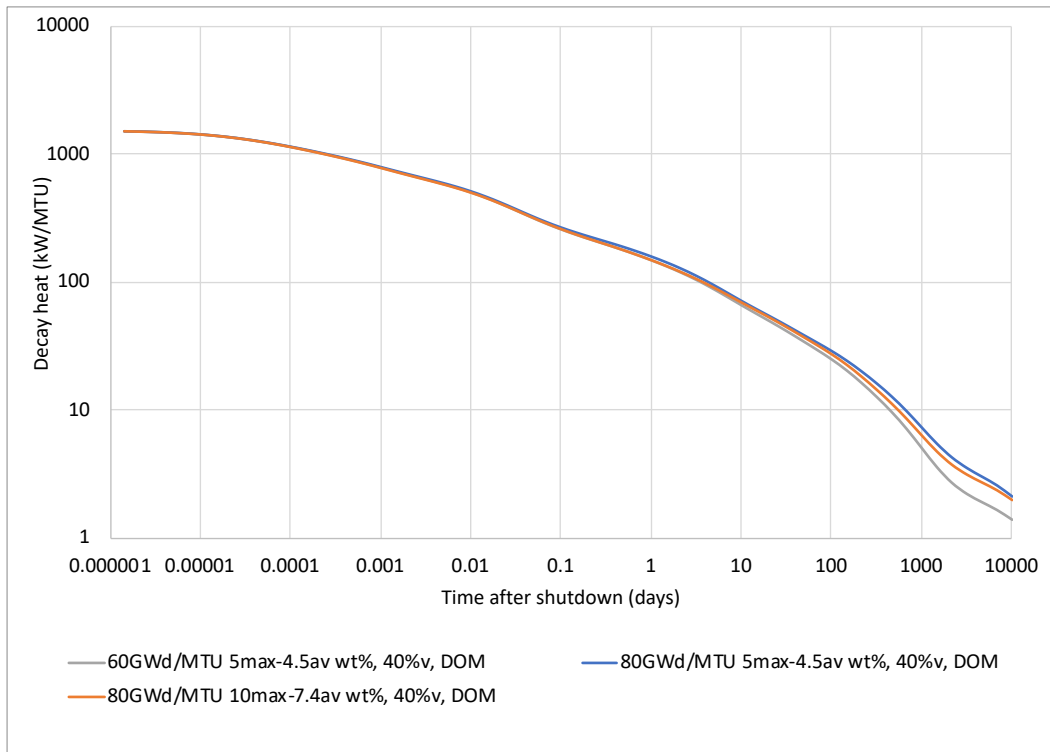


Figure 17. Decay heat as a function of cooling time (effect of enrichment and burnup)

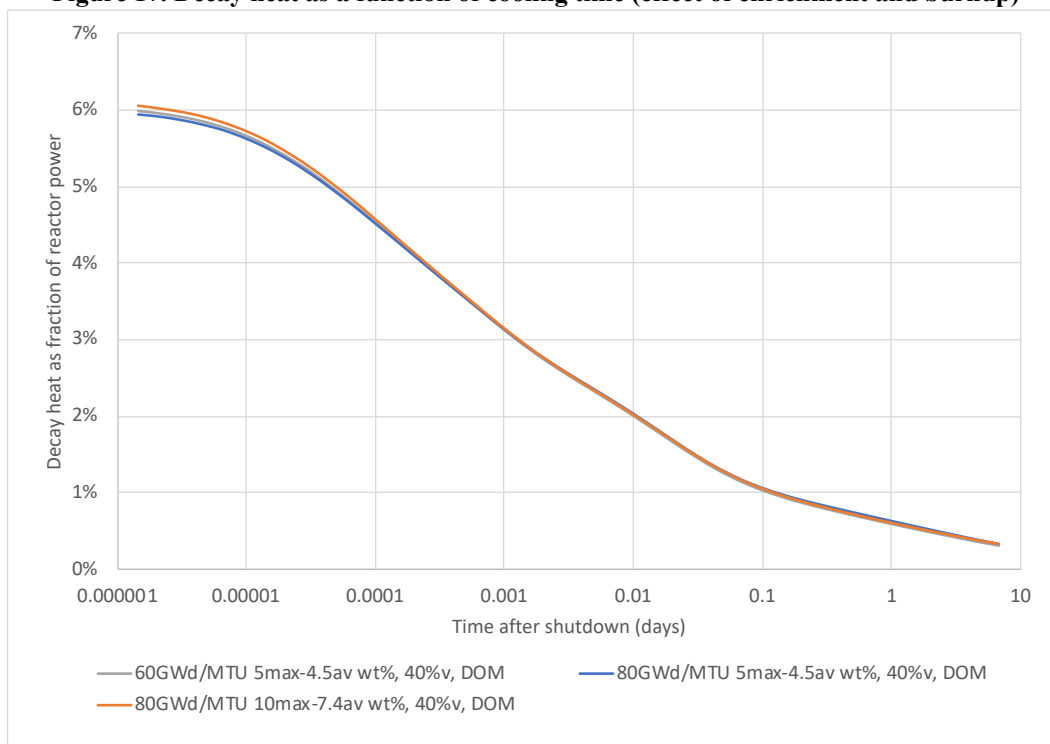


Figure 18. Decay heats as a fraction of full power vs cooling time.

$$Q_{rel}(t) = \frac{Q(t)}{Q_{ref}(t)} - 1 \quad (5)$$

where $Q(t)$ is the decay heat as a function of time and $Q_{ref}(t)$ is the decay heat for the reference 5max-4.5av wt% 60 GWd/MTU 40% void case.

In summary, shortly after reactor shutdown, operating power influences decay heat more than burnup and enrichment. As the short-lived fission products decay away, longer lived fission and activation products begin to contribute much more to decay heat, and decay heat begins to depend more on burnup and enrichment. Notably, no single isotope changed decay heat by more than 12% in any comparison evaluated below. Decay heat generally increased at later time points, when enrichment decreased, or burnup increased. This is consistent with the behavior of existing nuclear fuel.

Table 5 through Table 7 show the impact of HBU and EE on isotopics decay heats. Table 5 shows the impact on total decay heat for each isotope when enrichment increases from 5max-4.5av wt% to 10max-7.4av wt%. Table 6 shows the impact on total decay heat for each isotope when burnup increases from 60 to 80 GWd/MTU. Finally, Table 7 shows the combined impact of increasing both burnup and enrichment.

The values in Table 5 through Table 7 are the difference in decay heat for the isotope expressed as a percentage of total decay heat of the reference case. The relative difference in contribution of each isotope to the total heat production ($Q_{rel,i}$) is calculated from Eq. 6 and presented color coded, with blue indicating a decreasing decay heat from baseline, and red indicating an increasing decay heat from baseline.

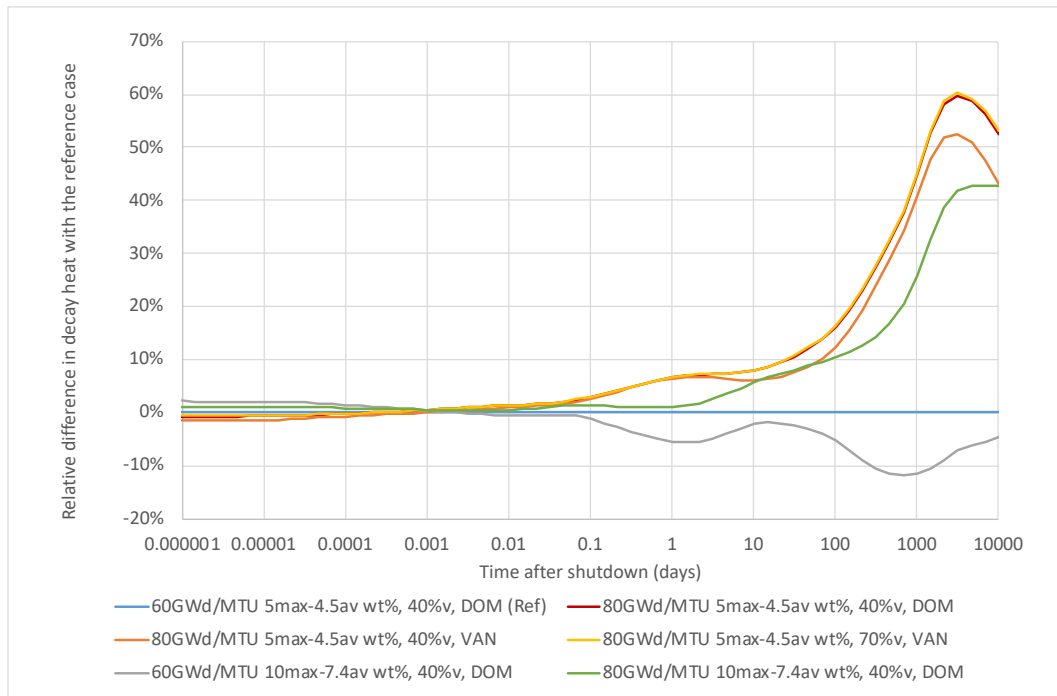


Figure 19. Decay heat relative to 60 GWd/MTU 5max-4.5av 40% DOM case

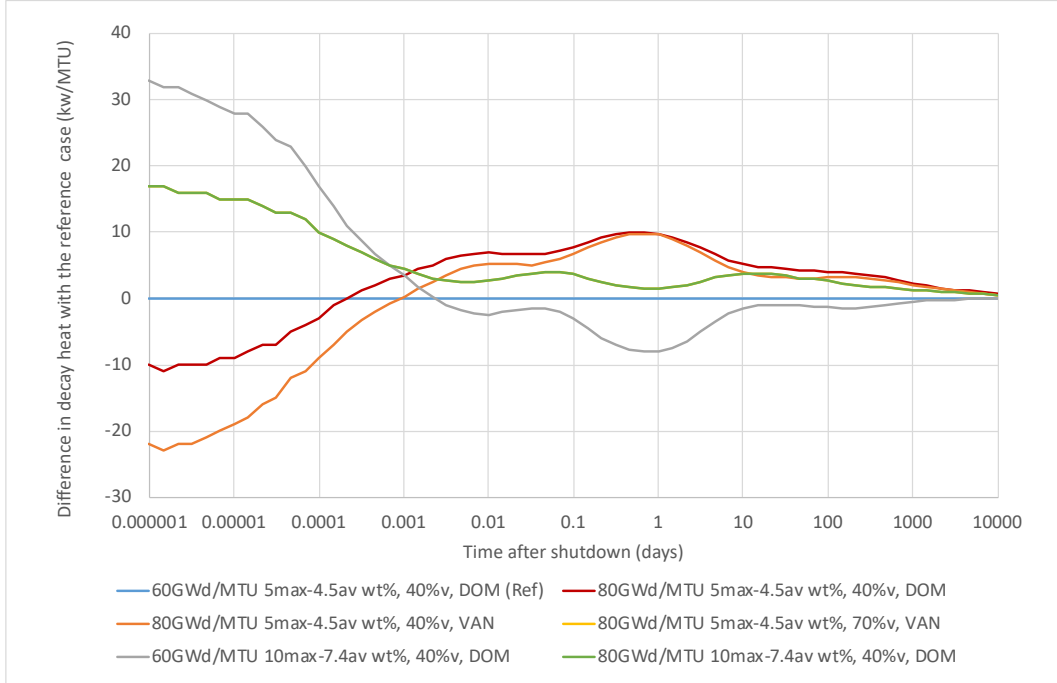


Figure 20. Decay heat difference with to 60 GWd/MTU 5max-4.5av 40% DOM case

$$Q_{rel,i} = \frac{Q_i - Q_{ref,i}}{Q_{ref}} \quad (6)$$

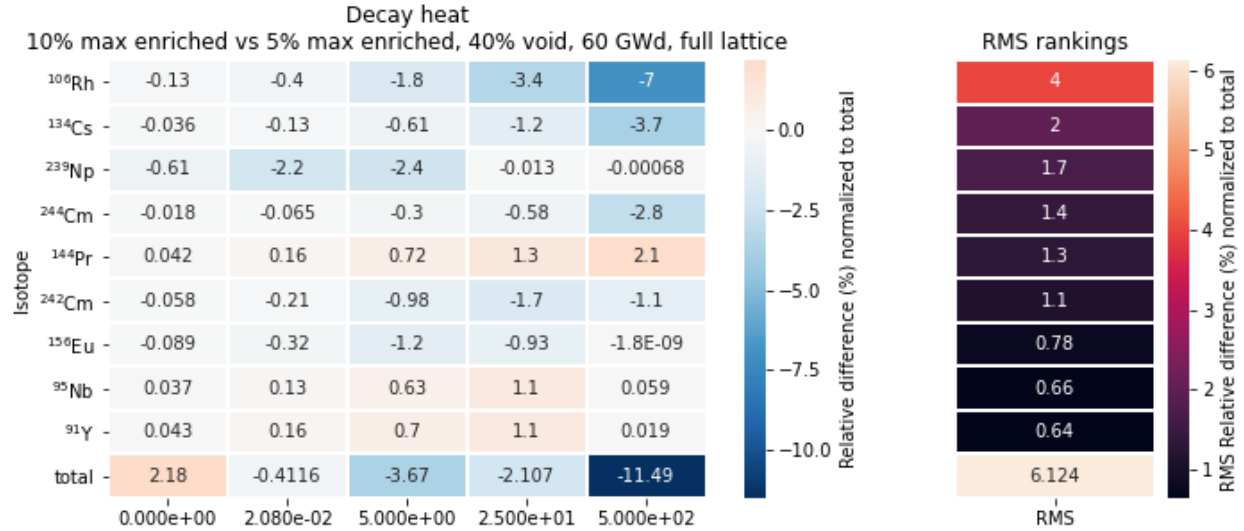
where Q_i is the decay heat for isotope i for HBU or EE, $Q_{ref,i}$ is the decay heat for isotope i for the reference case, Q_{ref} is the total decay heat for the reference case.

The top 10 isotopes are shown according to the RMS ranking introduced in Eq. (4). The RMS rankings in this report always exclude the time point 0 s after discharge. The row labeled *Total* is the total difference for the two cases reported by SCALE. Note that shortly after shutdown, many more isotopes than those listed contribute to decay heat, so the difference caused by the top 10 contributors by RMS ranking does not coincide with the total. At longer decay times, as short-lived fission products decay away, fewer isotopes are responsible for the decay heat, so the top 10 isotopes by RMS ranking correctly account for the majority of differences. For example, at 500 days with increased enrichment only (Table 5), the difference is driven by six isotopes— ^{106}Rh , ^{134}Cs , ^{144}Pr , ^{244}Cm , ^{242}Cm , and ^{90}Y —and the top 15 isotopes across all times (subtotal) coincide with the total of -10% change.

Increasing initial maximum pin enrichment from 5 to 10 wt% at 60 GWd/MTU (Table 5) leads to a reduction in the following isotopes: ^{106}Rh , ^{134}Cs , ^{239}Np , ^{244}Cm , and ^{242}Cm . These isotopes are neutron absorption products, or they tend to result from ^{239}Pu fission, which is in turn an indirect product of neutron absorption. ^{106}Rh has a ^{239}Pu cumulative fission yield of 4.1E-2. This

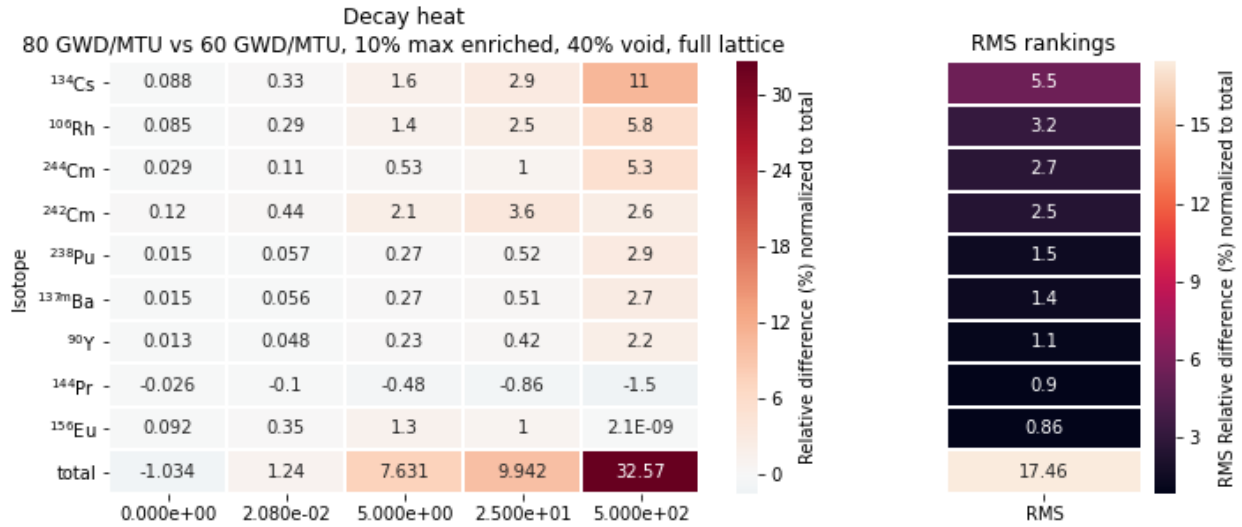
is an order of magnitude larger than its ^{235}U yield of $4.1\text{E-}3$, according to the Joint Evaluated Fission and Fusion File (JEFF) 3.3, as accessed through the International Atomic Energy Agency (IAEA) Live Chart of Nuclides. Note that ^{134}Cs results largely from neutron activation of ^{133}Cs which is mainly a stable fission product of ^{239}Pu fission (25x larger direct yield compared to ^{235}U fission); therefore, ^{134}Cs is an indicator for ^{239}Pu amount as well as magnitude of flux.

Table 5. Contributions of each isotope to total percent change in decay heat from enrichment increase



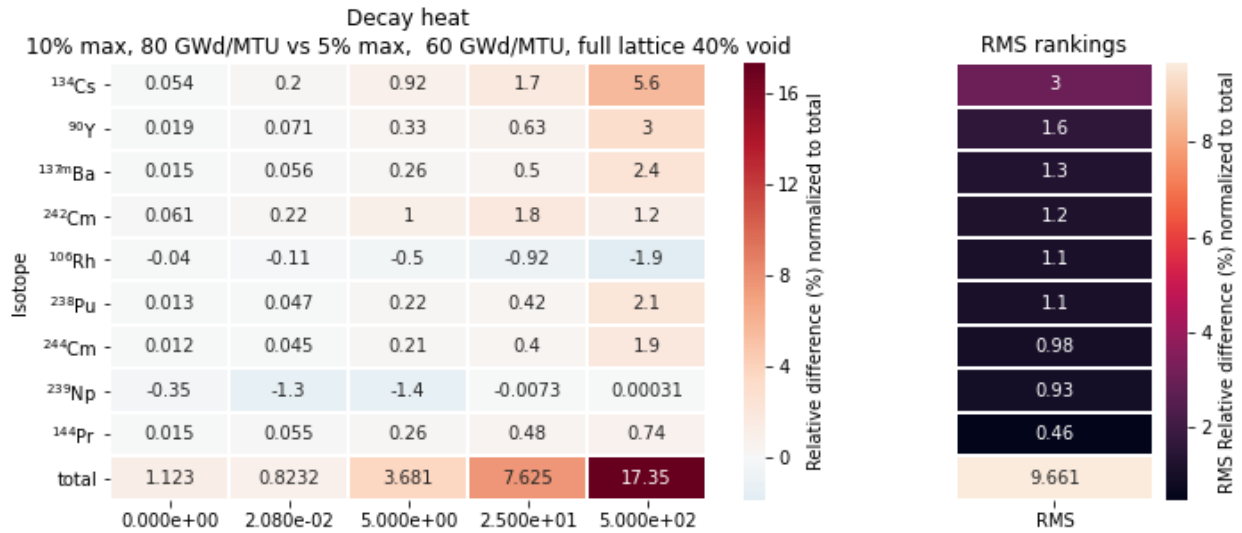
Effect of increasing burnup from the 60 GWd/MTU to 80 GWd/MTU for 10max-7.4av wt% enrichment case is shown in Table 6. In this case, both fission products and products of neutron absorption increase. The largest relative increases include isotopes created through neutron absorption: ^{244}Cm , and ^{242}Cm , or isotopes with ^{239}Pu cumulative fission yields that vastly exceed their ^{235}U yields. Notably, however, ^{239}Np is affected less by the burnup increase (due to 2.3 days half-life) than the enrichment increase discussed in the paragraph above. Increases in fission product decay heats are also notable with the burnup increase, specifically ^{90}Y and $^{137\text{m}}\text{Ba}$. The activity of $^{137\text{m}}\text{Ba}$ is proportional to burnup due to identical fission yields for ^{235}U and ^{239}Pu .

Table 6. Contributions of each isotope to total percent change in decay heat from burnup increase



The effect of increasing both enrichment and burnup from the 60 GWd/MTU 5max-4.5av wt% case to the 80 GWd/MTU 10max-7.4av wt% enrichment case is shown in Table 7. Almost all isotopes increase in abundance when both enrichment and burnup are increased, with the exception of ²³⁹Np and ¹⁰⁶Rh. The decay heat increases in fission products ⁹⁰Y and ^{137m}Ba.

Table 7. Contributions of each isotope to total percent change in decay heat from combined enrichment and burnup increase



¹⁴⁴Pr is generally a high-ranking decay heat contributor, behaving opposite of many of the other isotopes in the comparison charts. This is because it is preferentially produced by ²³⁵U fission and not ²³⁹Pu fission, so it increases with enrichment and can decrease with burnup, unlike many other isotopes. ¹⁴⁴Pr increases in abundance compared to 60 GWd/MTU 5max-4.5av wt% reference. It is the short-lived ($T_{1/2}=17$ min) progeny of ¹⁴⁴Ce ($T_{1/2}=284$ d). ¹⁴⁴Ce and ¹⁴⁴Pr are both progeny of ¹⁴⁴La. ¹⁴⁴La and its parents in the 144 amu beta decay series all have half-lives

on the order of tens of seconds or less. ^{144}La has a ^{239}Pu cumulative fission yield of 3.59% and a ^{235}U cumulative fission yield of 5.44%. ^{144}Pr cumulative fission yields are close to the ^{144}La values, with a ^{239}Pu fission yield of 3.75% and a ^{235}U fission yield of 5.47%. This indicates ^{144}La abundance in-core and generally reflects when the ^{144}Pr is produced. The plotting of the ^{144}La abundance shown in Figure 21 reflects the observations above. ^{144}Pr tracks with its parent ^{144}Ce . ^{144}La decreases as the proportion of the power produced by ^{235}U decreases.

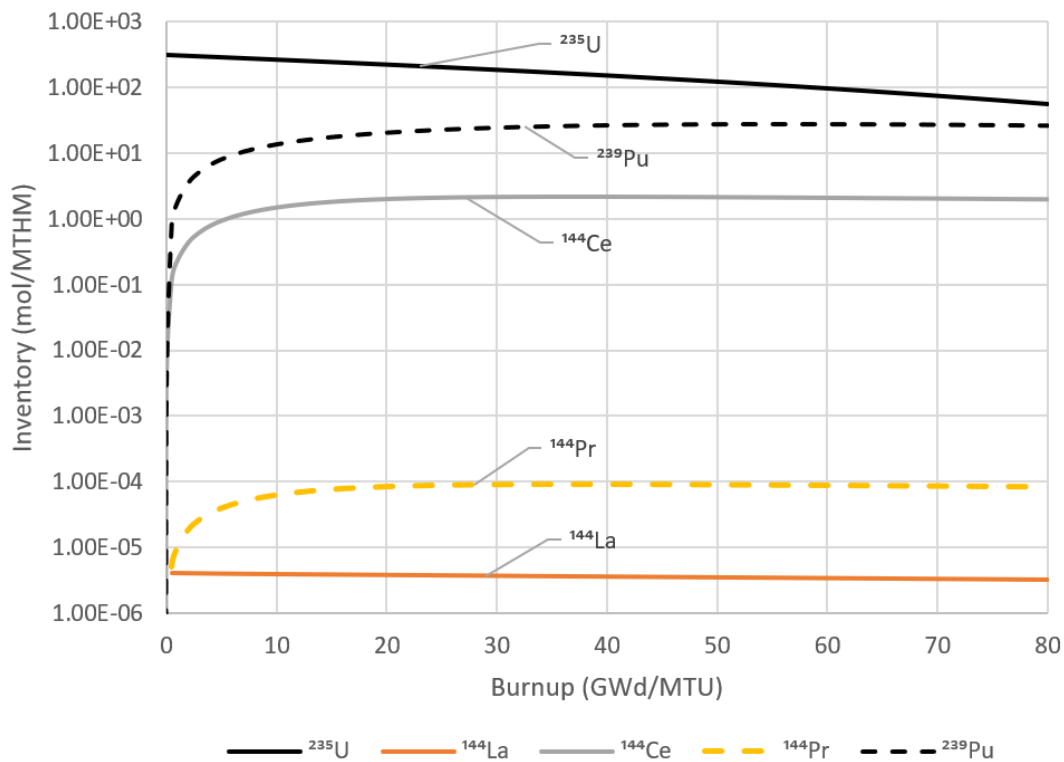


Figure 21. In-core abundances of ^{144}Pr beta chain isotopes for 10max-7.4av wt% initial enrichment.

Table 8 through Table 10 show the isotopes with the largest absolute changes for the same cases as Table 5 through Table 7. Decay heats for the isotopes are much higher shortly after discharge, and hundreds of isotopes contribute to total. Therefore, even the largest contributions look small compared to the total in the tables. Again, note that RMS values in this report always exclude the values at 0 seconds of cooling time.

Table 8. Difference in isotopic decay heats resulting from enrichment increase at various cooling times

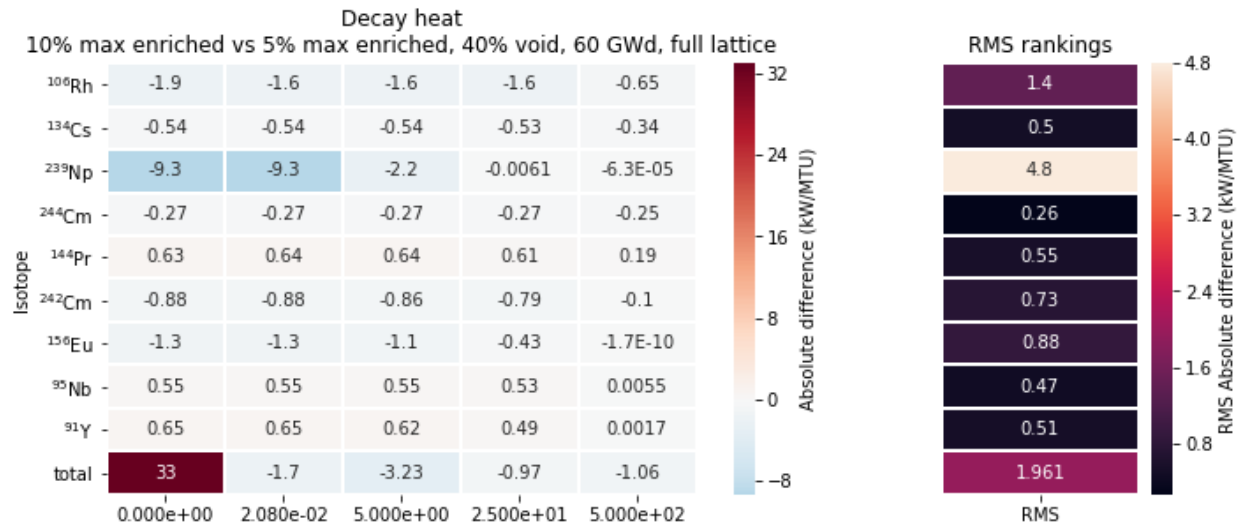


Table 9. Difference in isotopic decay heats resulting from burnup increase at various cooling times

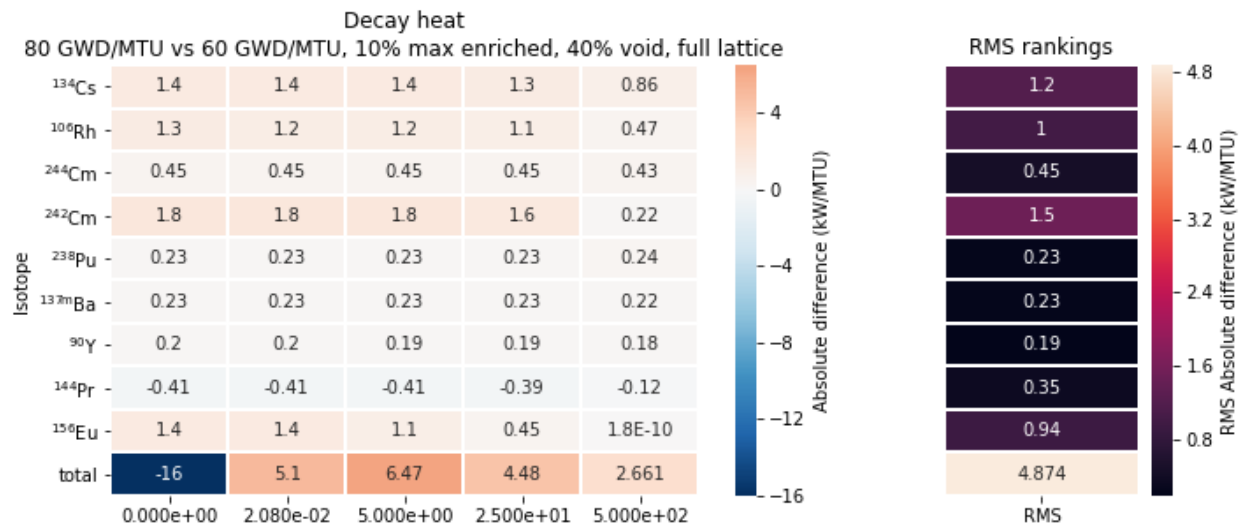
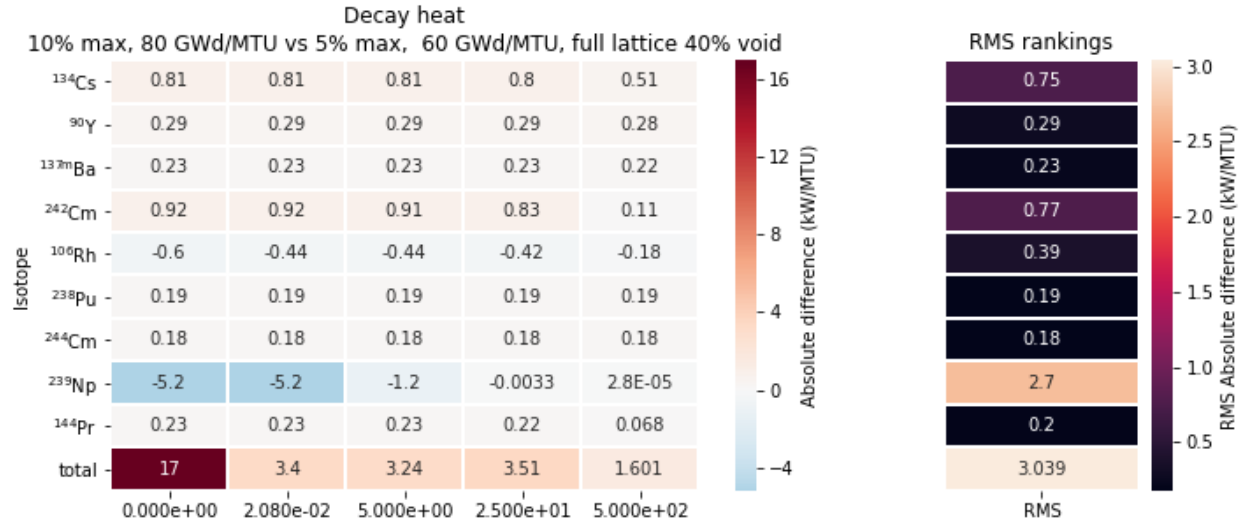


Table 10. Difference in isotopic decay heats resulting from burnup and enrichment increase at various cooling times



The BWR assembly experiences various combinations of void fractions and lattice designs along its axial length. To capture the impact of this variation, trends in enrichment, burnup, and combined enrichment and burnup are provided in Table 11 through Table 13 below. Specifically, the tables plot the signed RMS values of the change in decay heat from an isotope as a percentage of total decay heat, as in preceding tables. With signed RMS, a positive or negative sign is reintroduced to Eq. (2) result to reflect whether the isotope primarily increases or decreases with the burnup change.

Table 11 through Table 13 show that void fraction and lattice designs do not greatly affect the changes introduced by enrichment and burnup changes for the top-ranked isotopes. There is almost no change across lattice type and void fraction.

Table 11. Signed RMS change in isotope decay heat relative to total for enrichment increase from 5max-4.5av% to 10max-7.4av% enrichment

Full lattice 10% void	Full lattice 40% void	Vanished lattice 40% void	Vanished lattice 70% void	Relative difference (%) normalized to total
¹⁴⁴ Pr 1.4	¹⁴⁴ Pr 1.3	¹⁴⁴ Pr 1.5	¹⁴⁴ Pr 1.3	
⁹⁵ Nb 0.74	⁹⁵ Nb 0.66	⁹⁵ Nb 0.79	⁹⁵ Nb 0.67	
⁹¹ Y 0.72	⁹¹ Y 0.64	⁹¹ Y 0.77	⁹¹ Y 0.65	
⁹⁵ Zr 0.66	⁹⁵ Zr 0.58	⁹⁵ Zr 0.71	⁹⁵ Zr 0.6	
¹⁴⁰ La 0.65	¹⁴⁰ La 0.57	¹⁴⁰ La 0.7	¹⁴⁰ La 0.59	
¹⁵⁶ Eu -0.92	¹⁵⁶ Eu -0.78	¹⁵⁶ Eu -1	¹⁵⁶ Eu -0.8	
²⁴² Cm -1	²⁴² Cm -1.1	²⁴² Cm -1	²⁴² Cm -1.2	
²⁴⁴ Cm -1.3	²⁴⁴ Cm -1.4	²⁴⁴ Cm -1.4	²⁴⁴ Cm -1.5	
²³⁹ Np -1.9	²³⁹ Np -1.7	²³⁹ Np -2.1	²³⁹ Np -1.7	
¹³⁴ Cs -2.1	¹³⁴ Cs -2	¹³⁴ Cs -2.3	¹³⁴ Cs -2	
¹⁰⁶ Rh -4.4	¹⁰⁶ Rh -4	¹⁰⁶ Rh -4.6	¹⁰⁶ Rh -4.1	
total -6.269	total -6.124	total -6.61	total -6.391	

Table 12. Signed RMS change in isotope decay heat relative to total for burnup increase from 60 to 80 GWd/MTU at 10max-7.4av% enrichment

Full lattice 10% void	Full lattice 40% void	Vanished lattice 40% void	Vanished lattice 70% void	Relative difference (%) normalized to total
¹³⁴ Cs 5.6	¹³⁴ Cs 5.5	¹³⁴ Cs 5.7	¹³⁴ Cs 5.5	
¹⁰⁶ Rh 3.4	¹⁰⁶ Rh 3.2	¹⁰⁶ Rh 3.6	¹⁰⁶ Rh 3.3	
²⁴⁴ Cm 2.5	²⁴⁴ Cm 2.7	²⁴⁴ Cm 2.4	²⁴⁴ Cm 2.6	
²⁴² Cm 2.2	²⁴² Cm 2.5	²⁴² Cm 2.2	²⁴² Cm 2.5	
^{137m} Ba 1.4	²³⁸ Pu 1.5	^{137m} Ba 1.4	²³⁸ Pu 1.5	
²³⁸ Pu 1.3	^{137m} Ba 1.4	²³⁸ Pu 1.3	^{137m} Ba 1.4	
⁹⁰ Y 1.2	⁹⁰ Y 1.1	⁹⁰ Y 1.2	⁹⁰ Y 1.2	
¹⁵⁶ Eu 0.96	¹⁵⁶ Eu 0.86	¹⁵⁶ Eu 1	¹⁵⁶ Eu 0.87	
²³⁹ Np 0.89	²³⁹ Np 0.74	²³⁹ Np 0.98	²³⁹ Np 0.77	
⁹⁵ Nb -0.48	⁹⁵ Nb -0.43	⁹⁵ Nb -0.5	⁹⁵ Nb -0.44	
¹⁴⁴ Pr -0.98	¹⁴⁴ Pr -0.9	¹⁴⁴ Pr -1	¹⁴⁴ Pr -0.91	
total 17.23	total 17.46	total 17.24	total 17.51	

Table 13. Signed RMS change in isotope decay heat relative to total for enrichment and burnup increase from 5max-4.5av wt% 60 GWd/MTU to 10max-7.4av wt% enrichment at 80 GWd/MTU

Full lattice 10% void	Full lattice 40% void	Vanished lattice 40% void	Vanished lattice 70% void	
¹³⁴ Cs 2.9	¹³⁴ Cs 3	¹³⁴ Cs 2.8	¹³⁴ Cs 2.9	Relative difference (%) normalized to total
⁹⁰ Y 1.6	⁹⁰ Y 1.6	⁹⁰ Y 1.7	⁹⁰ Y 1.6	
^{137m} Ba 1.3	^{137m} Ba 1.3	^{137m} Ba 1.3	^{137m} Ba 1.3	
²⁴² Cm 1.1	²⁴² Cm 1.2	²⁴² Cm 1.1	²⁴² Cm 1.2	
²³⁸ Pu 0.97	²³⁸ Pu 1.1	²³⁸ Pu 0.91	²³⁸ Pu 1.1	
²⁴⁴ Cm 0.89	²⁴⁴ Cm 0.98	²⁴⁴ Cm 0.73	²⁴⁴ Cm 0.84	
¹⁴⁴ Pr 0.53	¹⁴⁴ Pr 0.46	¹⁴⁴ Pr 0.59	¹⁴⁴ Pr 0.49	
¹³⁷ Cs 0.37	¹³⁷ Cs 0.36	¹³⁷ Cs 0.37	¹³⁷ Cs 0.36	
²³⁹ U -0.34	²³⁹ U -0.3	²³⁹ U -0.36	²³⁹ U -0.3	
²³⁹ Np -1.1	²³⁹ Np -0.93	²³⁹ Np -1.1	²³⁹ Np -0.95	
¹⁰⁶ Rh -1.3	¹⁰⁶ Rh -1.1	¹⁰⁶ Rh -1.4	¹⁰⁶ Rh -1.2	
total 9.302	total 9.661	total 8.89	total 9.353	

As shown in Table 14, the effect of lattice type and void fraction on decay heat appears to be minimal. The table shows the signed RMS differences in decay heats from each isotope relative to the total decay heat of the assembly. Most of the change is driven by neutron absorption products such as ²⁴²Cm, ²⁴⁴Cm, ²³⁸Pu, and ¹³⁴Cs. ¹⁰⁶Rh is preferentially produced in fission of ²³⁹Pu.

Table 14. Signed RMS change in isotopic decay heat due to changes in lattice design and void fraction for 10max-7.4av wt% DOM lattice at 80 GWd/MTU

Full lattice 10% void	Full lattice 40% void	Vanished lattice 40% void	Vanished lattice 70% void	
¹⁰⁶ Rh 0	²⁴² Cm 0.53	¹⁴⁴ Pr 0.06	²⁴² Cm 0.53	Relative difference (%) normalized to total
¹³⁶ Cs 0	¹³⁴ Cs 0.45	⁹⁰ Y 0.052	¹³⁴ Cs 0.36	
¹³⁴ Cs 0	²⁴⁴ Cm 0.36	¹⁶⁰ Tb 0.0015	²³⁸ Pu 0.3	
¹⁶⁰ Tb 0	¹⁰⁶ Rh 0.29	¹³⁶ Cs -0.0051	²⁴⁴ Cm 0.28	
²³⁹ Np 0	²³⁸ Pu 0.29	¹⁵⁴ Eu -0.024	¹⁰⁶ Rh 0.18	
²³⁸ Pu 0	²³⁹ Np 0.17	²³⁹ Np -0.085	²³⁹ Np 0.12	
¹⁵⁴ Eu 0	¹⁵⁴ Eu 0.089	²³⁸ Pu -0.086	¹⁵⁴ Eu 0.094	
⁹⁰ Y 0	¹³⁶ Cs 0.067	²⁴² Cm -0.18	¹³⁶ Cs 0.084	
²⁴⁴ Cm 0	¹⁶⁰ Tb 0.055	²⁴⁴ Cm -0.2	¹⁶⁰ Tb 0.079	
²⁴² Cm 0	⁹⁰ Y -0.091	¹⁰⁶ Rh -0.21	¹⁴⁴ Pr -0.067	
¹⁴⁴ Pr 0	¹⁴⁴ Pr -0.097	¹³⁴ Cs -0.23	⁹⁰ Y -0.069	
total 0	total 1.847	total -0.7624	total 1.677	

5.2 ISOTOPES RELEVANT TO ACTIVITY

For all different enrichment and burnup cases studied (16 lattices), total activity per MTU is plotted in Figure 22. As in decay heat, all cases follow similar activity curve with time after shutdown. The activity curves start to split after 100 days and group in two curves based on the burnup of each case. Higher burnup cases exhibit higher activities at long cooling times.

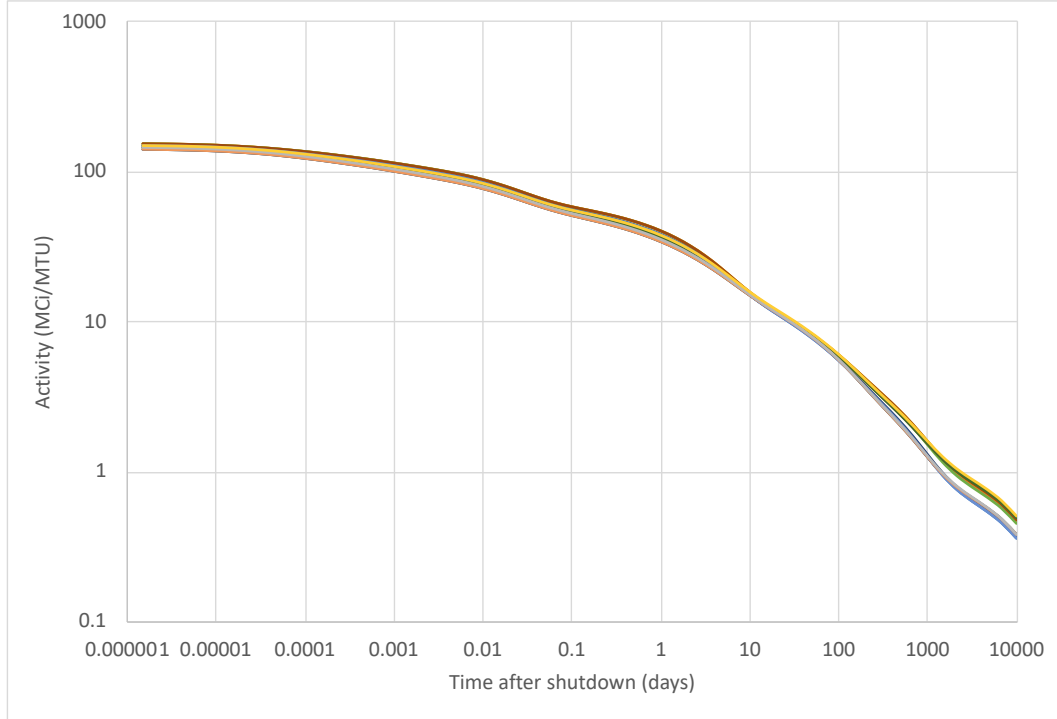


Figure 22. Activity as a function of cooling time for all 16 lattices.

In order to analyze the differences in activities in more detail, the relative (Eq. 7) and absolute differences in activities with respect to the reference, 5max-4.5av wt%, 60 GWd/MTU 40% void case are plotted in Figure 23, and Figure 24, respectively. The observed trends in in both figures are similar to the trends in decay heat. While increased enrichment reduces activity, increased burnup increases activity. However, as in decay heat the enrichment have a more muted effect on activity than the burnup after 10 days, so total activity is more dominated more by burnup.

$$A_{rel}(t) = \frac{A(t)}{A_{ref}(t)} - 1 \quad (7)$$

where $A(t)$ is the activity as a function of time and $A_{ref}(t)$ is the activity for the reference 5max-4.5av wt% 60 GWd/MTU 40% void case.

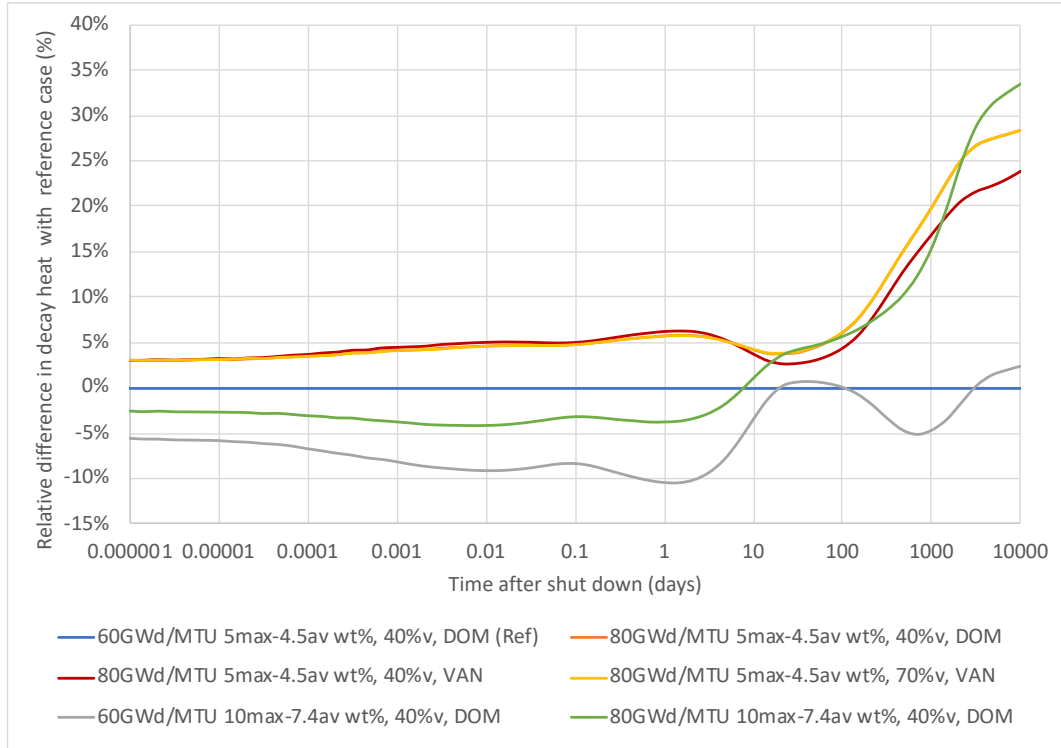


Figure 23. Relative difference in activity with the reference case a function of cooling time.

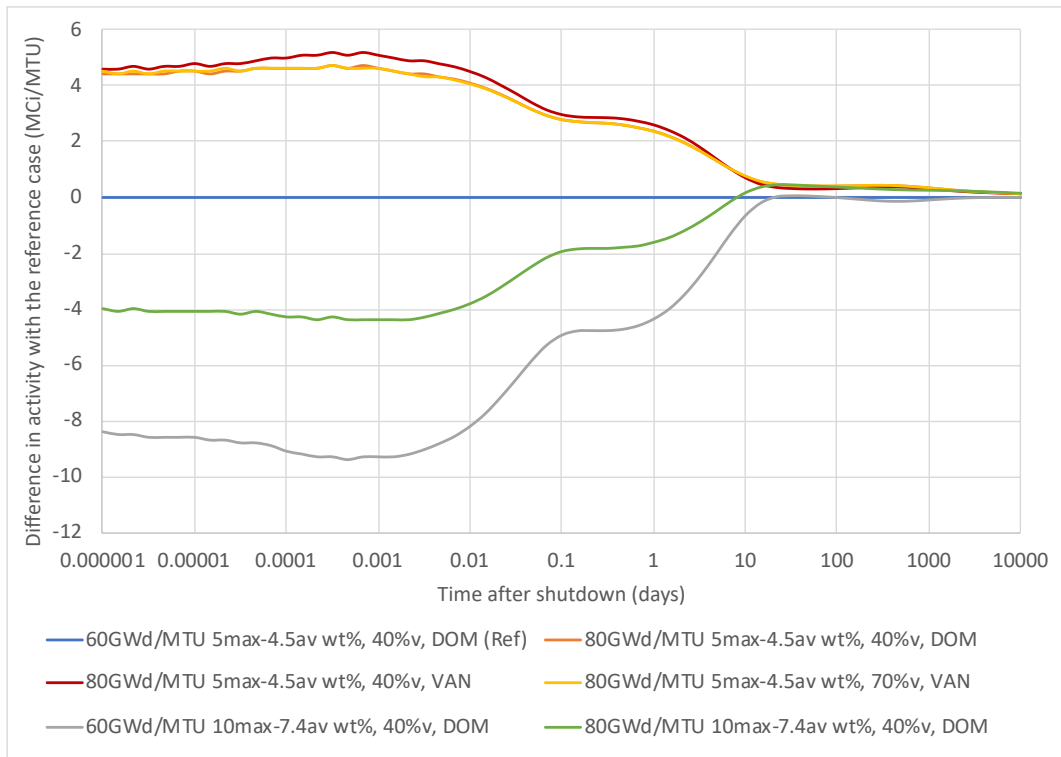


Figure 24. Difference in activity with the reference case a function of cooling time.

A procedure similar to that used for decay heat was performed to find isotopes with large changes in activity for extended enrichment and burnup.

Table 15 through Table 17 show the impact of HBU and EE on isotopic activities. Table 15 shows the impact on total activity for each isotope when enrichment increases from 5max-4.5av wt% to 10max-7.4av wt%. Table 16 shows the impact on total activity for each isotope when burnup increases from 60 to 80 GWd/MTU. Finally, Table 17 shows the combined impact of increasing both burnup and enrichment.

The values in Table 15 through Table 17 are the difference in activity for the isotope expressed as a percentage of total activity of the reference case. The relative difference in contribution of each isotope to the total activity ($A_{rel,i}$) is calculated from Eq. 8 and presented color coded, with blue indicating a decreasing activity from baseline, and red indicating an increasing activity from baseline.

$$A_{rel,i} = \frac{A_i - A_{ref,i}}{A_{ref}} \quad (8)$$

where A_i is the activity for isotope i for HBU or EE, $A_{ref,i}$ is the activity for isotope i for the reference case, A_{ref} is the total activity for the reference case

Many of the same trends observed for decay heat in Table 5 through Table 7 are observed for activity in Table 15 through Table 17. Most isotopes appearing in the activity tables that were not in the decay heat tables likely result from lower energy decays, some of which are isotopes in equilibrium with others in the decay heat ranking list that produce higher energy decays include ^{242}Cm , ^{244}Cm , and ^{238}Pu , which appear in the decay heat charts but not the activity charts.

As with decay heat, the activity is distributed across a larger number of isotopes at short cooling times and fewer isotopes at long cooling times. Like decay heat, the number of short-lived isotopes is large; however, these isotopes make a small contribution to change in total activity, with the exception of ^{239}Np and ^{239}U . At longer cooling times, fewer isotopes are decaying, so the total change in activity from the isotopes that are shown more closely matches the total calculated change in activity. No single isotope changes total activity by more than 5% in any of the comparisons.

Table 15. Contributions of each isotope to total percent change in activity from enrichment increase

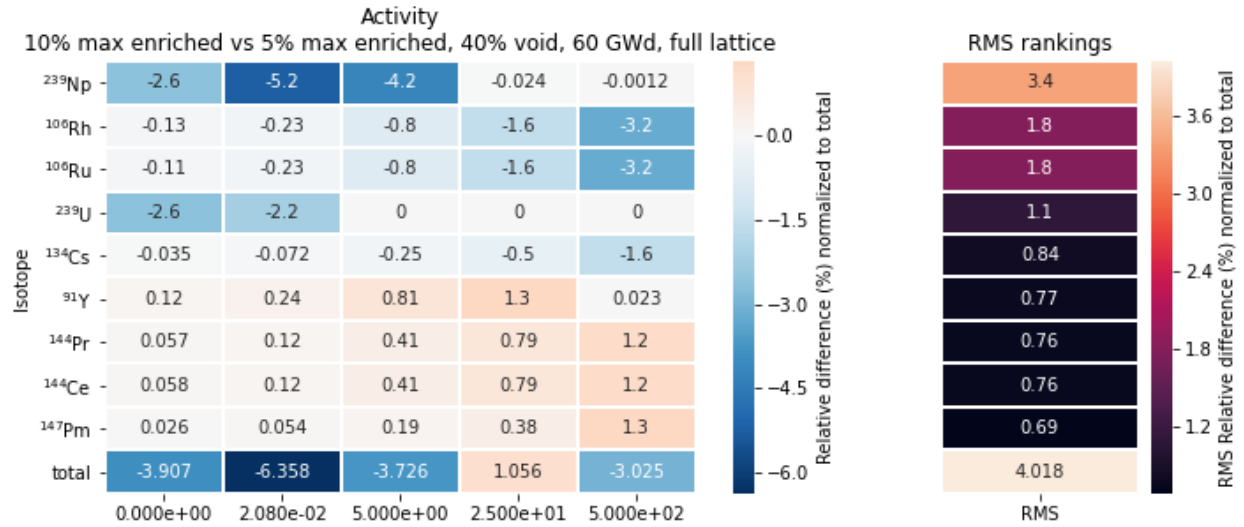


Table 16. Contributions of each isotope to total percent change in activity from burnup increase

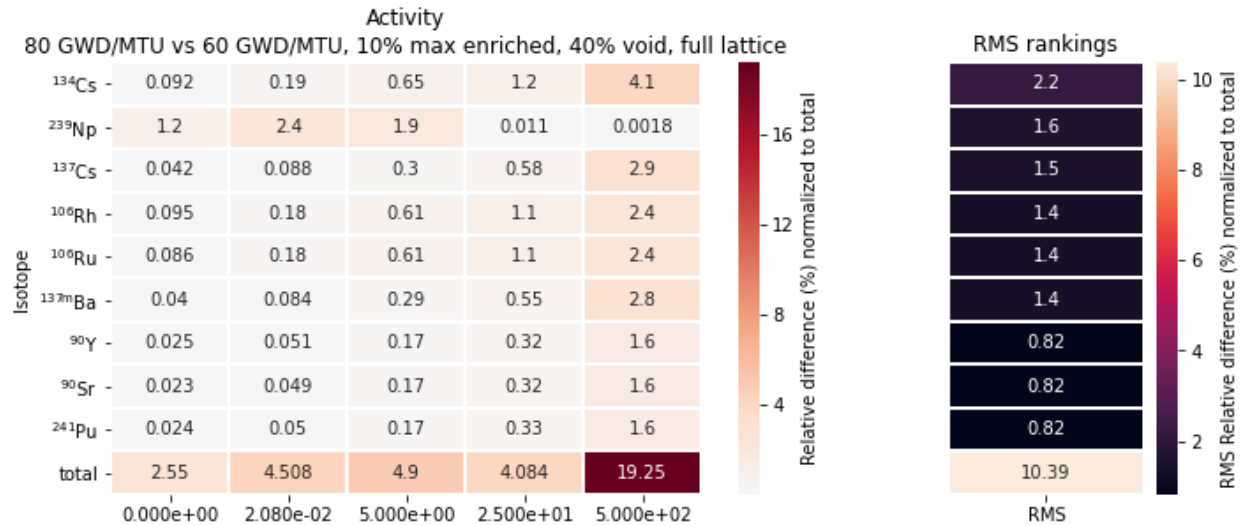
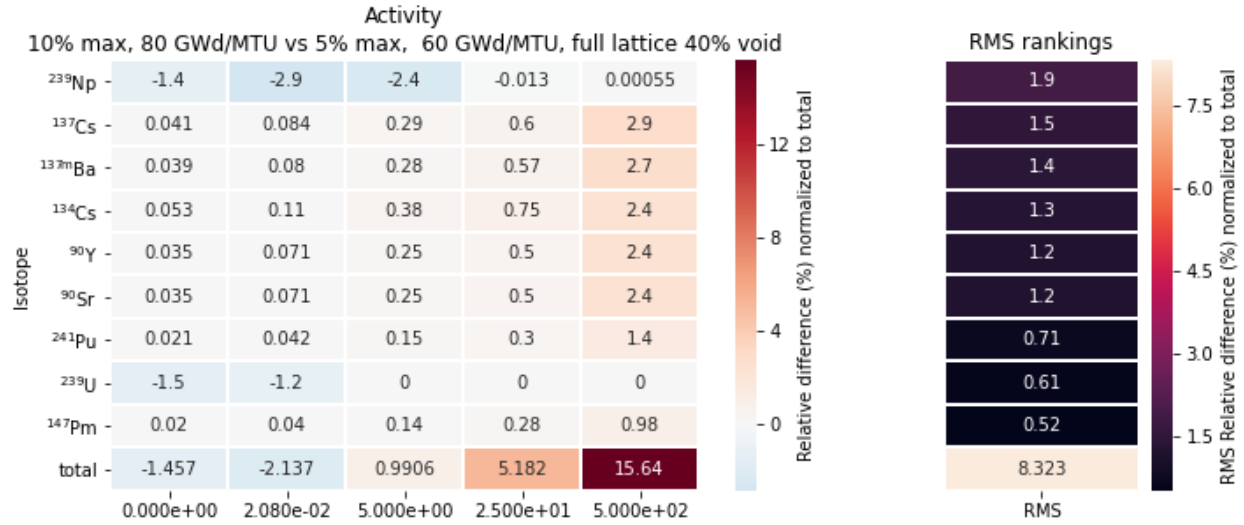


Table 17. Contributions of each isotope to total percent change in activity from combined enrichment and burnup increase



Since absolute differences in activity also follow the trends of the relative differences shown in Table 15 through Table 17, are not presented here. Again, ²³⁹Np dominated, and changes are larger at shorter cooling times than at longer cooling times due to its short half-life of 2.3 days. However, as seen in the case of decay heat, each isotope's change at a shorter cooling time is a smaller proportion of the total. Changes at shorter cooling times also depend more on specific power than burnup or initial enrichment.

Table 18 shows the effect of void fraction and lattice type on activity. Most of the small effect is concentrated in ²⁴¹Pu, ²³⁹Np, and ¹³⁴Cs. ²⁴¹Pu contributes approximately half of the activity change shown versus the DOM lattice at 10% void. Regardless, overall effect of lattice and void change on activity is rather small, being only about 1% of total activity.

Table 18. Signed RMS change in isotopic activity due to changes in lattice design and void fraction for 10max-7.4av wt% DOM lattice at 80 GWd/MTU

Full lattice 10% void	Full lattice 40% void	Vanished lattice 40% void	Vanished lattice 70% void	Relative difference (%) normalized to total
¹⁰⁶ Ru 0	²⁴¹ Pu 0.62	⁹⁰ Y 0.043	²⁴¹ Pu 0.6	
¹⁰⁶ Rh 0	²³⁹ Np 0.35	⁹⁰ Sr 0.041	²³⁹ Np 0.25	
⁹⁰ Sr 0	¹³⁴ Cs 0.2	¹⁴⁴ Pr 0.035	¹³⁴ Cs 0.15	
¹³⁴ Cs 0	¹⁰⁶ Rh 0.13	²⁴² Cm -0.021	¹⁰⁶ Ru 0.081	
²³⁹ U 0	¹⁰⁶ Ru 0.13	²³⁷ U -0.032	¹⁰⁶ Rh 0.081	
²³⁷ U 0	²³⁹ U 0.12	²³⁹ U -0.057	²³⁹ U 0.08	
²³⁹ Np 0	²³⁷ U 0.073	¹⁰⁶ Rh -0.098	²⁴² Cm 0.063	
²⁴¹ Pu 0	²⁴² Cm 0.064	¹⁰⁶ Ru -0.098	²³⁷ U 0.062	
⁹⁰ Y 0	¹⁴⁴ Pr -0.058	¹³⁴ Cs -0.1	¹⁴⁴ Pr -0.04	
²⁴² Cm 0	⁹⁰ Y -0.071	²³⁹ Np -0.18	⁹⁰ Y -0.054	
¹⁴⁴ Pr 0	⁹⁰ Sr -0.071	²⁴¹ Pu -0.21	⁹⁰ Sr -0.054	
total 0	total 1.221	total -0.4849	total 1.107	

5.3 ISOTOPES RELEVANT TO ACCIDENT RELEASE SOURCE TERM

In addition to isotopes that contribute to large changes in activity, some may also be important to the release source term. To screen for these, the list of elements in Regulatory Guide 1.183, *Alternative Radiological Source Terms for Evaluating Design Basis Accidents at Nuclear Power Reactors*, lists these elements that must be considered when considering the alternative release source terms provided in Table 5 of that document [8].

- Noble gases: Xe, Kr
- Halogens: I, Br
- Alkali metals: Cs, Rb
- Tellurium group: Te, Sb, Se, Ba, Sr
- Noble metals: Ru, Rh, Pd, Mo, Tc, Co
- Lanthanides: La, Zr, Nd, Eu, Nb, Pm, Pr, Sm, Y, Cm, Am
- Cerium: Ce, Pu, Np

Every isotope of these elements included in SCALE was modeled, but only those creating more than a 0.1% of total activity at any evaluated timepoint are listed in Table 19 through Table 21. Similar to previous sections, effect of EE and HBU are analyzed on release isotopes activities.

Comparisons showing the effects of increases in burnup and enrichment for a selection of isotopes are shown in Table 19 through Table 21. The relative difference in each isotope activity ($A_{rel,i}$) is calculated from Eq. 9. The observed trends are very similar to the trends observed for PWR assemblies [15]. The relative differences for negligible concentrations of ¹³³I and ¹³⁵I at 500 days were left blank in the tables.

$$A_{rel,i} = \frac{A_i - A_{ref,i}}{A_{ref,i}} \quad (9)$$

where A_i is the activity for isotope i for HBU or EE , $A_{ref,i}$ is the activity for isotope i for the reference case.

Table 19. Relative differences of selected release isotopes activities due to enrichment increase

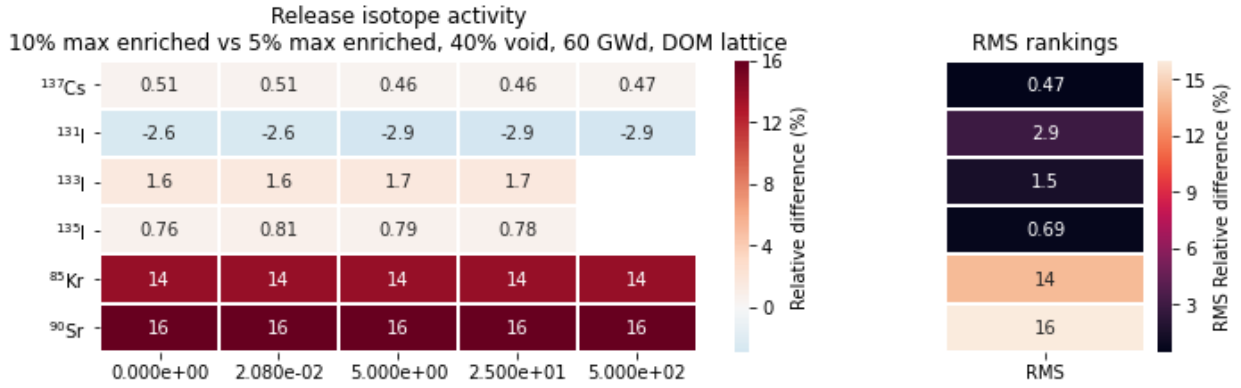


Table 20. Relative differences of selected release isotopes activities due to burnup increase

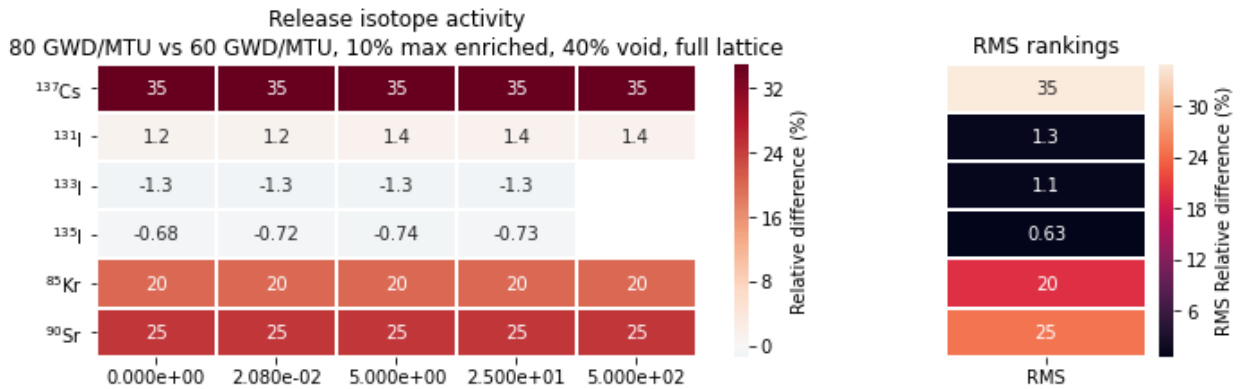
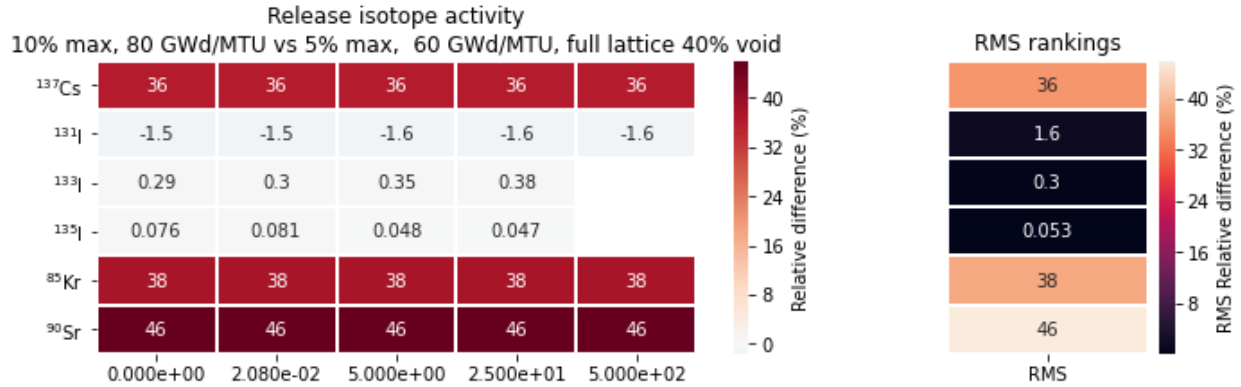
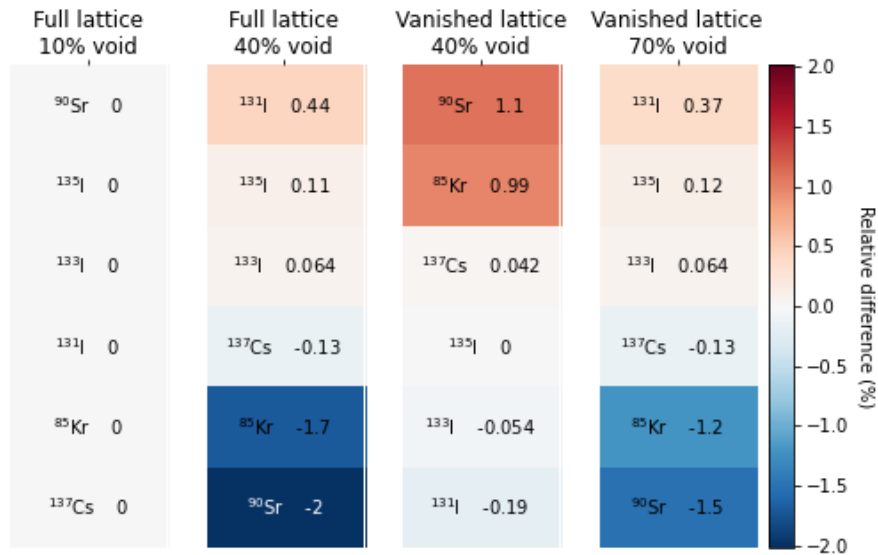


Table 21. Relative differences of selected release isotopes activities due to both enrichment and burnup increase



The effect of lattice type and void fraction on release isotopes is relatively small when both enrichment and burnup are increased. ⁹⁰Sr, and ⁸⁵Kr are the most affected isotopes, while decrease in void fraction increases inventories, DOM lattices show lower inventories compared to VAN lattices.

Table 22. Signed RMS relative differences in abundance of selected release isotopes due to changes in lattice design and void fraction for 10max-7.4av wt% DOM lattice at 80 GWd/MTU



5.4 ISOTOPES RELEVANT TO RADIATION SHIELDING SOURCE TERM

Changes in the isotopes important to cask shielding in NUREG 6700 [9] are evaluated in this section. This list of isotopes is developed for longer time frames such as 5 years. Given that relative contributions of short-lived isotopes are mostly dependent on operating power, this should be reasonable. Table 23 through Table 25 address the percent each isotope increases or

decreases in activity on an isotope basis. The relative difference for each isotope's activity is computed from Eq. 9.

Aside from the ^{238}Pu and Cm isotopes (addressed in section 5.5), given that there are no changes exceeding 100%, the existing methods for shielding should remain suitable. Values are similar to the PWR cases [15], with the exception of the higher actinides, which are more sensitive to operating conditions than fission products.

Table 23. Relative differences of selected shielding isotopes activities due to enrichment increase

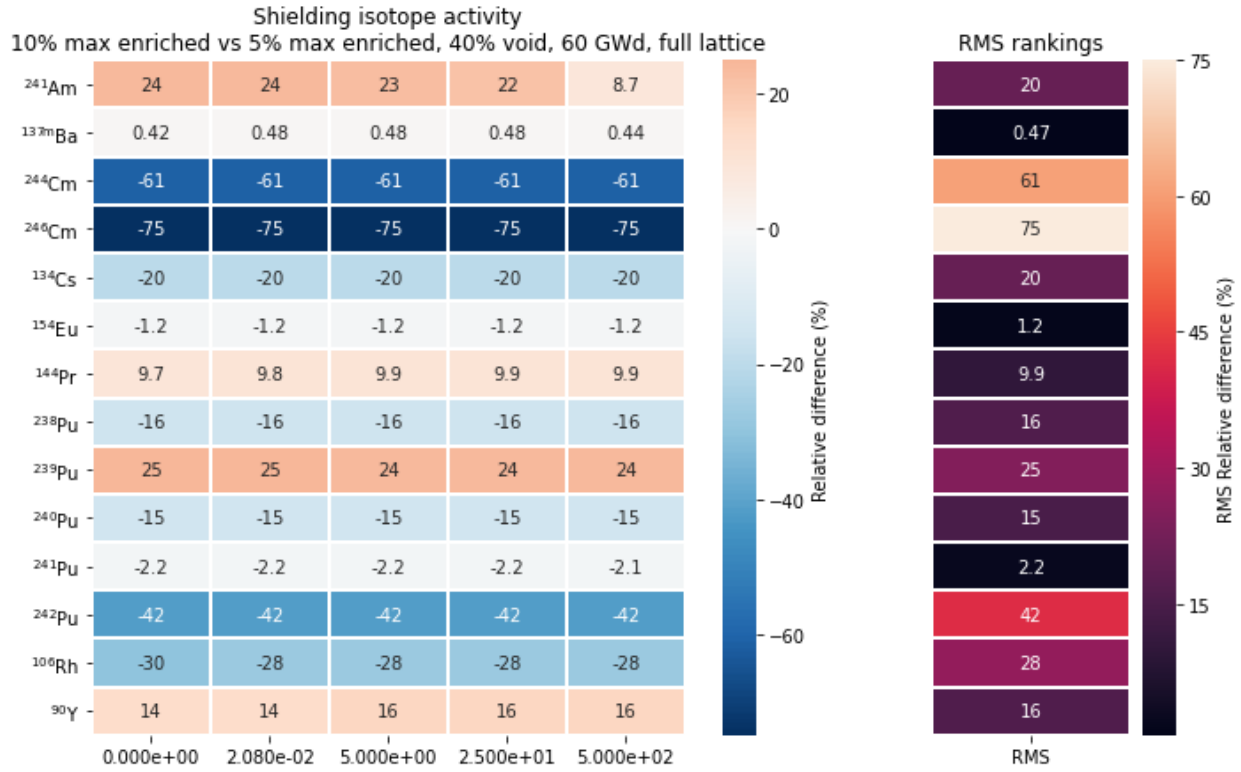


Table 24. Relative differences of selected shielding isotopes activities due to burnup increase

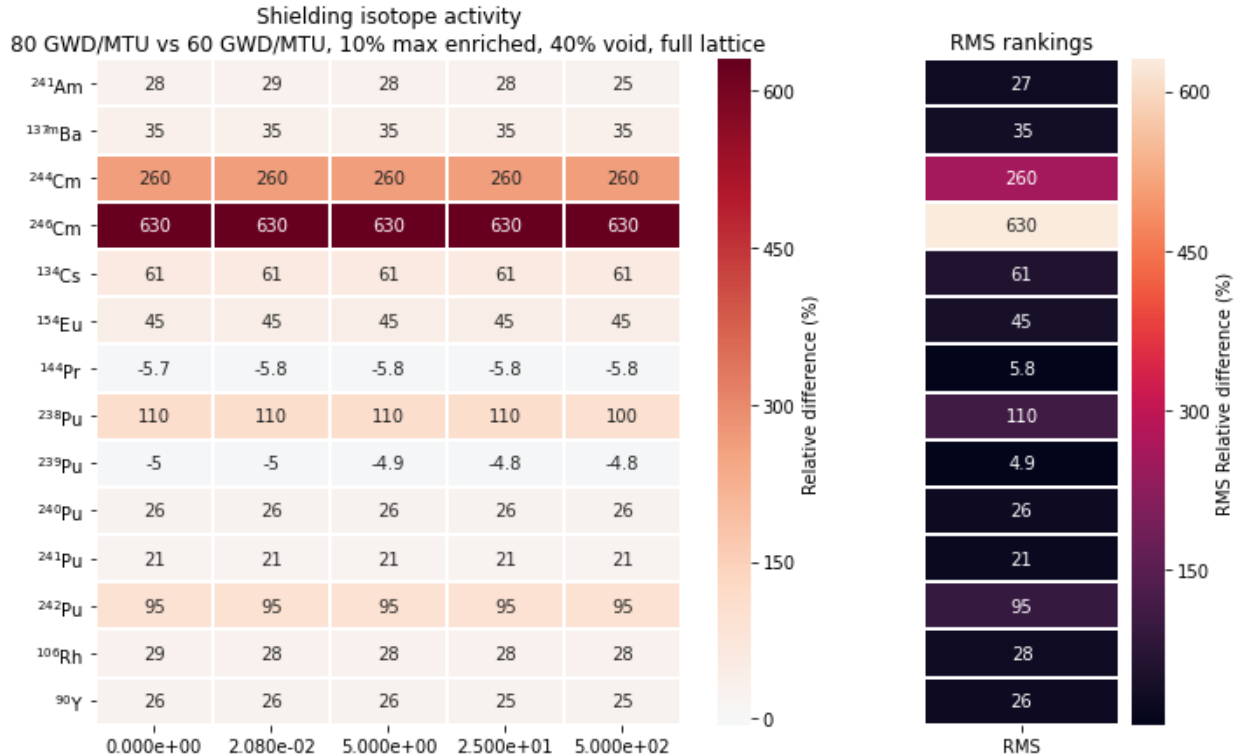


Table 25. Relative differences of selected shielding isotopes activities due to both enrichment and burnup increase

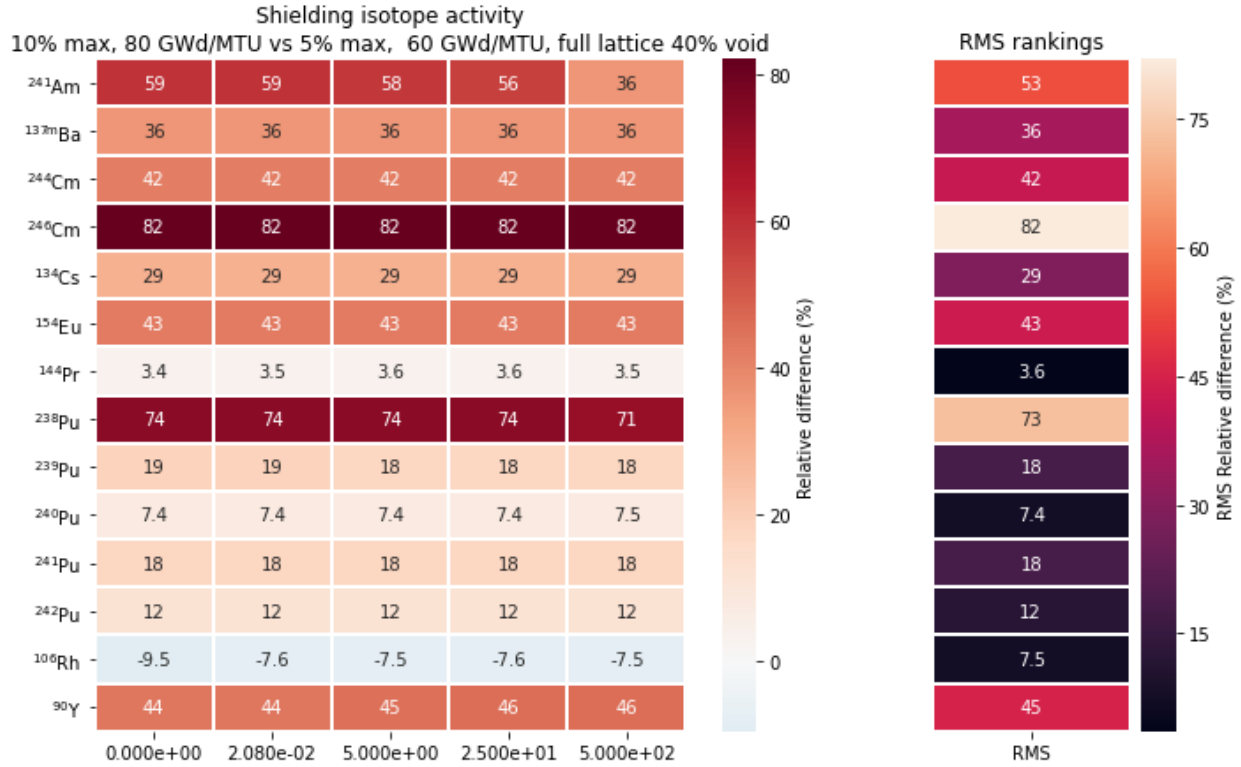


Table 26 shows effect lattice type and void fraction on RMS relative differences for the selected shielding isotopes for 10max-7.4av wt% lattice. Actinides like ²⁴⁴Cm concentrations can change significantly with void fraction (14% to 18%). Corollary, sensitivity to the lattice type due to change in moderation power is also expected (21 %). These differences are small compared to the effect of enrichment and burnup for the same isotopes; however, they imply that the trends seen in EE and HBU cases of DOM lattice at 40% void fraction may not apply to a VAN lattice at the same void fraction. Therefore, the analysis in this section should be repeated in the next phase of this study for VAN lattice as the reference lattice.

The curium isotopes in Table 24 are produced in small amounts and very sensitive to increasing burnup. Several isotopes on the activation chain leading to ²⁴⁴Cm and ²⁴⁶Cm are shown in Figure 25, along with ²³⁵U where the increasing sensitivity to burnup with increasing mass number is apparent.

Neutron emitters are important in some cask shielding applications, and the appearance of additional spontaneous fission neutron emitters could carry implications for shielding analyses. In the case evaluated, spontaneous fission neutron emitters such as ²⁴⁴Cm and ²⁴²Cm produce ~95% of neutrons post-discharge. To verify that no additional significant spontaneous fission source appeared, the difference in spontaneous fission source intensity between the 80 GWd/MTU 10max-7.4av wt% enrichment case and the 60 GWd/MTU 5max-4.5av wt% case are shown in Figure 26. It is clearly seen that ²⁴⁴Cm is the main isotope that changes the spontaneous neutron emission source substantially for the timescales in question. Isotopes with relative differences under 0.1% are not listed. Despite the 82% increase in ²⁴⁶Cm composition in the 80

GWd/MTU 10 wt% maximum enrichment case over the reference 60 GWd/MTU 5 wt% case seen in Table 25, this isotope due to long half-life (4700 years) should not substantially affect the neutron dose. Furthermore, no other new spontaneous fission isotopes become prominent. ^{242}Cm and ^{244}Cm increase in activity, and few actinides heavier than ^{244}Cm are produced because ^{245}Cm has a high neutron-induced fission probability.

Table 26. Signed RMS relative differences in abundance of selected shielding isotopes vs the dominant lattice with 10% void for 10% maximum enriched lattices burned to 80 GWd/MTU

Full lattice 10% void	Full lattice 40% void	Vanished lattice 40% void	Vanished lattice 70% void	
^{106}Rh 0	^{246}Cm 26	^{90}Y 1.2	^{239}Pu 25	Relative difference (%)
$^{137\text{m}}\text{Ba}$ 0	^{241}Am 25	^{144}Pr 0.48	^{241}Am 24	
^{134}Cs 0	^{239}Pu 25	$^{137\text{m}}\text{Ba}$ 0	^{246}Cm 20	
^{242}Pu 0	^{241}Pu 18	^{240}Pu -0.95	^{241}Pu 18	
^{241}Pu 0	^{154}Eu 15	^{106}Rh -1.8	^{154}Eu 16	
^{240}Pu 0	^{238}Pu 14	^{134}Cs -2.1	^{238}Pu 15	
^{144}Pr 0	^{244}Cm 14	^{242}Pu -2.9	^{244}Cm 11	
^{154}Eu 0	^{240}Pu 7.9	^{154}Eu -4.1	^{240}Pu 9.6	
^{246}Cm 0	^{134}Cs 4.1	^{238}Pu -4.3	^{134}Cs 3.3	
^{241}Am 0	^{106}Rh 2.6	^{241}Pu -6.1	^{106}Rh 1.5	
^{239}Pu 0	$^{137\text{m}}\text{Ba}$ -0.12	^{239}Pu -7	$^{137\text{m}}\text{Ba}$ -0.13	
^{238}Pu 0	^{144}Pr -0.8	^{244}Cm -7.7	^{144}Pr -0.55	
^{244}Cm 0	^{242}Pu -1.8	^{241}Am -8.2	^{90}Y -1.7	
^{90}Y 0	^{90}Y -2.1	^{246}Cm -13	^{242}Pu -5.3	

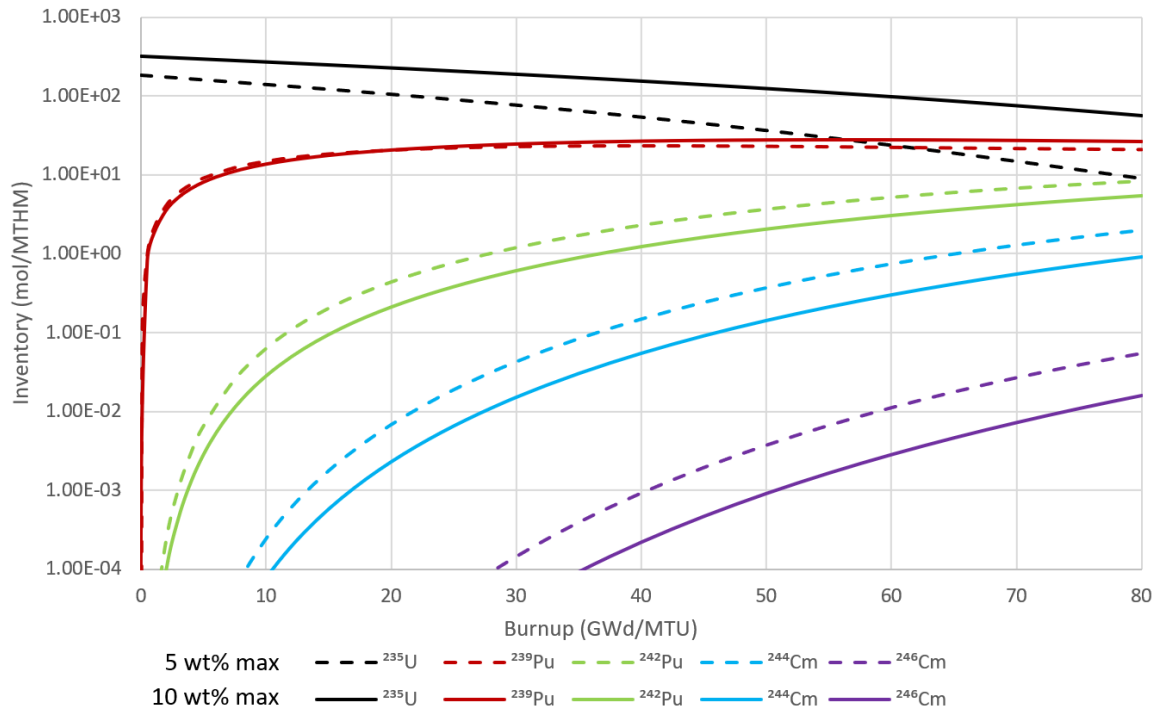


Figure 25. In-core abundances for isotopes in the activation chain for ^{244}Cm and ^{246}Cm .

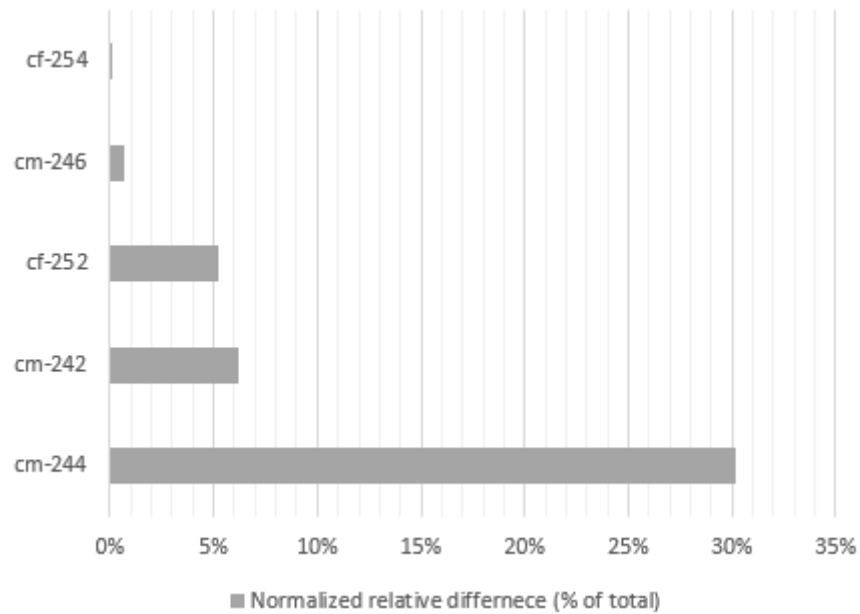


Figure 26. Relative difference in SF neutron emission on total SF neutron emission basis for time point 80 GWd/MTU 10max-7.4av wt% vs the reference case for 40% void fraction.

5.5 ISOTOPES FOR CRITICALITY

The impacts of high burnups and enrichments of isotopes found to substantially contribute to the multiplication factor in Section 4.1 are examined here. Table 27 through Table 29 show relative differences between isotope masses with respect to the reference case. The relative differences are computed as

$$M_{rel,i} = \frac{M_i - M_{ref,i}}{M_{ref,i}} \quad (10)$$

where M_i is the mass for isotope i for HBU or EE, $M_{ref,i}$ is the mass for isotope i reference 5max-4.5av wt% 60 GWd/MTU 40% void case.

In general, increasing enrichment decreases the abundance of actinides after ^{239}Pu in the neutron activation sequence. Other notable increases are in fission products ^{135}Xe and ^{149}Sm due to reduced flux levels. Varying burnup or initial enrichment alone creates large relative changes in isotopic content for heavier actinides such as ^{243}Am and ^{242}Pu . When increasing enrichment with burnup, the competing effects mostly cancel out for the heavier transuranics. This is because they are the products of multiple neutron absorptions, so their abundance increases with burnup. For a given burnup, increased enrichment results in lower overall neutron fluence, so neutron absorption products decrease with increasing enrichment.

Table 30 shows the percent change in mass for criticality isotopes due to changes in lattice types and void fractions. ^{235}U , ^{239}Pu , ^{241}Pu , ^{149}Sm , ^{151}Sm , ^{154}Eu have the largest relative changes in mass.

Table 27. Relative differences of criticality isotope masses due to enrichment increase

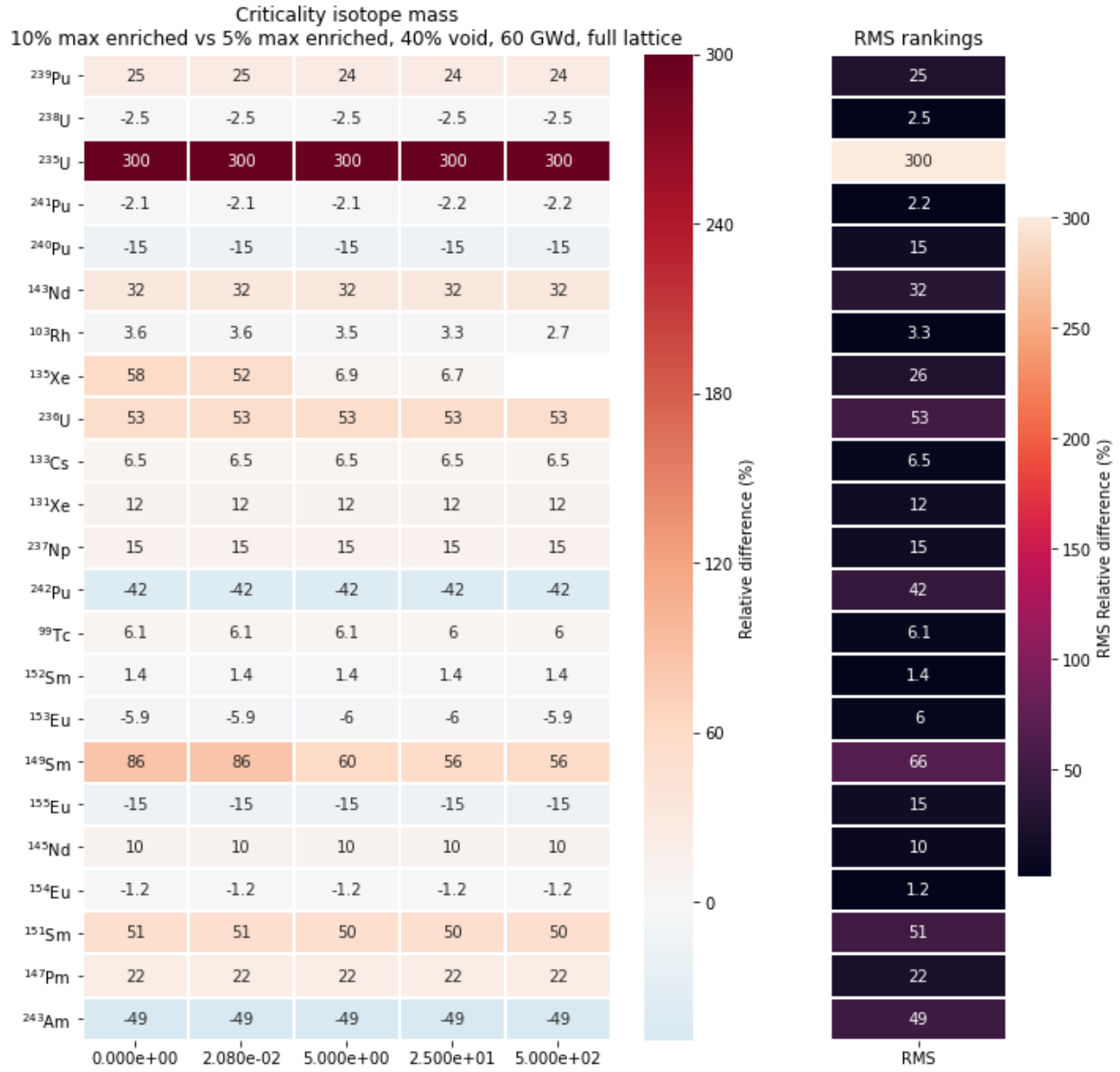


Table 28. Relative differences of criticality isotope masses due to burnup increase

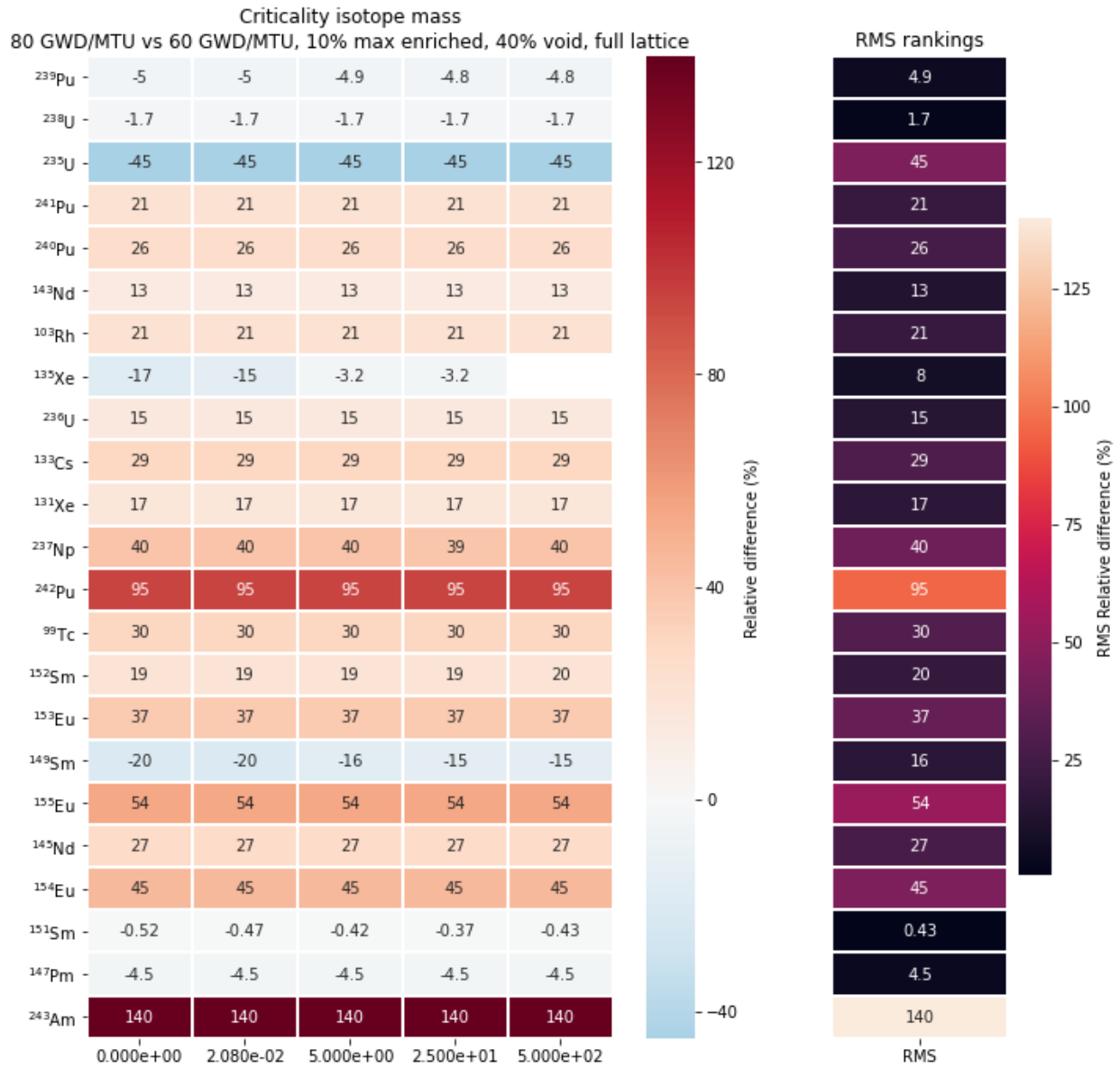


Table 29. Relative differences of criticality isotope masses due to both enrichment and burnup increase

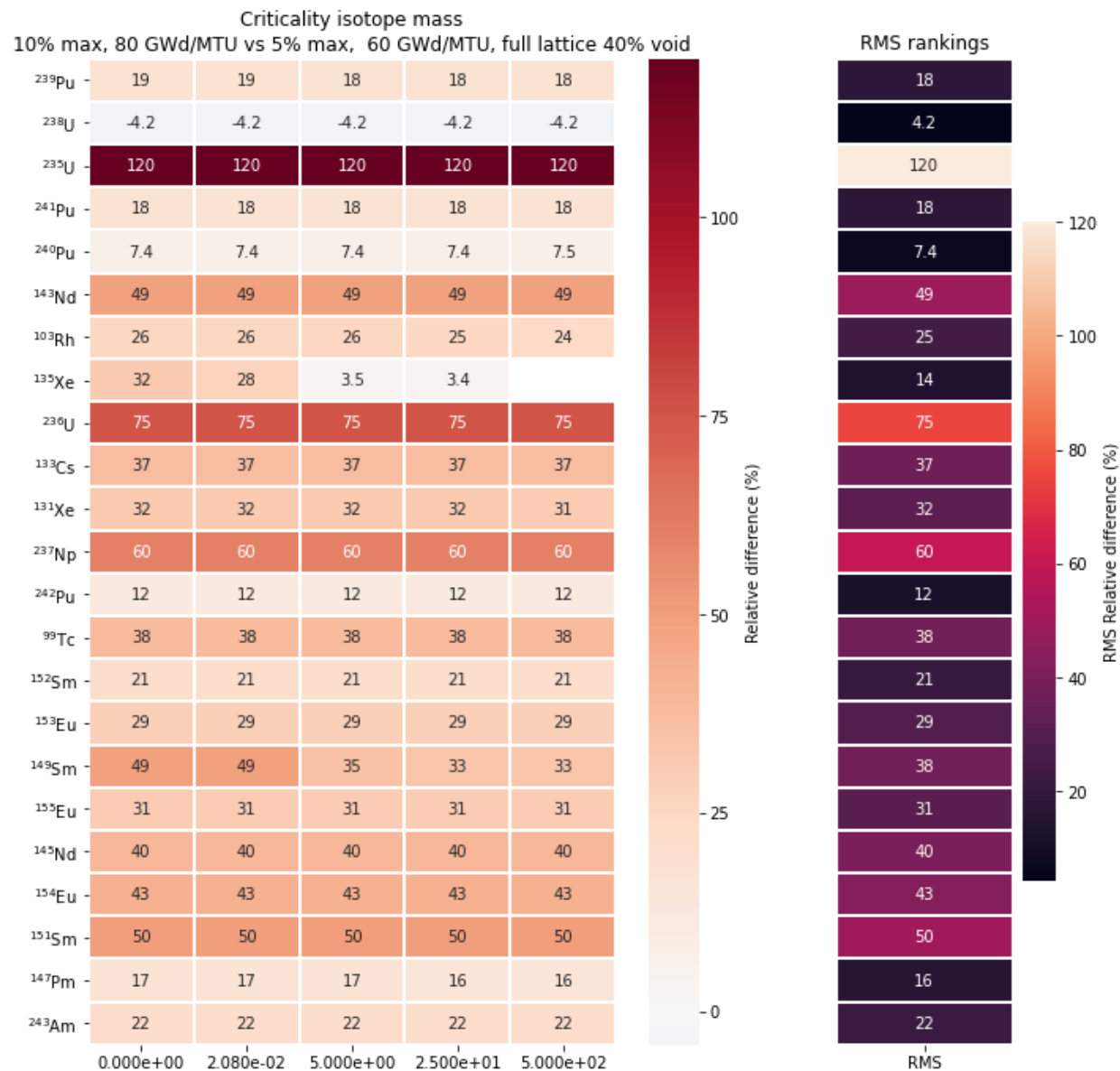
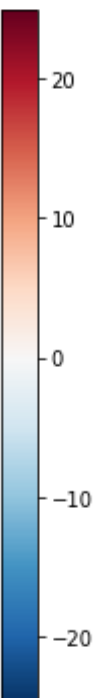


Table 30. Relative differences of criticality isotope masses due to changes in lattice design and void fraction for 10max-7.4av wt% DOM lattice at 80 GWd/MTU

Full lattice 10% void	Full lattice 40% void	Vanished lattice 40% void	Vanished lattice 70% void	
¹⁰³ Rh 0	²³⁹ Pu 25	¹⁵² Sm 1.8	²³⁹ Pu 25	
¹⁴⁵ Nd 0	¹⁴⁹ Sm 24	¹⁴⁷ Pm 1.3	¹⁵¹ Sm 23	
¹⁴³ Nd 0	¹⁵¹ Sm 22	²³⁶ U 1.1	¹⁴⁹ Sm 23	
⁹⁹ Tc 0	²⁴¹ Pu 18	¹³¹ Xe 0.96	²⁴¹ Pu 18	
¹³⁵ Xe 0	²³⁵ U 16	¹³³ Cs 0.75	¹⁵⁴ Eu 16	
¹³¹ Xe 0	¹⁵⁴ Eu 15	⁹⁹ Tc 0.63	²³⁵ U 13	
¹³³ Cs 0	¹³⁵ Xe 8.6	¹⁴⁵ Nd 0.6	²⁴⁰ Pu 9.6	
¹⁵² Sm 0	²³⁷ Np 8	²³⁸ U 0.15	¹³⁵ Xe 8.6	
¹⁴⁷ Pm 0	²⁴⁰ Pu 7.9	¹⁰³ Rh -0.69	¹⁴³ Nd 6.5	
¹⁴⁹ Sm 0	¹⁴³ Nd 5.4	¹⁵³ Eu -0.81	²³⁷ Np 6.4	
¹⁵⁵ Eu 0	¹⁵⁵ Eu 4.4	²⁴⁰ Pu -0.95	¹⁵⁵ Eu 4.8	
¹⁵⁴ Eu 0	²⁴³ Am 3.9	¹⁴³ Nd -0.97	²³⁶ U 2	
¹⁵³ Eu 0	¹⁰³ Rh 1.1	¹⁵⁵ Eu -1.1	¹⁰³ Rh 0.62	
¹⁵¹ Sm 0	²³⁶ U 0.64	¹³⁵ Xe -2.8	²⁴³ Am 0.35	
²³⁸ U 0	¹⁵³ Eu 0.47	²⁴² Pu -2.9	¹⁵³ Eu -0.33	
²³⁹ Pu 0	²³⁸ U -0.43	²³⁷ Np -4	²³⁸ U -0.42	
²⁴⁰ Pu 0	⁹⁹ Tc -1.1	¹⁵⁴ Eu -4.1	¹⁴⁷ Pm -0.63	
²⁴¹ Pu 0	¹³³ Cs -1.1	²⁴³ Am -4.9	¹³³ Cs -0.79	
²³⁶ U 0	¹⁴⁵ Nd -1.4	¹⁵¹ Sm -5.3	⁹⁹ Tc -0.85	
²³⁵ U 0	¹⁴⁷ Pm -1.5	²⁴¹ Pu -6.1	¹⁴⁵ Nd -1.4	
²³⁷ Np 0	²⁴² Pu -1.9	¹⁴⁹ Sm -6.9	¹³¹ Xe -1.5	
²⁴² Pu 0	¹³¹ Xe -1.9	²³⁹ Pu -7	²⁴² Pu -5.3	
²⁴³ Am 0	¹⁵² Sm -6.1	²³⁵ U -7.9	¹⁵² Sm -6.6	

5.6 COMPARISON OF 252g AND 56g MULTIGROUP LIBRARIES

Currently, 56-group libraries are recommended for the majority of Polaris calculations because their runtimes are faster than those in the 252-group library, and they have minimal impact on lattice eigenvalues for a wide range of internally investigated LWR configurations. The 10max-7.4av wt% enrichment VAN lattice with 70% void fraction was depleted to 80 GWd/MTU using 252 group cross section library to gauge the influence of group structure on isotopic results. The 70% void fraction VAN case was selected for this study to since it is the most different design compared to the PWR design used in the PWR report in Volume 1 [15]. The relative differences in isotope predictions (Eq.10) are calculated for isotopes with weights higher than 500 µg per metric ton of uranium. The relative differences larger than 1% are shown in Table 31. Two columns listing the percent change introduced from increasing enrichment from 5max-4.5av wt%

to 10max-7.4av wt% and burnup from 60 GWd/MTU to 80 GWd/MTU in addition to amount of each isotope per MTU of the fuel are included for comparison to demonstrate where the 56-group approximation may affect the takeaways in the isotope section. The change in most isotopes is only a fraction of the change introduced with EE and HBU. Except ^{234}U and ^{235}U , all of these isotopes appear on the release term list, but they are each a small component of the total term. ^{242}Pu and ^{240}Pu appear in the list of isotopes that influence both shielding and criticality. In the case of shielding, they contribute little to the overall activity of the spent nuclear fuel in the timescales studied in this work, so the impact on shielding is likely small. This is also seen in the analysis presented in NUREG CR-5700 [9], in which the isotopes contribute negligible amounts at 5 years of cooling but can be substantial source components at 100 years of cooling. Thus, the 56-group approximation used in work described in this section likely only impacts the ^{242}Pu values for criticality, as well as the quantities of some release nuclides. The 5–10% differences observed in the isotopics predicted by the 56-group library compared with the 252-group are larger than expected for the high enrichment and burnup case. Although, EE and HBU cases are beyond validation basis for these libraries, the biases observed in this study do not provide any information regarding relative differences in isotope concentrations when consistent libraries are used to analyze effect of EE and HBU. In the next phase of this study, more cases will be analyzed using 252-group library to verify findings of this report involving the nuclides identified in this section.

Table 31. Relative difference between 252- and 56-group cross section structures on isotope results (other comparisons shown for reference).

Isotope	Relative difference 252g vs 56g	Weight (g/MTU)	Relative difference between 5max-4.5av wt% vs. 10max-7.4av wt% (56g, 70% void)	Relative difference between 60 GWd/MTU vs. 80 GWd/MTU (56g, 70% void)	Shielding	Release	Decay	Activity
²⁴¹ Am	6.5%	7.2E+01	58%	28%	✓	✓		
²⁴² Am	2.8%	1.2E-01	4%	51%	✓			
²⁴³ Am	-6.7%	1.8E+02	-42%	142%	✓			
²⁴⁴ Am	-3.8%	7.8E-03	-53%	168%	✓			
^{244m} Am	-3.8%	5.0E-03	-53%	168%	✓			
²⁴² Cm	2.7%	2.2E+01	-1%	66%	✓	✓		
²⁴⁴ Cm	-4.5%	1.3E+02	-57%	263%	✓	✓	✓	
¹³⁶ Cs	9.4%	8.3E-01	0%	50%	✓	✓		
¹⁵³ Eu	3.5%	1.5E+02	1%	36%	✓			
¹⁵⁴ Eu	1.5%	3.7E+01	11%	44%	✓	✓	✓	
¹⁵⁵ Eu	10.2%	1.3E+01	-3%	54%	✓			
¹⁵⁶ Eu	-1.3%	3.5E+00	-33%	78%	✓	✓		
¹⁵⁵ Gd	6.5%	6.5E-01	42%	-14%				
²³⁸ Np	2.4%	1.3E+00	-9%	65%	✓	✓		
²⁴⁰ Np	-1.6%	4.1E-04	-41%	34%	✓			
¹⁰⁹ Pd	1.4%	8.3E-02	-33%	44%	✓			
¹¹¹ Pd	1.5%	4.0E-04	-28%	31%	✓			
¹¹² Pd	2.9%	1.0E-02	-28%	27%	✓			
^{148m} Pm	1.4%	9.0E-01	38%	-8%	✓			
²³⁸ Pu	3.3%	4.7E+02	-1%	107%	✓	✓	✓	
²³⁹ Pu	2.0%	3.7E+03	27%	-5%	✓	✓		✓
²⁴⁰ Pu	-6.3%	1.9E+03	-4%	27%	✓	✓		✓
²⁴¹ Pu	3.3%	1.1E+03	11%	21%	✓			✓
²⁴² Pu	5.1%	7.4E+02	-37%	98%	✓	✓		
²⁴³ Pu	-5.2%	1.0E-01	-44%	103%	✓			
⁸⁶ Rb	2.0%	2.8E-02	-4%	52%	✓			
¹⁰³ Rh	-2.6%	4.9E+02	10%	21%	✓			
¹²⁴ Sb	9.3%	3.6E-02	-30%	70%	✓			
¹²⁵ Sb	4.2%	7.4E+00	-14%	21%	✓			
¹²⁷ Sb	1.1%	1.5E-01	-13%	10%	✓			
¹⁴⁷ Sm	2.1%	1.6E+02	42%	25%	✓			
¹⁴⁹ Sm	2.9%	1.8E+00	71%	-20%	✓			
¹⁵¹ Sm	3.5%	1.2E+01	40%	-1%	✓			
^{125m} Te	4.1%	9.6E-02	-14%	23%	✓			
¹²⁷ Te	1.2%	1.4E-02	-11%	9%	✓			
^{127m} Te	2.1%	4.0E-01	12%	0%	✓			
²³⁴ U	4.5%	1.9E+02	151%	-20%				
²³⁵ U	1.2%	7.6E+03	546%	-47%				
¹³¹ Xe	2.8%	4.9E+02	21%	17%	✓			
^{131m} Xe	1.7%	5.2E-02	-3%	2%	✓			
¹³⁵ Xe	1.8%	1.2E-01	56%	-17%	✓			

6. CONCLUSIONS

Calculations were performed using the pre-release version of SCALE 6.3 Polaris and ORIGEN codes with 56 -group ENDF/B-VII.1 cross section library. The effects of EE and HBU on lattice depletion characteristics of a representative commercial BWR assembly (10×10 GNF-2) were evaluated. Similar to the first volume on PWR lattice behavior, the investigation focused on differences between depletion to conventional conditions with existing fuel (5max-4.5av wt% ²³⁵U enrichment depleted to 60 GWd/MTU) and depletion with enrichments up to 10max-7.4av wt% and burnup up to 80 GWd/MTU. Unlike the PWR volume, here a new lattice enrichment map was developed for each different EE case with limited optimization on gadolinia loading, pin peaking and depletion curves.

Key quantities of interest include lattice physics quantities, isotopic inventory at various decay times and their effect on decay heat, activity and shielding applications. Limited comparisons between predictions using SCALE 56-group ENDF/B-VII.1 cross sections and SCALE 252-group ENDF/B-VII.1 cross section are also presented. Conclusions from this evaluation are in general, very similar to the ones found the PWR Volume 1 report and are as follows.

1. No unexpected or anomalous trends were found that would call into question the accuracy of the Polaris code using SCALE 56-group ENDF/B-VII.1 data for depletion, lattice physics, and isotopic content calculations of the analyzed BWR fuel with enrichments up to 10max-7.4av wt% and burnup up to 80 GWd/MTU.
2. Increased enrichment and higher burnup are positively correlated due to the requirements of commercial BWR fuel management (fuel economics and reactor physics). This correlation tends to result in offsetting lattice physics effects when combined with single-assembly results to estimate core average characteristics.
3. Lattice physics results from the Polaris model depletion of GNF-2 10×10 DOM and VAN lattices with void fractions varying from 10% to 70% overall showed no unusual, unexpected, or adverse code performance trends.
 - a. Calculated fuel k_{inf} , peaking factors, and reactivity coefficients are smooth and continuous as a function of enrichment and burnup.
 - b. Lattice physics trends were predictable from first principles (e.g., spectral hardening resulting from increased ²³⁵U enrichment).
 - c. A first-order approximation shows that lattice average burnup is expected to 10 GWd/MTU for each 1 wt% increase in lattice average fuel enrichment above 5 wt%. This approximation can be used to extend the results of single-assembly lattice physics calculations to expected core average behavior.
 - d. Core average fuel temperature coefficient (DTC) and β -eff kinetics parameter are not expected to change substantially due to the offsetting effects of increased enrichment and increased burnup. However, moderator void coefficient depends on initial gadolinium loading, and the moderator void coefficient for a lattice at beginning of life was only

slightly negative for some lattices in this study. Thus special attention should be paid when optimizing enrichment maps.

4. Uncertainty in depletion k_{inf} due to cross section uncertainties changes negligibly for EE and HBU compared to the reference case. Increasing enrichment, increases k_{inf} uncertainty initially (~50 pcm); however, the uncertainty decreases with burnup and becomes lower than the reference case after 50 GWd/MTU.
5. Increasing enrichment from 5max-4.5av wt% to 10max-7.4av wt% at 60 GWd/MTU leads to minor changes in decay heat. At time = 0, decay heat increased by 3% and then decreased to -10% at 500 days and reaches to -5% at 1000 days relatively compared with the reference 5max-4.5av wt% case.
6. Increasing burnup from 60 to 80 GWd/MTU for 5max-4.5av wt% leads to a negligible change at time = 0 and a growing change from 10 days (7%) to 1000 days (43%) relatively compared with the reference 60 GWd/MTU. However absolute difference is negligible at 1000 days, the 80 GWd/MTU fuel has less than 1.5 kW/MTU decay heat difference compared with the reference 60 GWd/MTU case.
7. Effects of increases in burnup and enrichment on decay heat are in opposite directions, so the combined effect is a 18% increase at 500 days for increased enrichment and burnup compared with a 35% increase for only burnup. However, the absolute difference only makes 1 kW/MTU difference.
8. Decay heat calculations for VAN lattice show similar trends with DOM lattice. Increasing void fraction has negligible effect on decay heat compared to burnup and enrichment increase.
9. Activity shows similar trends to decay heat, but with less magnitude.
10. Isotopic results from the Polaris model depletion of GNF-2 10×10 DOM and VAN fuel lattices overall showed no unusual, unexpected, or adverse code performance trends.
 - a. No single isotope influenced decay heat by more than 11% in any case analyzed.
 - b. No single isotope changed activity by more than 5.2% in any case analyzed.
 - c. ^{244}Cm is the main isotope that changes the spontaneous neutron emission source substantially for the timescales in question.
 - d. Of the criticality-related isotopes evaluated, when increasing burnup to 80 GWd/MTU and enrichment to 10max-7.4av wt%, only ^{243}Am changed in composition by over a factor of 2 for the cases analyzed.
 - e. When changing from the 252- to the 56-group library, no isotope changed in mass by more than 10% for the 80 GWd/MTU, 10max-7.4av wt% VAN 70% void fraction case.

11. Each EE lattice requires a new enrichment loading pattern to be designed to match the reference case lattice design constraints. The loading patterns designed in for this study are adequate for the first phase. However, a more rigorous gadolinia loading and enrichment pattern optimization is needed for more realistic MVC and pin power distribution comparisons. Based on loading pattern trends in the industry, higher gadolinia loadings are expected. Increased gadolinia loading is also expected to further reduce the differences observed in the gadolinia depletion region for EE cases.
12. The results do not show significant changes when lattice type was changed, and void fraction was increased from the reference case. These inconsistent comparisons (DOM to VAN, 40% to 70% void fractions) show the bounding, conservative changes that could be expected for consistent comparisons (e.g., using 5max-4.5av wt% VAN lattice at 70% as the reference case and performing the same EE and HBU analyses). For the cases with the largest changes due to lattice type or void fraction change, this assumption should be verified in the next phase.
13. Higher than expected differences were observed in isotope contents calculated at 80 GWd/MTU with 56g vs 252g cross section libraries for some isotopes. However, these differences are negligible when compared to the magnitude of the change in isotopic contents when the reference case was compared to EE and HBU cases. Furthermore, comparison of 252g library results to the reference case results calculated from 56g library is an inconsistent bounding comparison to show that conclusions in this report would be valid when cross section library is changed. Reactivity coefficients calculated using 252g library in Appendix A confirms this conclusion. However, this assumption will be further verified in the next phase by repeating selected isotopic analyses with 252g library and confirming the findings.
14. Although no unexpected behavior was observed, verification basis for 56g and 252g cross section libraries will be extended to 80 GWd/MTU using continuous energy Monte Carlo depletion calculations in the next phase of this study.
15. Changes in pin power distributions were not analyzed in this phase because of their dependency to enrichment loading patterns which will be optimized in the next phase.

ACKNOWLEDGMENTS

Support for this work was provided by the US Nuclear Regulatory Commission Offices of Nuclear Regulatory Research, Nuclear Reactor Regulation, and Nuclear Material Safety and Safeguards. The authors would also like to thank many ORNL staff members for feedback on the contents and presentation in this report.

7. REFERENCES

1. M. Diaz, 2019, DSFM Regulatory Conference, “Advanced Fuels Update on the Front End of the Fuel Cycle,” <https://www.nrc.gov/docs/ML1925/ML19255F598.pdf>
2. F. Pimental et al., 2019, “The Economic Benefits and Challenges with Utilizing Increased Enrichment and Fuel Burnup for Light-Water Reactors,” Nuclear Energy Institute.
3. W. Marshall et al., 2015, *Technical Basis for Peak Reactivity Burnup Credit for BWR Spent Nuclear Fuel in Storage and Transportation Systems*, NUREG/CR-7194.
4. W. A. Wieselquist, R. A. Lefebvre, and M. A. Jessee, Eds., *SCALE Code System*, ORNL/TM-2005/39, Version 6.2.4, Oak Ridge National Laboratory, Oak Ridge, TN (2020).
5. K. Way and E. P. Wigner, *The Rate of Decay of Fission Products*, Phys. Rev. 73, 1318, 1948.
6. S Glasstone, *Nuclear Reactor Engineering* Princeton, N.J. Van Nostrand [1967]
7. N. E. Todreas and M. S. Kazimi, 1990, *Nuclear Systems I Thermal Hydraulic Fundamentals*. Taylor & Francis Group, LLC, New York, US Nuclear Regulatory Commission 2000.
8. *Regulatory Guide 1.183: Alternative Radiological Source Terms for Evaluating Design Basis Accidents at Nuclear Power Reactors*.
9. I. C. Gauld and J. C. Ryman, 2000, *Nuclide Importance to Criticality Safety, Decay Heating, and Source Terms Related to Transport and Interim Storage of High-Burnup LWR Fuel*, NUREG/CR-6700.
10. Nuclear Regulatory Commission, 2014, ML14113A088, LaSalle, Units 1 & 2, Updated Final Safety Analysis Report, Revision 20, Chapter 4.0, Reactor. <http://www.nrc.gov/docs/ML0813/ML081330057.pdf>
11. W. J. Marshall et. al., *Technical Basis for Peak Reactivity Burnup Credit for BWR Spent Nuclear Fuel in Storage and Transportation Systems*, NUREG/CR-7194 (ORNL/TM- 2014/240), prepared for the US Nuclear Regulatory Commission by Oak Ridge National Laboratory, Oak Ridge, TN (2015). <https://www.nrc.gov/docs/ML1509/ML15097A186.pdf>
12. LaSalle, Units 1 & 2, Submittal of Updated Final Safety Analysis Report (UFSAR), Revision 20, Chapter 4, ML14113A088, April 2014. <https://www.nrc.gov/docs/ML1411/ML14113A088.pdf>
13. D.J. Kelly, “Depletion of a BWR Lattice Using the RACER Continuous energy Monte Carlo Code “, Proc Int. Conf. on Math and Comp. Reactor Physics, and Env, Analysis, Portland, Oregon, USA, 1995,
14. M. L. Fensin. *Optimum Boiling Water Reactor Fuel Design Strategies to Enhance Reactor Shutdown by the Standby Liquid Control System*, Master’s Thesis, University of Florida (2004).
15. R. Hall et. al., “Isotopic and Fuel Lattice Parameter Trends in Extended Enrichment and Higher Burnup LWR Fuel Vol. 1: PWR Fuel”, ORNL/TM-202/1833

APPENDIX A. EFFECT OF CROSS SECTION LIBRARY

A separate analysis was performed to identify any effect in the reactivity, DTC, and MVC based on the cross-section library. The purpose of this comparison is to provide some qualitative insight into the impact of the 56-group cross section approximation used throughout this volume. The 10% lattice was depleted using SCALE 56-group ENDF/B-VII.1 cross sections and SCALE 252-group ENDF/B-VII.1 cross sections. Figure A.3. shows the difference in the reactivity for the dominant (DOM) and vanished (VAN) region lattices up to 80 GWd/MTU. This figure shows that the 56-group library consistently predicts greater reactivity for much of the depletion, with the exception being in the vanished lattice at 75+ GWd/MTU. Overall, the differences are small compared to the k_{inf} changes observed between lattice types, void fractions and enrichments seen in Figure 6.

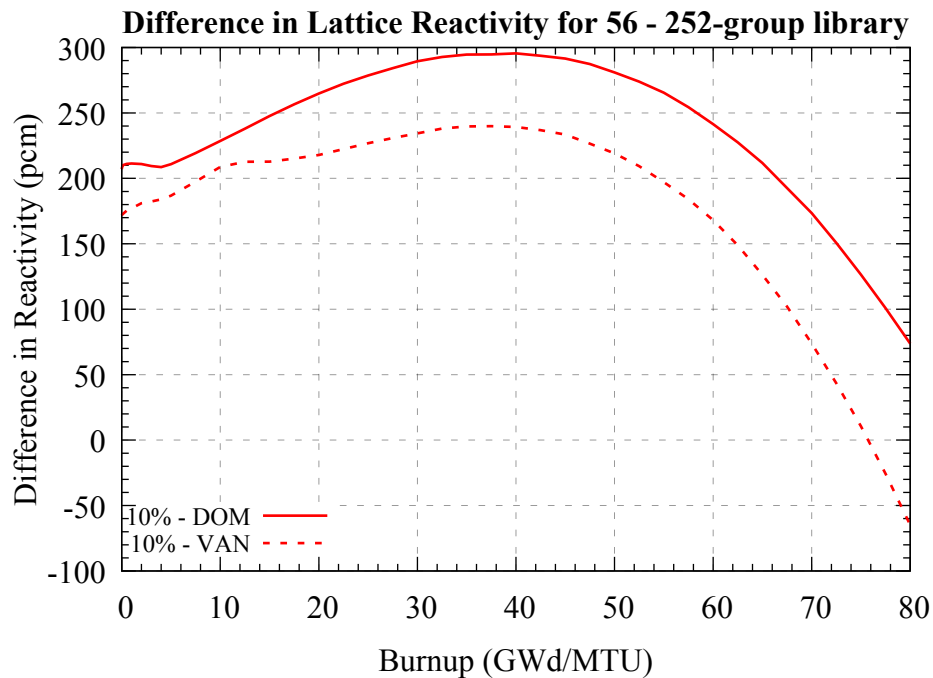


Figure 27. Difference in reactivity between the 252 and 56 g cross section libraries for the 10% limit dominant and vanished lattices.

Additionally, the DTC (Figure A.4.) and MVC (Figure A.5.) show consistent trends at higher burnups between the dominant and vanished lattices and the 56- and 252-group cross section libraries. Initially, the DTC for the 56-group library is greater until the lattice reaches ~20 GWd/MTU, at which point the DTCs for the 56- and 252-group intersect. Again, this is simply to provide some level of reassurance that there is little impact of cross section library approximation upon the conclusions reached in this volume.

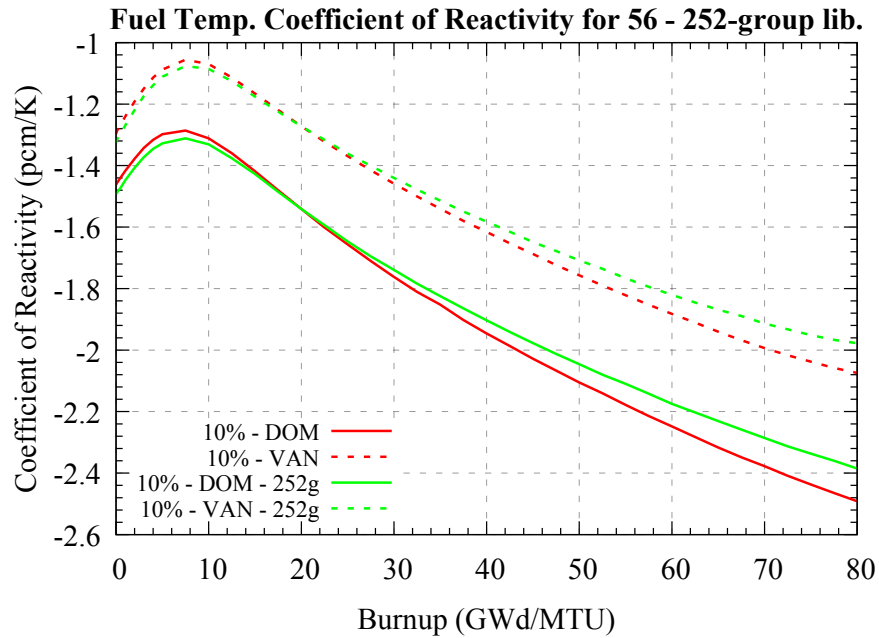


Figure 28. Comparison of the Doppler temperature coefficient (DTC) for the 252 and 56 g cross section libraries for the 10% limit dominant and vanished lattices.

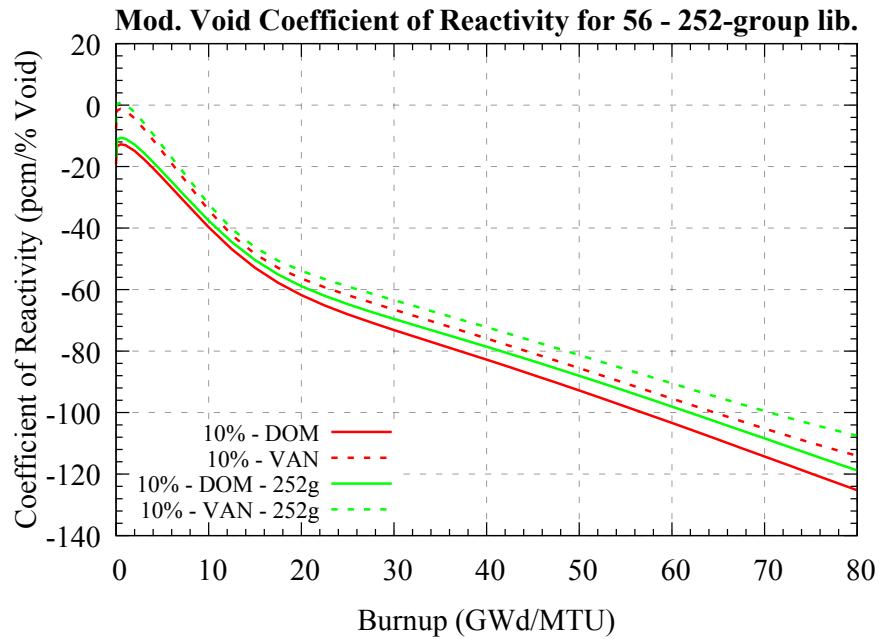


Figure 29. Comparison of the moderator void coefficient (MVC) for the 252 and 56 g cross section libraries for the 10% limit dominant and vanished lattices.

APPENDIX B. ARCHIVE FILE CONTENT

Lattice physics

Each Polaris simulation has an input file and 8 output file types. For the course of this study, only 2 files were used extensively, the input file (.inp) and the output file (.out). A summary of the file types and their contents is detailed below.

- *.inp - input file
- *.msg - simulation status message file
- *.out - simulation output file
- *.png - lattice illustration file - shows a snapshot of the lattice geometry and mesh
- *.t16 - Lattice physics parameters file
- *.f33 – ORIGEN library file

A. 5% Maximum Enrichment Lattices

1. Vanished Region Lattice with Void and Fuel Temperature Branch Case

5_percent_limit/VAN/GE14_5v40_van.x16
5_percent_limit/VAN/GE14_5v40_van.msg
5_percent_limit/VAN/GE14_5v40_van.out
5_percent_limit/VAN/GE14_5v40_van.t16
5_percent_limit/VAN/GE14_5v40_van.idc
5_percent_limit/VAN/GE14_5v40_van.inp
5_percent_limit/VAN/GE14_5v40_van.f33
5_percent_limit/VAN/GE14_5v40_van.png

2. Dominant Region Lattice with Void and Fuel Temperature Branch Case

5_percent_limit/DOM/GE14_5v40.x16
5_percent_limit/DOM/GE14_5v40.f33
5_percent_limit/DOM/GE14_5v40.png
5_percent_limit/DOM/GE14_5v40.idc
5_percent_limit/DOM/GE14_5v40.inp
5_percent_limit/DOM/GE14_5v40.out
5_percent_limit/DOM/GE14_5v40.msg
5_percent_limit/DOM/GE14_5v40.t16

3. Dominant Region Lattice with Control Rod Insertion Branch Case

5_percent_limit/DOM_cntl/GE14_5v40.x16
5_percent_limit/DOM_cntl/GE14_5v40.f33
5_percent_limit/DOM_cntl/GE14_5v40.png
5_percent_limit/DOM_cntl/GE14_5v40.idc
5_percent_limit/DOM_cntl/GE14_5v40.inp
5_percent_limit/DOM_cntl/GE14_5v40.out
5_percent_limit/DOM_cntl/GE14_5v40.msg
5_percent_limit/DOM_cntl/GE14_5v40.t16

B. 8% Maximum Enrichment Lattices

1. Vanished Region Lattice with Void Branch Case

8.5_percent_limit/VAN/void_branch/GE14_8v40_van.x16
8.5_percent_limit/VAN/void_branch/GE14_8v40_van.t16
8.5_percent_limit/VAN/void_branch/GE14_8v40_van.out
8.5_percent_limit/VAN/void_branch/GE14_8v40_van.msg
8.5_percent_limit/VAN/void_branch/GE14_8v40_van.inp
8.5_percent_limit/VAN/void_branch/GE14_8v40_van.idc
8.5_percent_limit/VAN/void_branch/GE14_8v40_van.png
8.5_percent_limit/VAN/void_branch/GE14_8v40_van.f33

2. Vanished Region Lattice with Temperature Branch Case

8.5_percent_limit/VAN/temp_branch/GE14_8v40_van.x16
8.5_percent_limit/VAN/temp_branch/GE14_8v40_van.t16
8.5_percent_limit/VAN/temp_branch/GE14_8v40_van.out
8.5_percent_limit/VAN/temp_branch/GE14_8v40_van.msg
8.5_percent_limit/VAN/temp_branch/GE14_8v40_van.inp
8.5_percent_limit/VAN/temp_branch/GE14_8v40_van.idc
8.5_percent_limit/VAN/temp_branch/GE14_8v40_van.png
8.5_percent_limit/VAN/temp_branch/GE14_8v40_van.f33

3. Dominant Region Lattice with Void and Fuel Temperature Branch Case

8.5_percent_limit/DOM/GE14_8v40.png
8.5_percent_limit/DOM/GE14_8v40.f33
8.5_percent_limit/DOM/GE14_8v40.inp
8.5_percent_limit/DOM/GE14_8v40.idc
8.5_percent_limit/DOM/GE14_8v40.t16
8.5_percent_limit/DOM/GE14_8v40.out
8.5_percent_limit/DOM/GE14_8v40.msg
8.5_percent_limit/DOM/GE14_8v40.x16

4. Dominant Region Lattice with Control Blade Insertion Branch Case

8.5_percent_limit/DOM_cntl/GE14_8v40.png
8.5_percent_limit/DOM_cntl/GE14_8v40.f33
8.5_percent_limit/DOM_cntl/GE14_8v40.inp
8.5_percent_limit/DOM_cntl/GE14_8v40.idc
8.5_percent_limit/DOM_cntl/GE14_8v40.t16
8.5_percent_limit/DOM_cntl/GE14_8v40.out
8.5_percent_limit/DOM_cntl/GE14_8v40.msg
8.5_percent_limit/DOM_cntl/GE14_8v40.x16

C. 10% Maximum Enrichment Lattices

252-group Cross section Library

1. Vanished Lattice with Void Branch

10_percent_limit/252group/VAN/void_branch/GE14_10v40_van_void.inp
10_percent_limit/252group/VAN/void_branch/GE14_10v40_van_void.idc
10_percent_limit/252group/VAN/void_branch/GE14_10v40_van_void.t16
10_percent_limit/252group/VAN/void_branch/GE14_10v40_van_void.out
10_percent_limit/252group/VAN/void_branch/GE14_10v40_van_void.msg
10_percent_limit/252group/VAN/void_branch/GE14_10v40_van_void.f33
10_percent_limit/252group/VAN/void_branch/GE14_10v40_van_void.png
10_percent_limit/252group/VAN/void_branch/GE14_10v40_van_void.x16

2. Vanished Lattice with Temperature Branch

10_percent_limit/252group/VAN/temp_branch/GE14_10v40_van.pbs
10_percent_limit/252group/VAN/temp_branch/GE14_10v40_van.x16
10_percent_limit/252group/VAN/temp_branch/GE14_10v40_van.f33
10_percent_limit/252group/VAN/temp_branch/GE14_10v40_van.png
10_percent_limit/252group/VAN/temp_branch/GE14_10v40_van.t16
10_percent_limit/252group/VAN/temp_branch/GE14_10v40_van.out
10_percent_limit/252group/VAN/temp_branch/GE14_10v40_van.msg
10_percent_limit/252group/VAN/temp_branch/GE14_10v40_van.inp
10_percent_limit/252group/VAN/temp_branch/GE14_10v40_van.idc

3. Dominant Lattice with Void Branch

10_percent_limit/252group/DOM/void_branch/GE14_10v40_void.x16
10_percent_limit/252group/DOM/void_branch/GE14_10v40_void.f33
10_percent_limit/252group/DOM/void_branch/GE14_10v40_void.png
10_percent_limit/252group/DOM/void_branch/GE14_10v40_void.t16
10_percent_limit/252group/DOM/void_branch/GE14_10v40_void.msg
10_percent_limit/252group/DOM/void_branch/GE14_10v40_void.out
10_percent_limit/252group/DOM/void_branch/GE14_10v40_void.inp
10_percent_limit/252group/DOM/void_branch/GE14_10v40_void.idc

4. Dominant Lattice with Temperature Branch

10_percent_limit/252group/DOM/temp_branch/GE14_10v40.png
10_percent_limit/252group/DOM/temp_branch/GE14_10v40.f33
10_percent_limit/252group/DOM/temp_branch/GE14_10v40.inp
10_percent_limit/252group/DOM/temp_branch/GE14_10v40.idc
10_percent_limit/252group/DOM/temp_branch/GE14_10v40.t16
10_percent_limit/252group/DOM/temp_branch/GE14_10v40.out
10_percent_limit/252group/DOM/temp_branch/GE14_10v40.msg
10_percent_limit/252group/DOM/temp_branch/GE14_10v40.x16

56-group Cross Section Library

1. Vanished Lattice with Void Branch (*_van_void*) and Temperature Branch

10_percent_limit/56group/VAN/GE14_10v40_van_void.inp
10_percent_limit/56group/VAN/GE14_10v40_van_void.idc
10_percent_limit/56group/VAN/GE14_10v40_van_void.t16
10_percent_limit/56group/VAN/GE14_10v40_van_void.out
10_percent_limit/56group/VAN/GE14_10v40_van_void.msg
10_percent_limit/56group/VAN/GE14_10v40_van.x16
10_percent_limit/56group/VAN/GE14_10v40_van_void.f33
10_percent_limit/56group/VAN/GE14_10v40_van_void.png
10_percent_limit/56group/VAN/GE14_10v40_van.f33
10_percent_limit/56group/VAN/GE14_10v40_van.png
10_percent_limit/56group/VAN/GE14_10v40_van_void.x16
10_percent_limit/56group/VAN/GE14_10v40_van.t16
10_percent_limit/56group/VAN/GE14_10v40_van.out
10_percent_limit/56group/VAN/GE14_10v40_van.msg
10_percent_limit/56group/VAN/GE14_10v40_van.inp
10_percent_limit/56group/VAN/GE14_10v40_van.idc

2. Dominant Lattice with Void Branch

10_percent_limit/56group/DOM/void_branch/GE14_10v40_void.x16
10_percent_limit/56group/DOM/void_branch/GE14_10v40_void.f33
10_percent_limit/56group/DOM/void_branch/GE14_10v40_void.png
10_percent_limit/56group/DOM/void_branch/GE14_10v40_void.t16
10_percent_limit/56group/DOM/void_branch/GE14_10v40_void.msg
10_percent_limit/56group/DOM/void_branch/GE14_10v40_void.out
10_percent_limit/56group/DOM/void_branch/GE14_10v40_void.inp
10_percent_limit/56group/DOM/void_branch/GE14_10v40_void.idc

3. Dominant Lattice with Temperature Branch

10_percent_limit/56group/DOM/temp_branch/GE14_10v40.png
10_percent_limit/56group/DOM/temp_branch/GE14_10v40.f33
10_percent_limit/56group/DOM/temp_branch/GE14_10v40.inp
10_percent_limit/56group/DOM/temp_branch/GE14_10v40.idc
10_percent_limit/56group/DOM/temp_branch/GE14_10v40.t16
10_percent_limit/56group/DOM/temp_branch/GE14_10v40.out
10_percent_limit/56group/DOM/temp_branch/GE14_10v40.msg
10_percent_limit/56group/DOM/temp_branch/GE14_10v40.x16

4. Dominant Lattice with Control Blade Insertion Branch

10_percent_limit/56group/DOM_cntl/GE14_10v40.png
10_percent_limit/56group/DOM_cntl/GE14_10v40.f33
10_percent_limit/56group/DOM_cntl/GE14_10v40.inp
10_percent_limit/56group/DOM_cntl/GE14_10v40.idc

10_percent_limit/56group/DOM_cntl/GE14_10v40.t16
10_percent_limit/56group/DOM_cntl/GE14_10v40.out
10_percent_limit/56group/DOM_cntl/GE14_10v40.msg
10_percent_limit/56group/DOM_cntl/GE14_10v40.x16

D. Convergence Study

1. Radial Element Convergence

i. 9-radial element mesh

Convergence_study/Convergence_Radial/9X/GE14_8v40.png
Convergence_study/Convergence_Radial/9X/GE14_8v40.f33
Convergence_study/Convergence_Radial/9X/GE14_8v40.inp
Convergence_study/Convergence_Radial/9X/GE14_8v40.idc
Convergence_study/Convergence_Radial/9X/GE14_8v40.out
Convergence_study/Convergence_Radial/9X/GE14_8v40.msg

ii. 6-radial element mesh

Convergence_study/Convergence_Radial/6X/GE14_8v40.png
Convergence_study/Convergence_Radial/6X/GE14_8v40.f33
Convergence_study/Convergence_Radial/6X/GE14_8v40.inp
Convergence_study/Convergence_Radial/6X/GE14_8v40.idc
Convergence_study/Convergence_Radial/6X/GE14_8v40.out
Convergence_study/Convergence_Radial/6X/GE14_8v40.msg

iii. 3-radial element mesh

Convergence_study/Convergence_Radial/3X/GE14_8v40.png
Convergence_study/Convergence_Radial/3X/GE14_8v40.f33
Convergence_study/Convergence_Radial/3X/GE14_8v40.inp
Convergence_study/Convergence_Radial/3X/GE14_8v40.idc
Convergence_study/Convergence_Radial/3X/GE14_8v40.out
Convergence_study/Convergence_Radial/3X/GE14_8v40.msg

iv. 1-radial element mesh

Convergence_study/Convergence_Radial/1X/GE14_8v40.png
Convergence_study/Convergence_Radial/1X/GE14_8v40.f33
Convergence_study/Convergence_Radial/1X/GE14_8v40.inp
Convergence_study/Convergence_Radial/1X/GE14_8v40.idc
Convergence_study/Convergence_Radial/1X/GE14_8v40.out
Convergence_study/Convergence_Radial/1X/GE14_8v40.msg

Convergence_study/Convergence_Radial/GE14_Radial.pdf
Convergence_study/Convergence_Radial/GE14_Radial_Difference.pdf

2. Burnup Step Size Convergence

i. 5 MWD/kgU Step

Convergence_study/Convergence_Burnup/5MWD/GE14_8v40.png
Convergence_study/Convergence_Burnup/5MWD/GE14_8v40.f33
Convergence_study/Convergence_Burnup/5MWD/GE14_8v40.inp
Convergence_study/Convergence_Burnup/5MWD/GE14_8v40.idc
Convergence_study/Convergence_Burnup/5MWD/GE14_8v40.out
Convergence_study/Convergence_Burnup/5MWD/GE14_8v40.msg
Convergence_study/Convergence_Burnup/GE14_Burnup.pdf

ii. 2.5 MWD/kgU Step

Convergence_study/Convergence_Burnup/2_5MWD/GE14_8v40.png
Convergence_study/Convergence_Burnup/2_5MWD/GE14_8v40.f33
Convergence_study/Convergence_Burnup/2_5MWD/GE14_8v40.inp
Convergence_study/Convergence_Burnup/2_5MWD/GE14_8v40.idc
Convergence_study/Convergence_Burnup/2_5MWD/GE14_8v40.out
Convergence_study/Convergence_Burnup/2_5MWD/GE14_8v40.msg

iii. 1 MWD/kgU Step

Convergence_study/Convergence_Burnup/1MWD/GE14_8v40.png
Convergence_study/Convergence_Burnup/1MWD/GE14_8v40.f33
Convergence_study/Convergence_Burnup/1MWD/GE14_8v40.inp
Convergence_study/Convergence_Burnup/1MWD/GE14_8v40.idc
Convergence_study/Convergence_Burnup/1MWD/GE14_8v40.out
Convergence_study/Convergence_Burnup/1MWD/GE14_8v40.msg

iv. 0.5 MWD/kgU Step

Convergence_study/Convergence_Burnup/0_5MWD/GE14_8v40.png
Convergence_study/Convergence_Burnup/0_5MWD/GE14_8v40.f33
Convergence_study/Convergence_Burnup/0_5MWD/GE14_8v40.inp
Convergence_study/Convergence_Burnup/0_5MWD/GE14_8v40.idc
Convergence_study/Convergence_Burnup/0_5MWD/GE14_8v40.out
Convergence_study/Convergence_Burnup/0_5MWD/GE14_8v40.msg

v. Current Simulation

Convergence_study/Convergence_Burnup/Current/GE14_8v40.png
Convergence_study/Convergence_Burnup/Current/GE14_8v40.f33
Convergence_study/Convergence_Burnup/Current/GE14_8v40.inp
Convergence_study/Convergence_Burnup/Current/GE14_8v40.idc
Convergence_study/Convergence_Burnup/Current/GE14_8v40.out
Convergence_study/Convergence_Burnup/Current/GE14_8v40.msg

E. Processed Data Files

Data files are organized based on output parameters for each of the Polaris Output files (*.out). Parameters of interest are extracted, and combined to form single tables to compare and plot.

processed_files/multiplication_factor_cntl.csv

Contains the multiplication factor as a function of burnup for 5%, 8.5%, and 10% max enrichment dominant and vanished region lattices with control rod inserted branch case.

processed_files/multiplication_factor.csv

Contains the multiplication factor as a function of burnup for 5%, 8.5%, and 10% max enrichment dominant and vanished region lattices for both temperature and void branch cases. temp+ is high temp (+200K). temp- is high temp (-200K). void+ is increased void (+30%). Void- is decreased void (-30%)

processed_files/flux_group1.csv

Fast Neutron Energies (20 - .625 MeV). Condensed version of the *Macroscopic Cross Sections* table at each burnup step for each enrichment and lattice region. Expanded tables are found in each of the output files

processed_files/flux_group2.csv

Thermal Neutron Energies (.625 - 1e-5 MeV). Condensed version of the *Macroscopic Cross Sections* table at each burnup step for each enrichment and lattice region. Expanded tables are found in each of the output files

processed_files/fission_macro_group1.csv

Fast Neutron Energies (20 - .625 MeV). Condensed version of the *Fission Macroscopic Cross Sections* table at each burnup step for each enrichment and lattice region. Expanded tables are found in each of the output files

processed_files/fission_macro_group2.csv

Thermal Neutron Energies (.625 - 1e-5 MeV). Condensed version of the *Fission Macroscopic Cross Sections* table at each burnup step for each enrichment and lattice region. Expanded tables are found in each of the output files.

processed_files/beta_eff.csv

Beta Eff. in the sum of decay groups row of the *Kinetic Parameters* table found in the output file. Data organized for each burnup step for each enrichment and lattice region.

processed_files/u_pu_sigma.csv

Summation of the Macroscopic fission cross section for plutonium over uranium isotopes $(\text{Pu}_{239} + \text{Pu}_{241}) / (\text{U}_{235} + \text{U}_{238})$. Data comes from the *Isotope*

Quantities table in the output file. Data organized for each burnup step for each enrichment and lattice region.

processed_files/power_level_over_burnup_rel.csv

Using the *Material Flux and Power Levels over Burnup Step* table, power levels for each ring from every rod in the lattice are extracted and normalized into Inner, middle, and outer regions. These are then condensed and outputted for every burnup step. This file contains inner, middle, and outer region power level for all three enrichments and both lattice regions.

F. Plots

plots/k.pdf

Plot of the multiplication factor for all enrichments and both lattice regions

plots/k_252.pdf

Plot of the pcm difference in reactivity between the 56-group and 252-group cross section library for the 10% enrichment case for both lattice regions

plots/cntl_blade_worth.pdf

Plot of the pcm change in reactivity by inserting the control plate at any burnup step

plots/abs.pdf

plots/abs_thermal.pdf

plots/abs_fast.pdf

Total effective abs. cross section - Fast energy effective abs. cross section -thermal effective abs. cross section for all three enrichments and both lattice regions

plots/fission.pdf

plots/fission_thermal.pdf

plots/fission_fast.pdf

Macroscopic fission cross section - Fast energy macroscopic cross section -thermal macroscopic fission cross section for all three enrichments and both lattice regions

plots/thermal_flux.pdf

plots/fast_flux.pdf

Fast and thermal neutron flux fraction for all three enrichments and both lattice regions

plots/CoR_Void.pdf

plots/CoR_Void_252.pdf

PCM difference in reactivity based on the instantaneous change in void for all three enrichments and both lattice regions, as well as comparison for 10% enrichment lattices using both 56-group and 252-group cross section libraries.

plots/CoR_Temp.pdf

plots/CoR_Temp_252.pdf

PCM difference in reactivity based on the instantaneous change in temperature for all three enrichments and both lattice regions, as well as comparison for 10% enrichment lattices using both 56-group and 252-group cross section libraries.

plots/U_Pu_ratio.pdf

Ratio of the macroscopic fission cross section for plutonium isotopes compared to uranium isotopes for all three enrichments and both lattice regions.

plots/beta.pdf

Total delayed neutron fraction for all three enrichments and both lattice regions.

plots/rings_total_power_5.pdf

plots/rings_total_power_8.pdf

plots/rings_total_power_10.pdf

Comparison of power production in inner, middle, and outer regions of the fuel for both lattice regions. Plots are organized by maximum enrichment.

plots/rings_inner_power.pdf

plots/rings_middle_power.pdf

plots/rings_outer_power.pdf

Comparison of power production in inner, middle, and outer regions of the fuel for both lattice regions. Plots are organized by the region of fuel rod.

Sensitivity

GE14_5v40_sampler.inp: input file for sampler run for 5% maximum enriched case with 40% void.

GE14_5v40_sampler.msg: message file for sampler run for 5% maximum enriched case with 40% void.

GE14_5v40_sampler.out: output file for sampler run for 5% maximum enriched case with 40% void.

GE14_5v40_sampler.samplerfiles: directory containing output files and glueup.x for 5% maximum enriched case with 40% void (a bash script to extract all the transport keff values into a single csv for later processing we had trouble getting sampler to do that.)

GE14_8v40_sampler.inp: input file for sampler run for 8% maximum enriched case with 40% void.

GE14_8v40_sampler.msg: input file for sampler run for 8% maximum enriched case with 40% void.

GE14_8v40_sampler.out: input file for sampler run for 8% maximum enriched case with 40% void.

GE14_8v40_sampler.samplerfiles: directory containing output files and glueup.x for 5% maximum enriched case with 40% void (a bash script to extract all the transport keff values into a single csv for later processing we had trouble getting sampler to do that.)

Isotopics

- Scale files

- Various suffixes indicate file's function

BASENAME_60Gorigen.000000000000000000.plt -- 60 GWD/MTU
origen case printout of nuclide masses
BASENAME_60Gorigen.000000000000000001.plt -- 60 GWD/MTU
origen case printout of neutron spectrum (not used)
BASENAME_60Gorigen.000000000000000002.plt -- 60 GWD/MTU
origen case printout of gamma spectrum (not used)
BASENAME_60Gorigen.000000000000000003.plt -- 60 GWD/MTU
origen case printout of decay heat
BASENAME_60Gorigen.000000000000000004.plt -- 60 GWD/MTU
origen case printout of activity
BASENAME_60Gorigen.000000000000000005.plt -- 60 GWD/MTU
origen case printout of decay heat for all decay time points
BASENAME_60Gorigen.000000000000000006.plt -- 60 GWD/MTU
origen case printout of activity for all decay time points
BASENAME_60Gorigen.f71 -- Binary output file with isotopics for
decay from 60 GWd/MTU
BASENAME_60Gorigen.inp -- Input file for isotopics for decay from 60
GWd/MTU
BASENAME_60Gorigen.msg -- Message file for isotopics for decay
from 60 GWd/MTU
BASENAME_60Gorigen.out -- Output file for isotopics for decay from
60 GWd/MTU
BASENAME_80Gorigen.000000000000000000.plt -- 80 GWD/MTU
origen case printout of nuclide masses
BASENAME_80Gorigen.000000000000000001.plt -- 80 GWD/MTU
origen case printout of neutron spectrum (not used)
BASENAME_80Gorigen.000000000000000002.plt -- 80 GWD/MTU
origen case printout of gamma spectrum (not used)
BASENAME_80Gorigen.000000000000000003.plt -- 80 GWD/MTU
origen case printout of decay heat
BASENAME_80Gorigen.000000000000000004.plt -- 80 GWD/MTU
origen case printout of activity
BASENAME_80Gorigen.000000000000000005.plt -- 80 GWD/MTU
origen case printout of decay heat for all decay time points
BASENAME_80Gorigen.000000000000000006.plt -- 80 GWD/MTU
origen case printout of activity for all decay time points
BASENAME_80Gorigen.f71 -- Binary output file with isotopics for
decay from 80 GWd/MTU
BASENAME_80Gorigen.inp -- Input file for isotopics for decay from 80
GWd/MTU

BASENAME_80Gorigen.msg -- Message file for isotopics for decay from 60 GWd/MTU
 BASENAME_80Gorigen.out -- Output file for isotopics for decay from 60 GWd/MTU
 BASENAME.bu -- Burnups extracted from output using postshell.x script. Output from a awk command
 BASENAME.bu_keff -- Burnups and keff values extracted from output using postshell_straightrun.x script. Output from a awk command. That only can be used if no branching is taking place so burnups and keff align right
 BASENAME.f33 -- Origen ARP library. Not used.
 BASENAME.f71 -- Isotopics file from Polaris run.
 BASENAME.inp -- Polaris input file
 BASENAME.keff -- keff values extracted from output using postshell.x script. Output from a awk command. It's not calculating, just pulling numbers next to text matches. QA is implicit because if the script errors, the results will be nonsensical (wrong number of values/trend makes no sense etc.)
 BASENAME.msg -- Polaris message file
 BASENAME.out -- Polaris output file
 BASENAME.pinpow -- File showing pin powers extracted from output using postshell.x script. Its a short script combining several unix commands that each extract text data from the output file.
 BASENAME.t16 -- lattice physics archive text file
 BASENAME.png -- lattice picture
 BASENAME.x16 -- lattice physics archive binary file

- Various prefixes (BASENAMEs) indicate the lattice being evaluated (Add 5% max prefixes)

GE14_8v10 -- 10 percent maximum enriched 10 % void full lattice
 GE14_8v40 -- 10 percent maximum enriched 40 % void full lattice
 GE14_8v40_van -- 10 percent maximum enriched 40 % void vanished lattice
 GE14_8v70_van -- 10 percent maximum enriched 70 % void vanished lattice
 GE14_8v70_van252 -- 10 percent maximum enriched 70 % void vanished lattice with 252 group cross sections
 GE14_8v40branches -- 10 percent maximum enriched 40 % void full lattice with branching for case with fuel temperature=1300K (not used)

- GE14_8v40.opus.inp – an opus input to extract time dependant isotopics from the GE14_8v40 Polaris case. It produces GE14_8v40.0000000000000.plt, which is a table listing the isotopic abundances for Inreactor inventories.xlsm

- Files relating to isotope worth
 - .loxs: Loss cross section outputs from obiwan. Filename prefixes are for the same cases as listed in the Scale files folder.
 - .fisxs: Fission cross section outputs from obiwan. Filename prefixes are for the same cases as listed in the Scale files folder.
 - .abncm.csv: Isotope abundances in depleted fuel taken from obiwan and cleaned to .csv format
 - Isotopeworths.csv: A spreadsheet to combine the cross sections and isotopic abundances and approximate isotope worths.
 - Obiwancommand.txt: The command to pull values with obiwan.
- Postprocessing files
 - IsotopePlotting.ipynb. This Jupyter notebook is a utility to show comparisons between cases in heatmaps. It also ranks isotopes by RMS of change. It's preferable to excel because every step is shown. The answers make intuitive sense and spot checks of the very few calculations are performed.
 - Heat maps

Plots comparing two types of discharged fuel across several decay times. For these plots the title includes information on what isotope set is being compared (activity, criticality, decay heat, release, or shielding) The figures themselves contain information on what comparison is being made (relative difference, absolute difference, or normalized relative difference).

 - Comparing burnup and enrichment at 40% void, full lattice
 - BuEnr_v40ActivityAbsDiff.png
 - BuEnr_v40Activity.png
 - BuEnr_v40Criticality isotope massAbsDiff.png
 - BuEnr_v40Criticality isotope mass.png
 - BuEnr_v40Decay heatAbsDiff.png
 - BuEnr_v40Decay heat.png
 - BuEnr_v40Release isotope activity.png
 - BuEnr_v40Shielding isotope activity.png
 - Comparing 80 GWd/MTU vs 60 GWd/MTU at 10 wt% max burnup and 40% void full lattice
 - Bu_f80e40v60GActivityAbsDiff.png
 - Bu_f80e40v60GActivity.png

Bu_f80e40v60GCriticality isotope
 massAbsDiff.png
 Bu_f80e40v60GCriticality isotope mass.png
 Bu_f80e40v60GDecay heatAbsDiff.png
 Bu_f80e40v60GDecay heat.png
 Bu_f80e40v60GRelease isotope activity.png
 Bu_f80e40v60GShielding isotope activity.png

- Comparing 80 GWd/MTU vs 60 GWd/MTU at 10 wt% max burnup and 40% void full lattice
 Enr_f40v60GActivityAbsDiff.png
 Enr_f40v60GActivity.png
 Enr_f40v60GCriticality isotope massAbsDiff.png
 Enr_f40v60GCriticality isotope mass.png
 Enr_f40v60GDecay heatAbsDiff.png
 Enr_f40v60GDecay heat.png
 Enr_f40v60GRelease isotope activity.png
 Enr_f40v60GShielding isotope activity.png
- Plots comparing RMS values for different lattices and voids to identify if there is a major change due to lattice type. Most of these are pretty boring. Suffix `_bu` indicates 80 GWd/MTU to 60 GWd/MTU are being compared at 10% max pin enrichment. Suffix `_enr` indicates comparison between 10 wt% max enrichment to 5% max enrichment at 60 GWd/MTU. Suffix `_enr+bu` indicates comparison between 10 wt% max enrichment, 80 GWd/MTU to 5% max enrichment at 60 GWd/MTU

RMSActivity_bu.png
 RMSActivity_enr+bu.png
 RMSActivity_enr.png
 RMSCriticality isotope mass_bu.png
 RMSCriticality isotope mass_enr+bu.png
 RMSCriticality isotope mass_enr.png
 RMSDecay heat_bu.png
 RMSDecay heat_enr+bu.png
 RMSDecay heat_enr.png
 RMSRelease isotope activity_bu.png
 RMSRelease isotope activity_enr+bu.png
 RMSRelease isotope activity_enr.png
 RMSShielding isotope activity_bu.png
 RMSShielding isotope activity_enr+bu.png
 RMSShielding isotope activity_enr.png

- Plots comparing RMS values for different lattices and voids to identify if there is a major change due to lattice type. Most of these are pretty boring. Suffix `_bu` indicates 80 GWd/MTU to 60 GWd/MTU are being compared at 10% max pin enrichment. Suffix `_enr` indicates comparison

between 10 wt% max enrichment to 5% max enrichment at 60 GWd/MTU. Suffix _enr+bu indicates comparison between 10 wt% max enrichment, 80 GWd/MTU to 5% max enrichment at 60 GWd/MTU

RMSvsBtmActivity_enr+bu.png
RMSvsBtmActivity_enr.png
RMSvsBtmCriticality isotope mass_enr+bu.png
RMSvsBtmCriticality isotope mass_enr.png
RMSvsBtmDecay heat_enr+bu.png
RMSvsBtmDecay heat_enr.png
RMSvsBtmRelease isotope activity_enr+bu.png
RMSvsBtmRelease isotope activity_enr.png
RMSvsBtmShielding isotope activity_enr+bu.png
RMSvsBtmShielding isotope activity_enr.png

G. Sources of figures and tables

Figure 1. Layout of the reference fuel assembly (5% - max) for dominant (left) and vanished (right) regions.

Figure 2. Layout of the 8.5% max enrichment fuel assembly for dominant (left) and vanished (right) regions.

Figure 3. Layout of the 10% max enrichment fuel assembly for dominant (left) and vanished (right) regions.

Figure 4. Spectra for 12GWd/MTU burnup for 252-group cases superimposed on notable macroscopic cross sections. Source: Resonance.xlsx Chart on Sheet 1.

Figure 5. Spectra for 10GWd/MTU burnup step for 56-group cases superimposed on notable macroscopic cross sections. Source: Resonance.xlsx Chart on Sheet 1.

Figure 6. Flux magnitude for cases evaluated. Source: 1 group flux.xlsx.

Figure 7. Concentrations of actinides with respect to burnup. Source: Inreactor inventories.xlsm. Sheet 5%.

Figure 8. Reactivity of both lattice regions for all three lattice enrichments.14
processed_files/multiplication_factor.csv

Figure 9. Ratio of thermal neutron flux to total flux (left) and ratio of fast neutron flux to total flux (right) for both lattice regions for all three lattice enrichments.15
processed_files/flux_group1.csv
processed_files/flux_group2.csv

Figure 10. The ratio of macroscopic cross sections for U and Pu isotopes vs fuel burnup.15
processed_files/u_pu_sigma.csv

Figure 11. Doppler temperature coefficient (DTC) vs burnup based on lattice.16
processed_files/multiplication_factor.csv

Figure 12. Moderator void coefficient (MVC) vs burnup based on lattice.17
processed_files/multiplication_factor.csv

Figure 13. Difference in reactivity between the 252 and 55 g cross section libraries for the 10% limit dominant and vanished lattices.18
processed_files/multiplication_factor.csv

Figure 14. Comparison of the Doppler temperature coefficient (DTC) for the 252 and 55 g cross section libraries for the 10% limit dominant and vanished lattices.18
processed_files/multiplication_factor.csv

Figure 15. Comparison of the moderator void coefficient (MVC) for the 252 and 55 g cross section libraries for the 10% limit dominant and vanished lattices.19
processed_files/multiplication_factor.csv

Figure 16. Power for each third of the fuel relative to the rod average power, averaged over all rods for the 10% limit lattices.20
processed_files/power_level_over_burnup_rel.csv

Figure 17. Power for the innermost third of the fuel relative to the rod average power averaged over all rods.20
processed_files/power_level_over_burnup_rel.csv

Figure 18. Power for the middle third of the fuel relative to the rod average power averaged over all rods.21
processed_files/power_level_over_burnup_rel.csv

Figure 19. Power for the outermost third of the fuel relative to the rod average power averaged over all rods.21
processed_files/power_level_over_burnup_rel.csv

Figure 20. Macroscopic thermal neutron absorption cross section vs burnup (left) and macroscopic fast neutron absorption cross section vs burnup (right).22
processed_files/flux_group1.csv
processed_files/flux_group2.csv

Figure 21. Macroscopic thermal fission cross section vs burnup (left) and macroscopic fast fission cross section vs burnup (right).22
processed_files/fission_macro_group1.csv
processed_files/fission_macro_group2.csv

Figure 22. Total delayed neutron fraction for all six lattices vs burnup.23
processed_files/beta_eff.csv

Figure 23. Control blade worth of the dominant lattice for three enrichments vs burnup.23
processed files/multiplication_factor_cntl.csv Figure 26. Uncertainty in keff arising
from cross section and fission yield uncertainty. Source: glueupKeff.v40.xlsx

Figure 27. Decay heat as a function of cooling time. 29 Source:decay_heat_and_activity.xlsx
Sheet:”Decay Heat”

Figure 28. Decay heats as a percentage of power vs cooling time. 30
Source:decay_heat_and_activity.xlsx Sheet:”Decay Heat”

Figure 29. Decay heat of highest decay heat lattice at 500 d decay time vs. lowest decay heat
lattice. 31 Source:decay_heat_and_activity.xlsx Sheet:”Decay Heat”

Figure 30. In-core abundances of 144Pr beta chain isotopes for 10 wt% maximum initial
enrichment. 34 Source: Inreactor inventories.xlsxm Sheet: 5%

Figure 31. Activity as a function of cooling time. 38 Source:decay_heat_and_activity.xlsx
Sheet: Activity

Figure 32. Activity of highest activity case at 500 GWd to lowest case. 39
Source:decay_heat_and_activity.xlsx Sheet: Activity

Figure 33. In-core abundances for isotopes in the activation chain for 244Cm and 246Cm.48
Source: Inreactor inventories.xlsxm Sheet: 5%

Figure 34. Relative difference in SF neutron emission on total SF neutron emission basis for time
point 80 GWd/MTU 10wt% maximum vs 60 GWd/MTU 5w% max, 40% void. 49 Source:
SpontaneousFission.xlsx

Figure A.1. Reactivity vs burnup of 8.5% limit dominant lattice based on the number of fuel
radial elements (left) and the difference in reactivity compared to a 9-radial element mesh (right).
A-1

Figure A.2. Reactivity vs burnup of 8.5% limit dominant lattice based on number of fuel sectors
(left) and difference in reactivity as compared to a 64-sector mesh (right). A-2

Figure A.3. Reactivity vs burnup of 8.5% limit dominant lattice based on the size of the burnup
step. A-2

Table 1. BWR fuel assembly design: assembled in document

Table 2. Lattice average 235U enrichment: assembled in document

Table 3. Fuel-to-moderator ratio for full and vanished lattices for various coolant void fractions
assembled in document

Table 4. Nuclide worth (10% void full lattice) 25 Source: Isotopeworhts.xlsm

Table 5. Predictions and relative standard deviations in masses when simulated with 100 perturbed cross section libraries 26 static_responses.1.stddev.8e.xlsx Sheet3

Table 6. Contributions of each isotope to total percent change in decay heat from enrichment increase Source: Enr_f40v60GDecay heat.png

Table 7. Contributions of each isotope to total percent change in decay heat from burnup increase Source: Bu_f80e40v60GDecay heat.png

Table 8. Contributions of each isotope to total percent change in decay heat from combined enrichment and burnup increase 33 Source: BuEnr_v40Decay heat.png

Table 9. Difference in isotopic decay heats resulting from enrichment increase at various cooling times 3Source: Enr_f40v60GDecay heatAbsDiff.png

Table 10. Difference in isotopic decay heats resulting from burnup increase at various cooling times 3Source: Bu_f80e40v60GDecay heatAbsDiff.png

Table 11. Difference in isotopic decay heats resulting from burnup and enrichment increase at various cooling times 35 Source: BuEnr_v40Decay heatAbsDiff.png

Table 12. Signed RMS change in isotope decay heat relative to total for enrichment increase from 5% to 10% maximum pin enrichment Source: RMSDecay heat_enr.png

Table 13. Signed RMS change in isotope decay heat relative to total for burnup increase from 60 to 80 GWd/MTU at 10% maximum pin enrichment Source: RMSDecay heat_bu.png

Table 14. Signed RMS change in isotope decay heat relative to total for enrichment and burnup increase from 5% 60 GWd/MTU to 10% maximum pin enrichment at 80 GWd/MTU Source: RMSDecay heat_enr+bu.png

Table 15. Contributions signed RMS effect of changing lattice and void vs full 10% void case 10% maximum pin enrichment at 80 GWd/MTU Source: RMSvsBtmDecay heat_enr+bu.png

Table 16. Contributions of each isotope to total percent change in activity from enrichment increase Source: Enr_f40v60GActivity.png

Table 17. Contributions of each isotope to total percent change in activity from burnup increase Source: Bu_f80e40v60GActivity.png

Table 18. Contributions of each isotope to total percent change in activity from combined enrichment and burnup increase Source: BuEnr_v40Activity.png

Table 19. Signed RMS effect of changing lattice and void vs full 10% void case 10 wt% maximum enriched at 80 GWd/MTU Source: RMSvsBtmActivity_enr+bu.png

Table 20. Relative differences of selected release isotopes activities due to enrichment increase
Source: Enr_f40v60GRelease isotope activity.png

Table 21. Relative differences of selected release isotopes activities due to burnup increase
43 Source: Bu_f80e40v60GRelease isotope activity.png

Table 22. Relative differences of selected release isotopes activities due to both enrichment and burnup increase Source: BuEnr_v40Release isotope activity.png

Table 23. Signed RMS relative differences in abundance of selected release isotopes vs the full lattice with 10% void, 10% maximum enrichment, and 80 GWd/MTU Source
RMSvsBtmRelease isotope activity_enr+bu.png

Table 24. Relative differences of selected shielding isotopes activities due to enrichment increase
Source: Enr_f40v60GShielding isotope activity.png

Table 25. Relative differences of selected shielding isotopes activities due to burnup increase
Source: Bu_f80e40v60GShielding isotope activity.png

Table 26. Relative differences of selected shielding isotopes activities due to both enrichment and burnup increase Source: BuEnr_v40Shielding isotope activity.png

Table 27. Signed RMS relative differences in abundance of selected shielding isotopes vs the full lattice with 10% void for 10% maximum enriched lattices burned to 80 GWd/MTU
Source: RMSvsBtmShielding isotope activity_enr+bu.png

Table 28. Percent differences in masses for a 3% enrichment increase at 60 GWd/MTU
Source: Enr_f40v60GCriticality isotope mass.png

Table 29. Percent differences in masses for a 20 GWd/MT burnup increase at 10 wt% maximum enrichment Source: Bu_f80e40v60GCriticality isotope mass.png

Table 30. Percent differences in masses for a 20 GWd/MT burnup increase and a 3 w% enrichment increase Source: BuEnr_v40Criticality isotope mass.png

Table 31. Change in activity of criticality isotopes for various lattice types at 10 wt% max, 80 GWd/MTU Source: RMSvsBtmCriticality isotope mass_enr+bu.png

Table 32. Order of magnitude changes in isotopic reactivity Source: ORM impact of isotopes.xlsx on the bottom of the Enr Change sheet.

Table 33. Relative difference between 252- and 56-group cross section structures on isotope results (other comparisons shown for reference). Source: Isotopes252vs56.xlsm Sheet1